TECHNISCHE UNIVERSITÄT DRESDEN

Fakultät Umweltwissenschaften, Fachrichtung Hydrowissenschaften, Institut für Grundwasserwirtschaft

Performance Assessment and Management of Groundwater in an Irrigation Scheme by Coupling Remote Sensing Data and Numerical Modeling Approaches

DISSERTATION

Zur Erlangung des akademischen Grades

Doktoringenieur
(Dr. – Ing.)

vorgelegt

der Fakultät Umweltwissenschaften, der Technischen Universität Dresden

von

Muhammad Usman, M.Sc.

Eingereicht am:

Datum der Verteidigung:

Kommissionsvorsitzender:

Prof. Dr. Olaf Kolditz,
Technische Universität Dresden / UFZ, Leipzig

Gutachter:

Prof. Dr. Rudolf Liedl,
Technische Universität Dresden

Prof. Dr. Niels Schütze,
Technische Universität Dresden

Prof. Dr. Martin Sauter,
Georg-August-Universität Göttingen

Erklärung des Promovenden

Die Übereinstimmung dieses Exemplars mit dem Original der Dissertation zum Thema:

"Performance Assessment and Management of Groundwater in an Irrigation Scheme by Coupling Remote Sensing Data and Numerical Modeling Approaches"

Wird hiermit bestätigt.

Dresden, 05-05-2016

Ort, Datum

Unterschrift

(Muhammad Usman)

This is for my father (late), mother, and wife, Sabeeha.

"Read in the name of your Lord who created"
"Created man, out of a (mere) clot of congealed blood"
"Read, and your Lord is the most Generous"
"Who taught by the pen"
"Taught man that which he knew not"
(Holy Quran 96:1-5)

"My Lord, save me from useless knowledge"
(Prophet Muhammad (PBUH))

Abstract

The irrigated agriculture in the Lower Chenab Canal (LCC) of Pakistan is characterized by huge water utilization both from surface and groundwater resources. Need of utilization of water from five rivers in Punjab province along with accelerated population growth has forced the construction of world's largest irrigation network. Nevertheless, huge irrigation infrastructure, together with inappropriate drainage infrastructure, led to a build-up of shallow groundwater levels, followed by waterlogging and secondary salinization in the soil profile. Following this era, decreased efficiency of irrigation supply system along with higher food demands had increased burdens on groundwater use, which led to a drop in groundwater levels in major parts of LCC. Previous studies in the study region revealed lacking management and maintenance of irrigation system, inflexible irrigation strategies, poor linkages between field level water supply and demands. No future strategy is present or under consideration to deal with this long time emerged groundwater situation particularly under unchanged irrigation water supply and climate change. Therefore, there is an utmost importance to assess the current profile of water use in the irrigation scheme and to device some workable strategies under future situations of land use and climate change. This study aims to investigate the spatio-temporal status of water utilization and performance of irrigation system using remote sensing data and techniques (SEBAL) in combination with other point data. Different irrigation performance indicators including equity, adequacy and reliability using evaporation fraction as main input parameter are utilized. Current profiles of land use/land cover (LULC) areas are assessed and their change detections are worked out to establish realistic future scenarios. Spatially distributed seasonal net recharge, a very important input parameter for groundwater modeling, is estimated by employing water balance approaches using spatial data from remote sensing and local norms. Such recharge results are also compared with a water table fluctuation approach. Following recharge estimation, a regional 3-D groundwater flow model using FEFLOW was set up. This model was calibrated by different approaches ranging from manual to automated pilot point (PP) approach. Sensitivity analysis was performed to see the model response against different model input parameters and to identify model regions which demand further improvements. Future climate parameters were downscaled to establish scenarios by using statistical downscaling under IPCC future emission scenarios. Modified recharge raster maps were prepared under both LULC and climate change scenarios and were fed to the groundwater model to investigate groundwater dynamics.

Seasonal consumptive water use analysis revealed almost double use for kharif as compared to rabi cropping seasons with decrease from upper LCC to lower regions. Intra irrigation subdivision analysis of equity, an important irrigation performance indicator, shows less differences in water consumption in LCC. However, the other indicators (ade-

quacy and reliability) indicate that the irrigation system is neither adequate nor reliable. Adequacy is found more pronounced during kharif as compared to rabi seasons with average evaporation fraction of 0.60 and 0.67, respectively. Similarly, reliability is relatively higher in upper LCC regions as compared to lower regions. LULC classification shows that wheat and rice are major crops with least volatility in cultivation from season to season. The results of change detection show that cotton exhibited maximum positive change while kharif fodder showed maximum negative change during 2005-2012. Transformation of cotton area to rice cultivation is less conspicuous. The water consumption in upper LCC regions with similar crops is relatively higher as compared to lower regions. Groundwater recharge results revealed that, during the kharif cropping seasons, rainfall is the main source of recharge followed by field percolation losses, while for rabi cropping seasons, canal seepage remains the major source. Seasonal net groundwater recharge is mainly positive during all kharif seasons with a gradual increase in groundwater level in major parts of LCC. Model optimization indicates that PP is more flexible and robust as compared to manual and zone based approaches. Different statistical indicators show that this method yields reliable calibration and validation as values of Nash Sutcliffe Efficiency are 0.976 and 0.969, % BIAS are 0.026 and -0.205 and root mean square errors are 1.23 m and 1.31 m, respectively. Results of model output sensitivity suggest that hydraulic conductivity is a more influential parameter in the study area than drain/fillable porosity. Model simulation results under different scenarios show that rice cultivation has the highest impact on groundwater levels in upper LCC regions whereas major negative changes are observed for lower parts under decreased kharif fodder area in place of rice, cotton and sugarcane. Fluctuations in groundwater level among different proposed LULC scenarios are within ±1 m, thus showing a limited potential for groundwater management. For future climate scenarios, a rise in groundwater level is observed for 2011 to 2025 under H3A2 emission regime. Nevertheless, a drop in groundwater level is expected due to increased crop consumptive water use and decreased precipitations under H3A2 scenario for the periods 2026-2035 and 2036-2045. Although no imminent threat of groundwater shortage is anticipated, there is an opportunity for developing groundwater resources in the lower model regions through water re-allocation that would be helpful in dealing water shortages. The groundwater situation under H3B2 emission regime is relatively complex due to very low expectation of rise in groundwater level through precipitation during 2011-2025. Any positive change in groundwater under such scenarios is mainly associated with changes in crop consumptive water uses. Consequently, water management under such situation requires revisiting of current cropping patterns as well as augmenting water supply through additional surface water resources.

Zusammenfassung

Die Bewässerungslandwirtschaft im Gebiet des Lower Chenab Canal (LCC) in Pakistan ist durch starke Wassernutzung sowohl aus ober- als auch unterirdischen Ressourcen charakterisiert. Das Erfordernis der Wassernutzung aus fünf Flüssen der Provinz Punjab hat zusammen mit einem beschleunigten Bevölkerungswachstum die Konstruktion des weltgrößten Bewässerungsnetzwerks vorangetrieben. Dennoch führte die enorme Bewässerungsinfrastruktur in Verbindung mit einem unzureichenden Dränageausbau zu einem Anstieg des oberflächennahen Grundwassers mit resultierender Bodenvernässung und -versalzung. Nach dieser Phase brachte die abnehmende Effizienz des Bewässerungssystems bei erhöhtem Nahrungsbedarf steigende Anforderungen bei der Grundwassernutzung mit sich, die ein Absinken der Grundwasserstände in weiten Teilen des LCC ergaben. Frühere Studien im Untersuchungsgebiet stellten die fehlende Betreuung und Wartung des Bewässerungssystems, unflexible Bewässerungsstrategien und schlechte Abstimmung zwischen Wasserdargebot und -bedarf auf der Feldskala heraus. Derzeit gibt es weder eine Strategie für die Zukunft noch entsprechende Planungen, um mit der über einen längeren Zeitraum entstandenen Grundwassersituation speziell bei unveränderten Bewässerungsbedingungen und unter dem Einfluss des Klimawandels umzugehen. Aus diesem Grund kommt der Bewertung des aktuellen Wassernutzungsprofils im Bewässerungsplan und der Ausarbeitung umsetzbarer Strategien für zukünftige Szenarien der Landnutzung und des Klimawandels allergrößte Bedeutung zu. Diese Arbeit setzt sich zum Ziel, die räumlich-zeitliche Wassernutzung und die Wirkungsweise des Bewässerungssystems unter Verwendung von Fernerkundungsdaten und -techniken (SEBAL) in Kombination mit weiteren Punktinformationen zu untersuchen. Unterschiedliche Indikatoren für die Bewässerungseffizienz wie Verteilungsgerechtigkeit, Angemessenheit und Zuverlässigkeit werden mit dem Verdunstungsanteil als Haupteingangsgröße verwendet. Gegenwärtige Landnutzungs- und -bedeckungsmuster werden bewertet und ihr Wandel wird herausgearbeitet, um realistische Zukunftsszenarien zu erstellen. Die räumlich differenzierte jährliche Grundwasserneubildung, die eine hochrelevante Eingangsgröße der Grundwassermodellierung darstellt, wird mittels Bilanzansätzen auf der Basis räumlicher Fernerkundungsdaten sowie örtlicher Normen und Vorschriften abgeschätzt. Die so resultierende Grundwasserneubildung wird zudem mit der Analyse von Wasserspiegelschwankungen verglichen. Im Anschluss daran wurde mittels FEFLOW ein 3D-Grundwasserströmungsmodell erstellt. Dieses Modell wurde mit verschiedenen Methoden, die von einem manuellen bis hin zum automatischen Pilot-point-Ansatz reichten, kalibriert. Eine Sensitivitätsanalyse wurde durchgeführt, um die Abhängigkeit der Modellergebnisse von unterschiedlichen Eingangsgrößen zu erkennen sowie Teile des Modellgebiets zu identifizieren, die einer verbesserten Abbildung bedürfen. Zur Berücksichtigung von zukünftigen IPCC-Emissionsszenarien wurde ein statistisches

Downscaling von Klimaparametern vorgenommen. Modifizierte Rasterkarten wurden sowohl für Landnutzungs- / Landbedeckungs- als auch für Klimawandelszenarien erstellt und für das Grundwassermodell nutzbar gemacht, um die Grundwasserdynamik zu untersuchen.

Eine Analyse des Wassergebrauchs auf Jahresbasis ergab nahezu die doppelte Menge für die Jahreszeit Kharif (Monsun- / Regenzeit) verglichen mit der Jahreszeit Rabi („Winter“) bei einer von ober- zu unterstromigen Regionen des LCC abnehmenden Tendenz. Vergleiche zwischen Untereinheiten des Bewässerungssystems hinsichtlich der Verteilungsgerechtigkeit, einem wesentlichen Tauglichkeitsindikator, lieferten geringere Unterschiede im Wasserverbrauch innerhalb des LCC. Allerdings zeigen die weiteren Indikatoren (Angemessenheit, Zuverlässigkeit), dass das Bewässerungssystem weder angemessen noch zuverlässig arbeitet. Die Angemessenheit ist während des Kharif stärker ausgeprägt als während des Rabi, wobei der Verdunstungsanteil 0.67 bzw. 0.60 beträgt. In ähnlicher Weise ist die Zuverlässigkeit in oberstromigen LCC-Regionen höher als in unterstromigen. Eine Landnutzungs- / Landbedeckungsklassifikation zeigt, dass Weizen und Reis die Hauptkulturen mit den geringsten Anbauveränderungen zwischen den Jahreszeiten sind. Die Analyse der Veränderungen ergab, dass Baumwolle im Zeitraum 2005 bis 2012 die stärkste Zunahme, Rabi-Viehfutter hingegen den stärksten Rückgang aufweist. Die Umwandlung von Baumwoll- in Reisanbaufläche ist weniger deutlich. Der Wassergebrauch in den oberstromigen LCC-Regionen ist bei vergleichbaren Kulturen höher als in den unterstromigen. Untersuchungen zur Grundwasserneubildung ergaben, dass zur Anbauzeit des Kharif Regen, gefolgt von Versickerungsverlusten auf den Feldern, die Hauptquelle für die Grundwasserneubildung darstellt, während zur Anbauzeit des Rabi die Versickerung aus den Kanälen dominiert. Die saisonale Grundwasserneubildungsrate ist während des Kharif hauptsächlich positiv, womit ein allmähliches Ansteigen der Grundwasserstände in weiten Teilen des LCC verbunden ist. Die Modellanpassung deutet darauf hin, dass die Pilot-point-Methode flexibler und robuster ist als manuelle und zonenbasierte Ansätze. Verschiedene statistische Kriterien zeigen, dass die genannte Methode eine zuverlässige Kalibrierung und Validierung ermöglicht (Nash-Sutcliffe-Effizienz: 0.978 bzw. 0.962, %BIAS: 0.026 bzw. -0.205, Wurzel des mittleren Abweichungsquadrats: 1.23 m bzw. 1.31 m).

Sensitivitätsuntersuchungen ergaben, dass die hydraulische Leitfähigkeit einen größeren Einfluss besitzt als die dränbare / wiederauffüllbare Porosität. Modellsimulationen für verschiedene Szenarien belegen, dass der Reisanbau die stärksten Auswirkungen auf Grundwasserstände in oberstromigen LCC-Regionen aufweist, während wesentliche negative Veränderungen in unterstromigen LCC-Regionen infolge der Aufgabe von Anbaufläche für Kharif-Viehfutter zugunsten von Reis, Baumwolle und Zuckerrüben auftreten. Grundwasserspiegelschwankungen zwischen verschiedenen Landnutzungs- / Landbedeckungsszenarien liegen innerhalb ±1 m, sodass sich hieraus ein begrenztes

Potenzial für Grundwasserbewirtschaftungsmaßnahmen ableiten lässt. Für zukünftige Szenarien ist infolge des Emissionsregimes H3A2 ein Anstieg der Grundwasserstände im Zeitraum von 2011 bis 2025 festzustellen. Demgegenüber ist aufgrund der zunehmenden Wassernutzung durch Anbaupflanzen und der gemäß dem H3A2-Szenario abnehmenden Niederschläge für die Zeiträume 2026 – 2035 und 2036 – 2045 ein Rückgang der Grundwasserstände zu erwarten. Obwohl dies mit keiner unmittelbaren Gefahr von Grundwasserknappheit verbunden ist, kann die Gelegenheit ergriffen werden, Grundwasserressourcen in den unterstromigen Teilen des Untersuchungsgebiets mittels Wasserumverteilung zu entwickeln, um so dem Wassermangel zu begegnen. Für das Emissionsregime H3B2 erweist sich die Grundwassersituation als sehr komplex, da für den Zeitraum 2011 – 2025 ein sehr geringer Anstieg der Grundwasserstände infolge von Niederschlägen zu erwarten ist. Jedwede positive Entwicklung der Grundwasservorräte ist bei diesen Szenarien hauptsächlich auf Veränderungen der Wassernutzung durch die angebauten Kulturen zurückzuführen. In der Folge erfordert das Wassermanagement in dieser Situation sowohl eine Neubewertung der gegenwärtigen Anbaumuster als auch eine Verbesserung der Wasserversorgung durch zusätzliche Oberflächenwasserressourcen.

Table of Contents

Acronyms

3-D	Three Dimensional
ASTER	Advanced Space-borne Thermal Emission and Reflection Radiometer
AVHRR	Advanced Very High Resolution Radiometer (AVHRR)
CBD	Convention on Biological Diversity
CGIAR	Consultative Group for International Agricultural Research
COMSATS	Commission on Science and Technology for Sustainable Development in the South
CSI	Consortium for Spatial Information
DD	Dynamic Downscaling
DEM	Digital Elevation Model
DS	Dual Simplex
EF	Evaporation Fraction
EVI	Enhanced Vegetation Index
FAO	Food and Agricultural Organization
GCM	General Circulation Model
GIS	Geographical Information System
GOP	Government of Pakistan
GW	Groundwater
HadCM3	Hadley Centre Coupled Model version 3
IBIS	Indus Basin Irrigation System
ICA	International Cooperation Administration
IPCC	International Panel on Climate Change
ISD	Irrigation Subdivision
IWASRI	International Waterlogging and Salinity Research Institute
IWMI	International Water Management Institute
LANDSAT	Land Satellite
LCC	Lower Chenab Canal
MODIS	MODerate Resolution Imaging Spectroradiometer
NCEP	National Centers for Environmental Prediction
NCEP	National Centers for Environmental Prediction
NDVI	Normalized Difference Vegetation Index
NOAA	National Oceanic and Atmospheric Administration
OLS	Ordinary Least Square
PEST	Parameter Estimation Tool
PID	Punjab Irrigation Department
PLPROC	Parameter List Processor

PMD	Pakistan Meteorological Department
PP	Pilot Point
PWP	Pakistan Weather Portal
QB	Qadirabad Balloki
RADARSAT	Radar Satellite
RCM	Reginal Circulation Model
RF	Rainfall
SCARP	Salinity Control and Reclamation Project
SCS	Soil Conservation Services
SDSM	Statistical Downscaling Model
SEBAL	Surface Energy Balance Algorithm
SMO	Salinity Monitoring Organization
SPOT	Système Pour l'Observation de la Terre
SRTM	Shuttle Radar Topography Mission
TM	Thematic Mapper
TRMM	Tropical Rainfall Measuring Mission
TS	Trimu Sidhnai
UN	United Nations
UNCED	United Nations Conference on Environment and Development
UNDESA	United Nations Department of Economic and Social Affairs
UNEP	United Nations Environment Program
USDA	United States Department of Agriculture
USGS	United States Geological Survey
WAPDA	Water and Power Development Authority
WBM	Water Balance Method
WTF	Water Table Fluctuation
WWAP	World Water Assessment Program

Chapter 1

General Introduction

1. Groundwater for irrigated agriculture

Irrigated agriculture is the largest consumer of groundwater resource accounting for about 70% of the global fresh water abstraction and 90% of consumptive water use (FAO, 2010; Döll, 2009). According to Llamas (2005), during the last 20-30 years, there is a boom in the utilization of groundwater resources for irrigation in areas subject to extended dry seasons and/or regular droughts. Globally, an area of about 300 million ha (Mha) is under irrigation and 38% of this land are equipped for irrigation with groundwater amounting to 545 km^3/yr (Siebert et al., 2010). Extended groundwater use is not only restricted to semi-arid regions, but also occurs in many humid areas (Fig. 1). It is envisaged that groundwater use for irrigated agriculture will continue to expand due to many possible reasons including: (a) it is usually found close to point of use, (b) it can be developed quickly by individual private investment at low capital cost, (c) it is available directly for crop needs, (d) it is suited to pressurized irrigation and, (e) it has permitted irrigated agriculture outside of canal command regions (Shah et al., 2007). Groundwater use has been the crux of the green revolution in agriculture across many Asian nations. Currently, the nations with highest groundwater use are India (39 Mha), China (19 Mha) and USA (17 Mha) (Siebert et al., 2010; Madramootoo, 2012). Groundwater use in developing countries is likely to continue and the pressure on groundwater resources over next 25 years in Asia will come from demographic increase, agriculture and increasing water demand per capita, industrial activity and energy demand (Gunatilaka, 2005). It is predicted that the world population will increase from 6.9 billion in 2010 to 8.3 billion in 2030 and to 9.1 billion in 2050, most of which will occur in Asia (Christmann et al., 2009; UNDESA, 2009). This increase in population will expand food demand by 50% in 2030 and by 70% in 2050. Nevertheless, Ayars et al. (2006) reported that future scenarios predict a worldwide fresh irrigation water scarcity which is even higher in arid and semi-arid regions. This fact emphasizes that the role of water should be properly regarded as socio-economic and life sustaining commodity demanding management procedures and be implemented through water conservation and resource assessment and reuse (UNCED, 2002). Otherwise poor management of groundwater resources will nullify the social gains made so far (Mukharji and Shah, 2005).

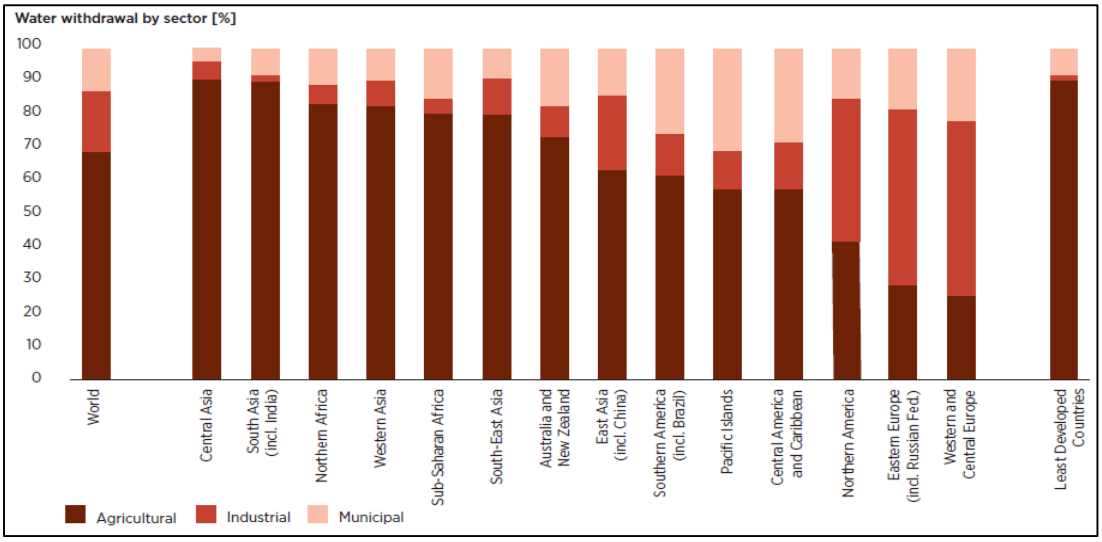

Fig. 1 Water withdrawal by sector by region in 2005 (Source: UNESCO, 2012)

2. Groundwater development in Pakistan

The Indus Basin Irrigation System (IBIS) of Pakistan was designed about a century ago and is one of the largest contiguous irrigation systems in the world. Its design objectives were to prevent crop failure, avoid famine and expand settlement opportunities (Jurriens and Mollinga, 1996) by constructing reservoirs, barrages and main canals which are now serving an area of 16 Mha with some 172 billion m^3 of river water flow per year (Aslam and Prathapar, 2006). The IBIS is supported by the basin of the Indus river and its tributaries including the Kabul, Jehlum, Chenab, Ravi and Satluj rivers. The irrigation system is comprised of three major storage reservoirs, 19 barrages, 12 link canals, 45 major irrigation canal commands and over 120,000 field water channels. The total canal length is about 60,000 km, with additional 1.8 million km comprising of watercourses, farm channels and field ditches (COMSATS, 2003). The rivers of IBIS have glaciated headwaters and snowfields that provide about 50-80% of surface water flow out of the total volume of 137 x 10^9 m^3. The remaining volume is due to monsoon runoff. It is estimated that effective rainfall contributes about 200-300 mm in total crop water availability in the north of the country and some 50 mm in the south (Qureshi et al., 2010).

The IBIS was designed for an annual cropping intensity (ratio of effective crop area harvested to the physical area) of about 75% with the intention of spreading the irrigation water over large areas to expand settlement opportunities (Qureshi et al., 2010), and has grown up to 200% (Kazmi et al., 2012) because more than one crop cycle per year has become possible. Also many canals have lost their design capacity over time due to siltation and erosion of their banks (Badruddin, 1996). The result is further limitation of canal water availability per unit of irrigated land (Sarwar, 2000).

Huge crop yield losses, land degradation and social instability were observed during the 1970s due to inadequacy, inequity and unreliability of surface water supplies, which resulted in large scale migration of populations from rural areas to cities (Postel, 2003). Nevertheless, large farming communities also came forward to rescue themselves against this situation and huge investment is made to extract groundwater by installing agricultural wells for crops. The government also helped farmers by subsidizing the power supply after realizing the benefits of groundwater irrigation for expansion of irrigated areas and to maintain higher crop production levels. In the early days, open wells, Persian wheels, karezes, hand pumps and reciprocating pumps were used for groundwater abstraction. Introduction of indigenous small diesel engines and subsidized energy supply cause a dramatic increase in the number of private tubewells (i.e. individual farmer owned) in the country. By the end of the 1990s, canal irrigation dominated the irrigated agriculture in the country, but in the early 1990s, groundwater irrigation had surpassed canal irrigation (Van der Velde and Kijne, 1992). According to Chaudhary et al. (2002), more than 50% of irrigated lands in the country are irrigated by groundwater wells. More than 70% of the farmers in the Punjab province depend directly or indirectly on groundwater for agriculture (Qureshi et al., 2003). About 80% of total tubewells in the country are private owned. According to some estimates, the investment in the private tubewells is of the order of Rs. 25 billion (US$ 400 million) whereas, the annual benefits are of the order of Rs. 150 billion (US$ 2.3 billion) in the form of agricultural production (Shah et al., 2003; Qureshi et al., 2010). According to Government of Pakistan, on average, every fourth farming family owns a tubewell and a large proportion of farmers without tubewell ownership purchase water through local groundwater markets (Government of Pakistan (GOP), 2000; Qureshi and Akhtar, 2003). Figure 2 depicts the development and distribution of tubewells in each province of Pakistan.

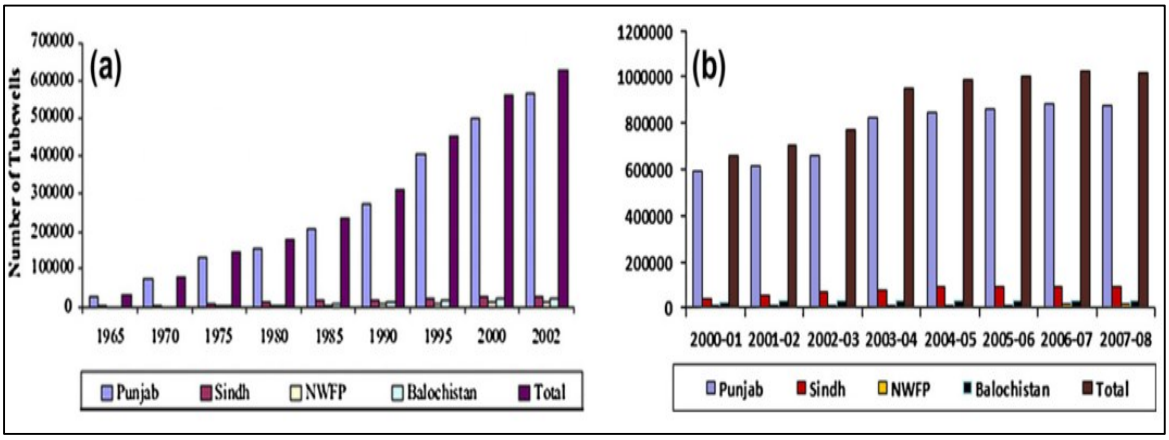

Fig. 2 Number of tubewells in Pakistan (a) Qureshi et al. (2010) (b) Agricultural Statistics of Pakistan (2008-09)

3. Study area

Lower Chenab Canal (LCC), Punjab, Pakistan has been chosen as the study region (Fig. 3). The LCC irrigation system originates at the Khanki headworks which distribute water to its eastern and western parts through seven branch canals. This irrigation system was designed in 1892-1898 and its command area lies in Rechna Doab which comprises of the land mass between rivers Ravi and Chenab.

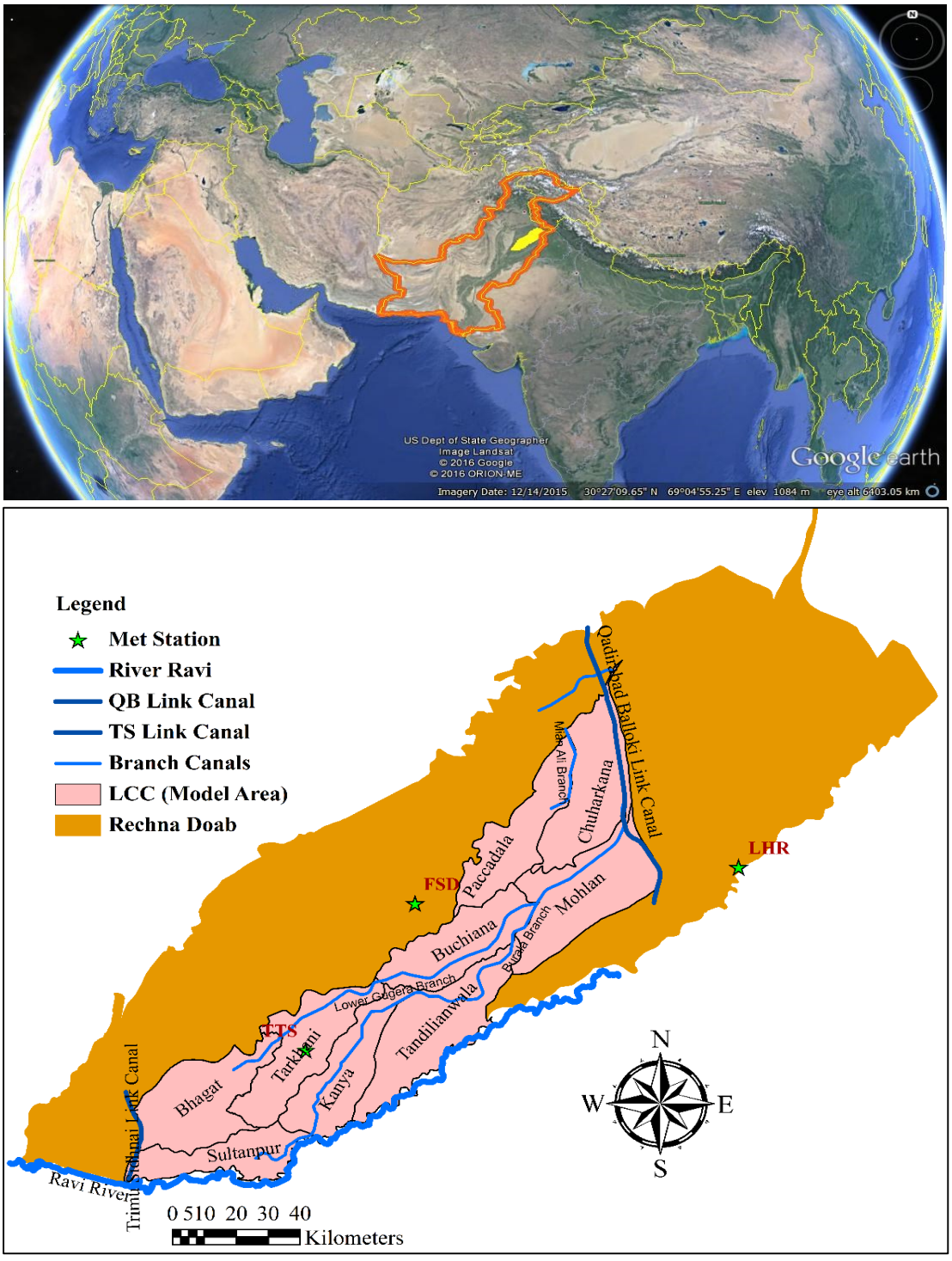

Fig. 3 Location of the study area in Rechna Doab, Punjab, Pakistan

The location of the area is between latitude 30° 36' and 32° 09' N and longitude 72° 14' and 77° 44' E. The present study mainly focuses on the eastern part of LCC. Two link canals namely Qadirabad-Balloki (QB) and Trimu-Sidhnai (TS) flow from north to south and fall into river Ravi. Major part of LCC east lies in the districts of Faisalabad and Toba Tek Singh. Administratively, the entire study area is split into 9 irrigation subdivisions: Chuharkana, Paccadala, Mohlan, Buchiana, Tandlianwala, Kanya, Tarkhani, Bhagat and Sultanpur. Irrigation subdivision is considered as the smallest management unit of the irrigation system in LCC. The structuring of these irrigation subdivisions ensures the equitable distribution of canal water among different consumers.

4. History of groundwater use in the study area

Punjab province of Pakistan is called 'the land of five rivers' and covers an area of about 127,000 km^2. These rivers include Indus, Jhelum, Chenab, Ravi and Sutlej from west to east. The land between any two rivers is known as 'doab'. These doabs include Thal (between rivers Indus and Jhelum), Chaj (between rivers Chenab and Jhelum), Rechna (between rivers Chenab and Ravi) and Bari (between rivers Ravi and Sutlej) and the plains of these doabs have been formed by alluvial deposits and are very fertile. During the 1900s, during the rule of British over the subcontinent, an extensive network of irrigation canal was constructed in order to develop the barren land and to utilize the water of these five rivers. These practices paid off the investment of millions of rupees for construction of canals and headworks within a few years as the area converted into lush green fields (Hassan and Bhutta, 1996). The period of prosperity proved very short as intensive irrigation application coupled with poor subsurface drainage resulted in a gradual increase of groundwater. By the late 1930's and early 1940's, several million acres of land had been affected by waterlogging and salinization, both of which were spreading alarmingly every year (Malmberg, 1975). In some areas the groundwater rise was about 24.4 m with an average rate of rise of 0.46 m/yr (Hassan and Bhutta, 1996). According to Soomro (1975), waterlogging was first identified in the upper parts of Rechna doab within few years of opening of the Lower Chenab Canal (LCC).

A comprehensive study of the geology and hydrology of the Indus Plain was carried out in 1954 by the Government of Pakistan in cooperation with the U.S. International Cooperation Administration (ICA) to assess the groundwater potential of the Northern Plain in order to formulate reclamation measures that would solve the problems of waterlogging and salinity and restore the productive capacity of the land (Malmberg, 1975). The results of these studies provided the basis for the reclamation projects utilizing deep tubewells to lower the groundwater level and supplement the canal water supply. The launch of the first project phase took place in 1960 with the first Salinity Control and Reclamation Project (SCARP-1). The interfluvial area between the Ravi and Chenab rivers was selected for construction of SCARP-1. This project was the first of 18 planned reclamation projects that ultimately

included about 21 million acres and more than 28,000 production and drainage wells (Malmberg, 1975).

Large scale groundwater extraction for irrigated agriculture in Rechna started by the launching of SCARP. Thousands of large capacity tubewells were installed under this program. In the initial phase more than 10,000 public tubewells (supplying an area of 2.6 Mha) with an average discharge capacity of 80 l/s were installed (Bhutta and Smedema, 2007; Kazmi et al., 2012). The project resulted not only in the lowering of the water table but also in supplemented irrigation. This also encouraged farmers to own their individual tubewells and led to a proliferation with a typical tubewell discharge capacity of 28 l/s or less. The results of SCARP-1 indicated that it managed to lower the groundwater level below 1.5 m over an area of 2 Mha and below 3 m over 4 Mha, thereby overcoming the problem of waterlogging significantly. It also reclaimed salt affected area from 4.5 to 7.0 Mha (Qureshi et al., 2010). Moreover, the additional groundwater abstraction by SCARP tubewells increased cropping intensities from 80 to 120% in most of the SCARP project areas (IWASRI, 1998).

5. Research agenda

5.1. Problem statement

The drought of 1998-2002 in Pakistan is considered to be the worse in last 50 years which resulted in a huge decrease of canal flows (Pakistan Weather Portal (PWP), 2011). Moreover the population of the country had an annual growth rate of 2.61% from 1961 to 2011 (Mustafa et al., 2013). The outcome of this situation emerged in the form of increased groundwater abstraction for agricultural use as production of important crops grew by an annual rate of 3% from 1962 to 2010. As stated earlier, farmers did prefer groundwater due to issues of canal water supply and because of flexibility which groundwater granted them in their irrigation strategies along with government support in terms of subsidized energy provision. It is witnessed from that fact that the number of tubewells in the country increased dramatically from 10,000 in 1960 to about 0.60 million in 2002 and about 0.80 million in 2006 (Qureshi et al., 2003; World Bank, 2007). Every farmer is absolutely free to install a tubewell of any discharge capacity anywhere on his farm without any control on groundwater abstraction and detrimental effects of his action on this precious resource and on others.

Evolution of groundwater in the study region showed that its management has two contradictory aspects. First there was a rise of the groundwater level due to increased water losses from irrigation canals and field percolations, which also caused secondary salinization in many parts by transporting of salts from deeper layers to the vadose zone. Secondly in fresh water zones, overexploitation of groundwater resulted in depletion of the aquifer and fall of the water table (Kijne, 1999). Excessive lowering of the groundwater level is making groundwater pumping expensive and wells are going out of production, which is escalating crop production costs and net profits of growers started declining.

There are many reasons of these opposite effects, and the spatial differences between water demand and supply is one of them. The country is still practicing a century old water distribution plan called 'warabandi'. The biggest limitation of this system is its inflexibility as farmers have to attain their water share according to a rigid irrigation plan ignoring the fact whether they require water or not. Moreover, this system does not guarantee farmers to adjust their cropping patterns, rather they will get the similar amount of water on land area basis without accommodating their cropping patterns. The consequence is overdependence on groundwater as farmers have to do less planning, it provides a great level of control over the crop calendar and there is no wait for the availability of canal water (Plusquellec, 2002). Nevertheless, this situation has shown the inefficiency of the irrigation system with lower crop water productivity (Ahmad et al., 2008; Usman et al., 2014). Moreover, the unplanned changes in land use / land cover has escalated the miseries of groundwater along with climate change. According to Immerzeel et al. (2010), many developing countries including Pakistan are going to face changes in agricultural production due to climate change.

Under the current circumstances of the irrigation system and environmental variabilities, there is a dire need to follow a holistic approach to maintain the advantages of groundwater as a valuable resource for current and future generations. Management of groundwater needs to be more strategic and proactive to cope with potential impacts of climate variabilities which has unfortunately been ignored by this time (Kundzewicz et al., 2007).

5.2. Objectives and scope of the study

The ever-growing use of groundwater in the study region raises the question to investigate the groundwater resources for their sustainable use on large time scales without hampering environment for the coming generations. This is performed by setting up a hydrogeological model as a key tool. Such models often lack several spatially distributed input data, both biotic (vegetation) and environmental. Meeting this challenge requires the integration of field surveys and advanced remote sensing technologies (e.g. satellite images). This is achieved by bringing research approaches from different scientific disciplines together. Based on the evaluation of the current performance of the irrigation system and future model simulations, potential options and measures are implemented to reduce the risk of groundwater deterioration. The findings of the current study are generally applicable to the present study area, but the results are also relevant to nearby areas with similar agro-ecological conditions. More specifically, the following research questions are addressed in the current study:

1. To carry out the current performance evaluation of the irrigation system along with spatio-temporal variation in consumptive water use (Article I).
2. To classify major land use/land cover for diagnosing current patterns and for exploring change detection (Article II).

3. To estimate spatio-temporal seasonal net groundwater recharge in irrigated agricultural area (Article III).
4. To set up a numerical model for regional groundwater flow, its calibration and validation through multiple inverse approaches (Article IV).
5. To assess groundwater dynamics under future land use/land cover and climate changes for sustainable use of water resources (Article V).

Figure 4 depicts the conceptual framework of the current study to carry out the research work to achieve these objectives and the interdependencies for accomplishing the overall task of sustainable groundwater management.

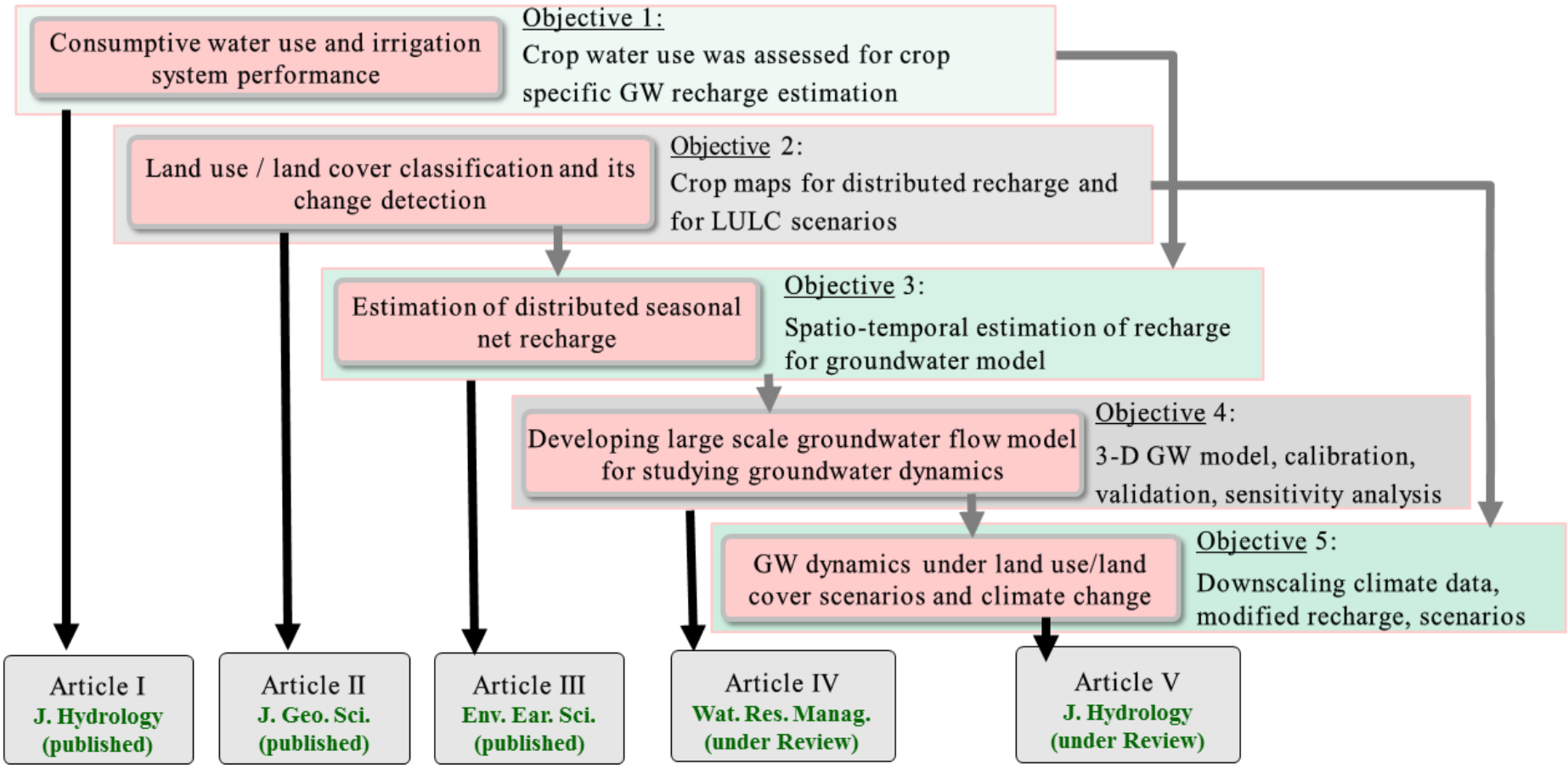

Fig. 4 Conceptual framework for the current study

Chapter 2

Overview of Publications

The thesis comprises of three chapters including five research articles. The **first article** gives an overall account of the spatio-temporal estimation of consumptive water use using modern satellite data along with some local meteorological data. The article also describes the current patterns of water use in different regions of the study area which leads to the analysis of the irrigation system performance. The analysis carried out in this article also encompasses patterns of water use and its availability on different spatio-temporal scales both for kharif (i.e. mainly summer season) and rabi (i.e. mainly winter season) cropping seasons. Evaporative Fraction (EF) representing the key element to assess the three very important performance indicators of equity, adequacy and reliability, was determined by the Surface Energy Balance Algorithm (SEBAL) using Moderate Resolution Imaging Spectroradiometer (MODIS) images. Spatially based estimations were performed at irrigation subdivisions, lower and upper LCC and, whole LCC scales, while temporal scales covered months, seasons and years for the study period from 2005 to 2012. The assessment of equitable water distribution indicates smaller coefficients of variation and hence less inequity within each subdivision except Sagar (0.08) and Bhagat (0.10). Both adequacy and reliability of water resources are found lower during kharif as compared to rabi with variation from head to tail reaches. Reliability is quite low from July to September and in February/March. This is mainly attributed to seasonal rainfalls. Average consumptive water use estimations indicate almost doubled water use (546 mm) in kharif as compared to (274 mm) in rabi with significant variability for different cropping years. Crop specific consumptive water use reveals rice and sugarcane as major water consumers with average values of 593 mm and 580 mm, respectively, for upper and lower LCC, followed by cotton and kharif fodder. The water uses for cotton are 555 mm and 528 mm. For kharif fodder, corresponding values are 525 mm and 494 mm for both regions. Based on the differences in consumptive water use, different land use land cover change scenarios were evaluated with regard to savings of crop water. It is found that such analyses need to be complemented at more fine spatial resolutions (i.e. irrigation subdivisions).

The **second article** investigates the current and historic cultivation patterns of major land use/ land cover classes as agriculture is the major water consumer in the region. Normalized Difference Vegetation Index (NDVI) is used for characterization of different classes and areal estimation of these classes is carried out. Moreover, the potential patterns of land use/land cover changes are identified. The extent of volatilities from one class to another

along with their potential change regions are identified by utilizing multiple spatial techniques. In the end, multiple scenarios of land use/land cover are developed to utilize for groundwater modeling. Wheat and rice are found to be major crops in rabi and kharif seasons, respectively. Accuracy assessment of prepared maps is performed using three different techniques: error matrix approach, comparison with ancillary data and with previous study. Producer and user accuracies for each class are calculated along with kappa coefficients (K). The average overall accuracies for rabi and kharif are 82.83% and 78.21%, respectively. Producer and user accuracies for individual class range respectively between 72.5% to 77% and 70.1% to 84.3% for rabi and 76.6% to 90.2% and 72% to 84.7% for kharif. The K values range between 0.66 to 0.77 for rabi with average of 0.73, and from 0.69 to 0.74 with average of 0.71 for kharif. LULC change detection indicates that wheat and rice have less volatility of change in comparison with both rabi and kharif fodders. Transformation between cotton and rice is less common due to their completely different cropping conditions. Results of spatial and temporal LULC distributions and their seasonal variations provide useful insights for establishing realistic LULC scenarios for hydrological studies.

The **third article** elaborates the results of groundwater recharge. Recharge is a very important input parameter to groundwater modeling in the current study region due to excessive application of irrigation for agriculture and seasonal monsoon rainfalls. Due to the very complex irrigation system, multiple recharge estimation methods are adopted including water balance approach and water table fluctuation method. For the water balance method, recharge contributions from different organs of the irrigation system are estimated along with data from remote sensing. Spatial recharge is estimated for both rabi and kharif cropping seasons and results are validated with recharge obtained from the water table fluctuation method. Moreover, limitations of the conventional groundwater abstraction approach and of different recharge estimation methods employed herein are discussed. Groundwater abstraction estimation from conventional utilization factor method overstates results both for kharif and rabi cropping seasons. Recharge results obtained from water balance method and water table fluctuation approach are comparable both at irrigation subdivision and 1 km^2 spatial scales. During the kharif cropping seasons, rainfall is the main source of recharge followed by field percolation losses while for rabi cropping seasons, canal seepage remains the major source. Net groundwater recharge is mainly positive during all kharif seasons. A gradual increase in groundwater level is observed in major parts of the study area. Improvement in results from water table fluctuation method is possible by better distribution and increased intensity of piezometers while for water balance approach, it is possible by adopting alternative buffer zones for canal seepage. Detailed sensitivity and uncertainty analyses of input/output variables are needed to present the results with confidence interval and hence to support sustainable and economical operation of irrigation system.

In the **fourth article**, a conceptual model of the current study area is set up which is further used to build a numerical groundwater flow model using FEFLOW-3D simulation package. Modeling setup, data requirements, boundary conditions and hydrogeological setting are discussed and the model is calibrated using multiple approaches ranging from manual to automated techniques. The comparison of different calibration techniques is performed followed by a sensitivity analysis with regard to important model input parameters. The results indicate that Pilot Point (PP) is more flexible and robust as compared to other approaches. Different statistical indicators show that this method yields reliable calibration and validation as values of Nash Sutcliffe efficiency (ME) are 0.976 and 0.969, percent BIAS are 0.026 and -0.205 and root mean square errors (RMSE) are 1.23 m and 1.31 m, respectively. The results of output sensitivity suggest that hydraulic conductivity is a more influential parameter in the study area than drain/fillable porosity. Parameter error along with sensitivity demonstrates the strength/weaknesses of available field data. Different observation sensitivity plots highlight sensitive/insensitive regions for each observation point to guide planners to perform further field activities accordingly. Under considering the limitations of the current study, it is recommended to perform global sensitivity and linear uncertainty analysis for better certainty of modeling results.

The **fifth article** explores the groundwater dynamics under changing land use/land cover and climate conditions. The results of land use/ land cover scenarios are retrieved from the third article, while the future climate change scenarios are synthesized using a statistical downscaling approach under International Panel on Climate Change (IPCC) emission scenarios H3A2 and H3B2. Actual evapotranspiration and precipitation are utilized as potential downscaling parameters. The values of relative change of such parameters is used to prepare modified recharge maps. The simulation is carried out under different scenarios for future periods and valuable information is extracted to support the management of groundwater resources in the study region. The water budget for the calibration and validation period shows a total horizontal water inflow of 2844 Mm^3 to LCC and an outflow of 2720.2 Mm^3. The water outflow through pumping is about 17374.43 Mm^3 as compared to groundwater recharge of 19933.20 million m^3 (Mm^3). The comprising surplus of 2682.87 Mm^3 raises groundwater levels in major parts of LCC. Changes in rice cultivation show the highest impact on groundwater levels in upper irrigation subdivisions of LCC whereas higher negative changes are observed for lower parts of LCC when fodder is replaced by rice, cotton, and sugarcane. Fluctuations in groundwater level among different scenarios are within ±1 m range thus showing a limited potential for groundwater management due to LULC changes. For future climate scenarios, a rise in groundwater level is observed under the H3A2 emission regime for 2011 to 2025. Nevertheless, a drop in groundwater level is expected due to increased crop consumptive water use and decreased precipitation under the H3A2 scenario for the periods 2026-2035 and 2036-2045. Although no imminent threat of groundwater shortage is anticipated, there is an opportunity for developing groundwater resources in the

lower LCC regions through water re-allocation that would help to deal with anticipated water shortages in the study region. The groundwater situation under the H3B2 emission regime is relatively complex as very little rise in groundwater level through precipitation is expected during 2011-2025. Any positive change in groundwater under such scenarios is mainly associated with changes in crop consumptive water uses. Consequently, water management requires revisiting of current cropping patterns as well as augmenting water supply through additional surface water resources. Considering the limitations of the current study, it is recommended to update the model with modifications in river flow due to climatic changes. Moreover, it is regarded helpful to investigate groundwater dynamics under combined effects of LULC and climate change.

Finally, a concluding part **(Chapter 3)** summarizes the main findings of the overall research along with major empirical conclusions of the five articles.

Chapter 3

General conclusions and policy recommendations

The current study was conducted in the irrigated agricultural Lower Chenab Canal (LCC) region of Punjab, Pakistan, to investigate the current profile of water resources use and its impact on groundwater dynamics. High spatio-temporal remote sensing data and state of the art numerical modeling techniques were employed for this purpose. The results of the current investigations are generally applicable for LCC, however, they could also be used for similar agro-climatic surrounding regions. The main conclusions emerging form this study are:

- Traditionally, irrigated agriculture in LCC was solely dependent on surface water resources but the increase in cropping intensities due to accelerated population and lower performance of irrigation system forced farmers to use it in conjunction with groundwater. Some recent drought periods (i.e. from 1998-2002) have also increased its importance for agriculture and presently its share is almost half in total irrigation water requirements.

- The present situation of high demand for groundwater and its major drop in levels at locations of LCC during the last 10-15 years has urged the need to explore the reasons and future fate of groundwater resources in the presence of current irrigation system performance, cropping practices and their adaptation to future climate conditions. The results indicate that canal water supply in LCC is more variable during rabi seasons as compared to kharif seasons. Monthly consumptive water use is almost double for kharif seasons as compared to rabi seasons. Moreover, consumptive water use becomes higher during monsoon in kharif season and after winter rains in rabi season due to more water availability for crops.

- The trend in consumptive water use is generally decreasing from upper regions of LCC as compared to lower regions. This tendency is more pronounced during kharif seasons than rabi seasons. The irrigation performance indicator ‘equity’ shows a lower difference of water availability in the majority of LCC regions. Results of other performance indicators including ‘adequacy’ and ‘reliability’ of irrigation system indicate poor depiction. Inadequacy is higher during kharif season than rabi season, while reliability is relatively high in upper LCC regions than lower regions.

- Rice and wheat are major crops during kharif and rabi seasons. Wheat is cultivated in all regions of LCC during rabi season while cultivation of rice is more pronounced in upper regions with better rainfall and canal water availability. The cultivation of

cotton is found in lower regions as fewer rainfalls are suitable for its growth. Sowing of sugarcane is mostly adopted in low-sloping areas especially alongside river Ravi. Just like wheat, both rabi and kharif fodder are cultivated everywhere in LCC.

- Quantification of both groundwater recharge and abstraction is possible by indirect approaches using remote sensing which is highly responsive to fluctuations in canal water supply, land use changes and rainfall variability. During kharif, rainfall is the major source of recharge to groundwater (37%) followed by field percolation (30%), canal seepage (13%), watercourse seepage (9%), and distributary seepage (8%). The rest is lateral groundwater inflow. Groundwater abstraction is found highest in one upper and two lowest irrigation subdivisions including Chuharkana, Bhagat and Sultanpur. This is mainly driven by the availability of canal water supply in these regions and partly due to cultivation of high water demand crops including rice and sugarcane. During rabi seasons, rainfall is no longer an important recharge component but major recharge share come from canal seepage and field percolation. Groundwater abstraction is found to be highest in most of the upper LCC regions due to decreased canal flow instead of lower crop water demands during this season.

- The estimation of field percolation losses by the conventional fixed percentage value approach with crop specific percolation values is different for rice and wheat but it is in accordance for mixed cropping patterns. A considerable share of field percolation in groundwater recharge also indicates lower irrigation efficiencies which results in considerable loss of canal water below crop roots without crop utilization. This results in overuse of groundwater and thus considerable energy demand for groundwater pumping.

- The net groundwater recharge is largely variable in space and time. During kharif season in most parts of LCC, net groundwater recharge is positive except in two irrigation subdivisions at lower regions (Bhagat and Sultanpur) owing to more groundwater dependence. During rabi seasons, the recharge results are quite variable from year to year even for the same locations. The majority of the regions of LCC show gently increasing trends in groundwater level except Sagar irrigation subdivision at upper locations and Bhagat and Sultanpur irrigation subdivisions at lower locations.

- After the successful calibration and validation of the FEFLOW-3D model by both automated and conventional manual approaches, the model was used to simulate groundwater levels under different land use/land cover (LULC) and future climate scenarios. Real changes in LULC during the study period are investigated and real-

istic change scenarios are proposed in consultation with local experts. For future climate change scenarios, a statistical downscaling approach was utilized to work out the changes in precipitation and actual crop water utilization in reference to baseline periods considering IPCC emission scenarios H3A2 and H3B2. Modified recharge data were prepared considering cropping variability and such data were utilized in the numerical groundwater model for future simulations.

- The proposed LULC scenarios indicate that change in rice cultivation has the highest impact on groundwater in upper irrigation subdivisions. The groundwater levels for lower LCC regions indicate high negative changes under decreased fodder area replaced by rice, cotton and sugarcane. The highest positive change is observed for Bhagat irrigation subdivision under third scenario followed by Tarkhani and Kanya irrigation subdivisions under fourth scenario. Fluctuations in groundwater level among different scenarios are within ±1 m, which shows that proposed LULC changes have limited potential for groundwater management.

- The groundwater dynamics under future climate scenarios show a rise in groundwater level for whole LCC during the period 2011 to 2025 under the H3A2 emission scenario. The changes for upper irrigation subdivisions are relatively higher. These positive changes in different irrigation subdivisions are because of decreased consumptive water use by crops and also due to increase in precipitation. However, the change is relatively higher due to consumptive water use at upper parts, and in lower parts it is relatively higher due to increased precipitation.

- At present there is no threat of shortage of groundwater. Rather, there is a need of reallocation of surface water resources to supply more water to lower areas in order to safeguard and develop groundwater resources in these regions. It would also safeguard against any threat of water logging in some parts of upper LCC.

- Judicious utilization of groundwater resources during 2011-2025 is also important considering the groundwater behaviour for periods 2026-2035 and 2036-2045. During these periods, a drop in groundwater is expected due to increased consumptive water use by crops and decreased precipitation under H3A2 scenario. Hence, proper water management during 2011-2025 could safeguard against possible water shortages. The other solutions could be the alteration of current cropping patterns to grow crops with less water demand. There is a need to breed similar crops which consume less water without affecting the farmer's crop yield.

- There is an urgent need to revamp the monitoring and operation of the irrigation system. For instance, the area is lacking modern data loggers for recording groundwater levels, canal flows, groundwater quality parameters, and real time online crop and climate data etc., which is highly important for conducting research of high quality. Moreover, it is high time to change the canal water supply policy from supply driven to demand driven.

- The present study does not accommodate groundwater quality issues. This could be very important and a demanding issue to be investigated in the future under altering situations of groundwater use and fertilizer applications for changing LULC and climate conditions.

References

Ahmad MD, Turral H, Nazeer A (2009) Diagnosing irrigation performance and water productivity through satellite remote sensing and secondary data in a large irrigation system of Pakistan. Agricultural Water Management (96): 551–564. doi:10.1016/j.agwat.2008.09.017

Aslam M, Prathapar SA (2006) Strategies to mitigate secondary salinization in the Indus Basin of Pakistan: A selective review. Research Report 97. Colombo, Sri Lanka: International Water Management Institute (IWMI)

Ayars JE, Christen EW, Soppe RW, Meyer WS (2006) The resource potential of in-situ shallow ground water use in irrigated agriculture: a review. Irrig. Sci. 24: 147–160

Badruddin M (1996) Country profile. Pakistan Internal Report. International Water Management Institute (IWMI): Lahore, Pakistan

Bhutta MN, Smedema K (2007) One hundred years of waterlogging and salinity control in the Indus valley, Pakistan: A historical review. Irrigation and Drainage (56): S81-S90

Chaudhary MR, Bhutta NM, Iqbal M, Subhani KM (2002) Groundwater resources: use and impact on soil and crops. Paper presented at the Second South Asia Water Forum, 14–16 December, Islamabad, Pakistan

Christmann S, Martius C, Bedoshvili D et al (2009) Food Security and Climate Change in Central Asia and the Caucasus. Sustainable Agriculture in Central Asia and the Caucasus Series No.7. CGIAR-PFU, Tashkent, Uzbekistan

COMSATS (Commission on Science and Technology for Sustainable Development in the South) (2003) Water Resources in the South: Present Scenario and Future Prospects. Islamabad: COMSATS

Döll P (2009) Vulnerability to the impact of climate change on renewable groundwater resources: a global-scale assessment, Environ. Res. Lett., 4, 035006, doi:10.1088/1748-9326/4/3/035006

FAO (2010) AQUASTAT – FAO's global information system on water and agriculture, FAO, http://www.fao.org/nr/aquastat

GOP (2000) Agricultural statistics of Pakistan. Ministry of Food, Agriculture and Livestock, Economics Division, and Govt of Pakistan, Islamabad

Gunatilaka A (2005) Groundwater woes of Asia. Asian Water, January/February

Hassan ZH, Bhutta MN (1996) A water balance model to estimate groundwater recharge in Rechna Doab. Irrig Drain Syst (10):297–317

Immerzeel WW, Beek LPH, Bierkens MFP (2010) Climate change will affect the Asian water towers. Sci 328:1382−1385

IWASRI (International Waterlogging and Salinity Research Institute) (1998) Integrated water resources management program for Pakistan. Economic, social and environmental matters. Internal Report 98/5, Lahore, Pakistan

Jurriens R, Mollinga PP (1996) Scarcity by design: protective irrigation in India and Pakistan. ICID Journal 45(2): 31–53

Kazmi SI, Ertsen MW, Asi MR (2012) The impact of conjunctive use of canal and tube well water in Lagar irrigated area, Pakistan. Physics and Chemistry of the Earth, Parts A/B/C 47-48: 86–98. doi:10.1016/j.pce.2012.01.001

Kijne JW (1999) Improving the Productivity of Pakistan's Irrigation: the Importance of Management Choices. International Water Management Institute: Colombo, Sri Lanka

Kundzewicz ZW, Mata LJ, Arnell NW, Döll P, Kabat P, Jime´nez B, Miller KA, Oki T, Sen Z, Shiklomanov IA (2007) Freshwater resources and their management. In: Parry ML, Canziani OF, Palutikof JP, van der Linden PJ, Hanson CE (eds) Climate change 2007: impacts, adaptation and vulnerability. Contribution of working group II to the fourth assessment report of the ıntergovernmental panel on climate change. Cambridge University Press, Cambridge, pp 173–210

Llamas MR & Martinez-Santos P (2005) Intensive groundwater use: silent revolution and potential source of social conflicts. ASCE Journal Water Resources Planning & Management 131: 337-341

Madramootoo CA (2012) Sustainable groundwater use in agriculture. Irrigation and Drainage 61: 26–33. doi:10.1002/ird.1658

Malmberg GT (1975) Reclamation by tubewell drainage in Rechna doab and adjacent areas, Punjab region, Pakistan. Geological Survey water Supply paper 1608-O. United States Government Printing Office, Washington, 1975

Mukherji A, and Shah T (2005) Socio-Ecology of Groundwater Irrigation in South Asia: An Overview of Issues and Evidence', in Selected Papers of the Symposium on Intensive Use of Groundwater, held in Valencia (Spain), 10-14 December 2002, IAH Hydrogeology Selected Papers, Balkema Publishers

Mustafa D, Akhter M, Nasrallah N (2013) Understanding Pakistan's water-security nexus. United States Institute of Peace, Peaceworks No. 88. ISBN: 978-1-60127-184-6

Plusquellec H (2002) Is the daunting challenge of irrigation achievable? Irrig. Drain. (51): 185–198

Postel SL (2003) Securing water for people, crops and ecosytems: new mindset and new priorities. Natural Resource Forum (27): 89–98

PWP (2011) Monsoon of Pakistan. http://pakistanweatherportal.com/ monsoon-of-pakistan/.

Qureshi AS, Akhtar M (2003) Effect of electricity pricing policies on groundwater management in Pakistan. Pak JWater Resour 7(2):1–9

Qureshi AS, Gill MA, Sarwar A (2010) Sustainable groundwater management in Pakistan: Challenges and opportunities. Irrigation and Drainage (59): 107–116. doi:10.1002/ird.455

Qureshi AS, McCornick PG, Sarwar A, Sharma BR (2010) Challenges and Prospects of Sustainable Groundwater Management in the Indus Basin, Pakistan. Water Resour Manag 24(8):1551–1569

Qureshi AS, Shah T, Mujeeb A (2003) The Groundwater Economy of Pakistan. IWMI working paper No. 19

Sarwar A (2000) A transient model approach to improve on-farm irrigation and drainage in semi-arid zones. PhD dissertation, Wageningen University, The Netherlands

Shah T, Burke J, and Villholth K (2007) Groundwater: a global assessment of scale and significance, in: Water for Food, Water for Life, edited by: Molden, D., Earthscan, London, UK and IWMI, Colombo, Sri Lanka, 395–423

Shah, T (2003) Governing the groundwater economy: comparative analysis of national institutions and policies in South Asia, China and Mexico. Water Perspectives, 1(1): 2–27

Siebert S, Burke J, Faures JM, Frenken K, Hoogeveen J, Döll P, Portmann FT (2010) Groundwater use for irrigation – a global inventory. Hydrology and Earth System Sciences 14, 1863–1880. doi:10.5194/hess-14-1863-2010Soomro, A.B. (1975). A Review of Problem of Waterlogging and Salinity in Pakistan. Master Thesis No. 915, Asian Institute of Technology, Bangkok, Thailand

UNCED (2002) Conservation and management of resources for development. United Nations Conference on Environment and Development. Joahannesburg Summit, 26th Aug-04th Sep, Agenda 21, Ch: 14- 18

UNDESA (United Nations Department of Economic and Social Affairs, Population Division) (2009) World Population Prospects: The 2008 Revision, Highlights, Working Paper No. ESA/P/WP.210. New York, UN

Usman M, Liedl R, Shahid MAM (2014) Managing irrigation water by yield and water productivity assessment of a Rice-Wheat system using remote sensing. Journal of Irrigation and Drainage Engineering. doi:10.1061/(ASCE)IR.1943-4774.0000732

Van der Velde EJ, Kijne JW (1992) Salinity and irrigation operations in Punjab. Pakistan: are there management options? Paper at Workshop on IIMI-India Collaborative Research in Irrigation Management (Lahore, IIMI)

World Bank (2007) Punjab Groundwater Policy – Mission Report. WB-SA-PK-Punjab GW Mission report, June 2007. www.worldbank.org/ gwma

Annexes

Annex A

List of publications

1. Usman M, Liedl R, Awan UK (2015) Spatio-temporal estimation of consumptive water use for assessment of irrigation system performance and management of water resources in irrigated Indus Basin, Pakistan. Journal of Hydrology. doi:10.1016/j.jhydrol.2015.03.031

2. Usman M, Liedl R, Shahid MA, Abbas A (2015) Land use / land cover classification and its change detection using multi-temporal MODIS NDVI data. Journal of Geographical Sciences 25, 1479–1506. doi:10.1007/s11442-015-1247-y

3. Usman M, Liedl R, Kavousi A (2015) Estimation of distributed seasonal net recharge by modern satellite data in irrigated agricultural regions of Pakistan. Environmental Earth Sciences. doi:10.1007/s12665-015-4139-7

4. Usman M, Reimann T, Liedl R (submitted) Test and application of different inverse methods for an inverse parameterization of a large scale groundwater flow model. Journal of Water Resources Management, Springer

5. Usman M, Liedl R (submitted) Assessing groundwater dynamics under future land use/land cover and climate change scenarios in irrigated Indus Basin, Pakistan. Journal of Hydrology, Elsevier

Article I

Usman M, Liedl R, Awan UK (2015) Spatio-temporal estimation of consumptive water use for assessment of irrigation system performance and management of water resources in irrigated Indus Basin, Pakistan. Journal of Hydrology. doi:10.1016/j.jhydrol.2015.03.031.

Download link: http://www.sciencedirect.com/science/article/pii/S0022169415002024

Article II

Usman M, Liedl R, Shahid MA, Abbas A (2015) Land use / land cover classification and its change detection using multi-temporal MODIS NDVI data. Journal of Geographical Sciences 25, 1479–1506. doi:10.1007/s11442-015-1247-y

Download link: http://link.springer.com/article/10.1007%2Fs11442-015-1247-y

Article III

Usman M, Liedl R, Kavousi A (2015) Estimation of distributed seasonal net recharge by modern satellite data in irrigated agricultural regions of Pakistan. Environmental Earth Sciences. doi:10.1007/s12665-015-4139-7

Download link: http://link.springer.com/article/10.1007/s12665-015-4139-7

Article IV

Test and application of different inverse methods for an inverse parameterization of a large scale groundwater flow model

Muhammad Usman, Thomas Reimann & Rudolf Liedl

Abstract

The subsistence of agriculture in Pakistan is not possible without significant use of groundwater (GW). Numerical modeling is an option to manage GW resources and to predict its behaviour under consideration of different scenarios. Calibration and validation are sensitive activities while evaluating groundwater resources with numerical models. Conventionally, calibration is performed by trial and error, eventually resulting in user dependent bias. The use of automated inverse methods allows efficient model calibration. This study employs PEST to calibrate a large catchment scale transient groundwater flow model built up with FEFLOW-3D. To demonstrate the effects of different calibration methods for such large catchment-scale models, a comparison of manual, zone based and state-of-the-art pilot point (PP) calibration was made. An advanced Tikhonov regularization algorithm was employed for carrying out the PP method using PEST. The results indicate that PP is more flexible and robust as compared to other approaches. Different statistical indicators show that this method yields reliable calibration and validation as values of Nash Sutcliffe efficiency (ME) are 0.976 and 0.969, % BIAS are 0.026 and -0.205 and root mean square errors (RMSE) are 1.23 m and 1.31 m, respectively. The results of output sensitivity suggest that hydraulic conductivity is a more influential parameter in the study area than drain/fillable porosity. Parameter error along with sensitivity demonstrates the strength/weaknesses of available field data. Different observation sensitivity plots highlight sensitive/insensitive regions for each observation point to guide planners to perform further field activities accordingly. Under considering the limitations of the current study, it is recommended to perform global sensitivity and linear uncertainty analysis for better certainty of modeling results.

Keywords: Groundwater, Sensitivity analysis, Pilot-point-approach, Tikhonov regularization, PEST, Inverse parameterization

1. Introduction

Groundwater supply is compulsory for the subsistence of agriculture in Pakistan. It is believed that about 40% of irrigation needs in Punjab, the main food producing province in the country, are met from groundwater (Kazmi et al., 2012; Shah et al., 2003). However, its

present unregulated and uncontrolled application is repleted with serious threats and consequences to water resources (Qureshi et al. 2010). Effects of ample use of groundwater can discern in form of declined water table in most of the canal commands in Punjab and Sindh provinces (Sarwar and Eggers, 2006; Kazmi et al. 2012). Rapidly falling groundwater levels are causing deterioration of its quality and lowering of crop yields against their potential levels (Qureshi et al. 2009), and hence need to be addressed by adequate management strategies.

Groundwater modeling could be a suitable tool to represent the natural groundwater flow in the environment and to predict the fate and movement of solutes and potential contaminants under natural or hypothetical scenarios (Zhou and Li, 2011). Such models can be used to predict the effects of groundwater abstraction and irrigation developments with regard to the aquifer and to simulate various water management scenarios (Barlow, 2005). Nevertheless, groundwater modeling involves a variety of data requirements, whereas poor data availability may lead to fallacious results.

The process of model calibration is mandatory for acquiring reliable modeling results from prediction models. A good model calibration ensures that residuals between measured and computed data are minimized and parameter uncertainties are low. This can be verified by subsequent model validation (i.e. run the model with data that are not used for calibration). According to Doherty and Johnston (2003), a good calibration should only be acknowledged under a wide range of hydrologic conditions. Model calibration can be broadly classified into (1) traditional manual calibration (Reilly and Harbaugh, 2004) and (2) automated calibration using inverse techniques (Doherty and Hunt, 2010). Historically and under consideration of the available computational power, model calibration was manually performed by adjusting model parameters with a more or less trial and error process. This approach has been widely used for several complex regional models, e.g. Refsgaard, 1997; Senarath et al. 2000; Blasone et al. 2007. However, manual calibration is time consuming, tedious and very subjective in nature (Madsen et al. 2002). The accuracy of results from this approach requires good experience of the modeler and thorough understanding of the system and is also characterized by the strategies employed to adjust the model parameters (Blasone et al. 2007). In recent times, manual calibration has been partly substituted by automated approaches, which are also recognized as nonlinear parameter estimation techniques (Doherty, 2003). The use of these techniques in groundwater modeling is now commonplace (Hunt et al. 2015; Bratefield and White, 2015; Black and Black, 2012), because of their high speed to determine best fit parameters, their low subjectivity in the calibration procedure and the availability of generic software that can be easily linked to different hydrological models. It is very likely that the results from automated calibration techniques may be better than from manual techniques along with the simultaneous possibility of carrying out sensitivity and uncertainty analyses (Bahremand and Smedt, 2007; 2010).

Despite the fact of advantages of automated calibration techniques, their application is still limited by a number of factors, which are well represented by Black and Black (2012) in the context of United Kingdom regional groundwater flow models. However, the concerns are common in many parts of the world especially where data sampling is not satisfactory. One possible reason is the limited computational capacity for regional models with distributed data inputs (Bahremand and Smedt, 2007). Moreover such models generally possess high spatio-temporal variability which causes enormous nonlinearity and high correlation between different model parameters. The result may be unrealistic model parameter distributions and also the calibration process descends into one local minimum without exploring other depressions (Abbaspour et al. 2001). This problem is pronounced in local search strategies as compared to global search strategies (Doherty and Johnston, 2003; Abbaspour et al, 2001). Nevertheless, computational costs are remarkably reduced by local strategies to explore objective function minima (Doherty and Johnston, 2003). According to Blasone et al. (2007), it is very difficult to conclude about the effectiveness and efficiency of both techniques as their performance varies with the intended use of a model.

Uncertainty may not only emerge from imprecisely known model parameters, but also from inadequate simplification of the real system. In particular, calibration of any groundwater model is based on some method of spatial parameter characterization or zonation. This usually implies to subdivide the model domain into different hydrogeological units based on geological properties and other evidence. Then uniform hydraulic properties are assumed for each zone (Yeh and Mock, 1996). This simplification means that values of hydraulic properties at any location are weighted averages of their true values over a large area (Black and Black, 2012). This use of discrete zones for hydraulic parameters may result in unnecessary structural uncertainties of the model system and, therefore, produce more unrealistic parameter values and also present geological heterogeneity in “unnatural” appearance (Doherty, 2003). An alternative approach can be the pilot point method (De Marsily et al. 1984), which interpolates hydraulic property values from a set of points distributed throughout the model domain (Doherty, 2003). The result is a smoother parameter distribution with reduced structural uncertainty as compared to conventional zone-based parameter assignment approaches. Nevertheless, the use of a larger number of pilot points could result in enhanced model run times. However, implementation of some advanced regularization technique like Tikhonov regularization (Tikhonov et al. 1995) can overcome this potential deficiency (Tokin and Doherty, 2005). Further, increase of hardware performance (e.g. multicore processors, incorporation of graphic card processors) could facilitate the application of inverse methods for groundwater modeling.

Model calibration either from manual or automated techniques does not guarantee full reliability of model predictions as groundwater flow and transport simulations are never closed systems and both independent and dependent variables of such systems are laden with

inference and assumptions (Oreskes et al. 1994). Parameter values obtained during calibration are only as realistic as the validity of the model assumptions and hence modeling is only a reflection of the real physical process (Muleta and Niclow, 2004; Gallagher and Doherty, 2007). Sensitivity analysis is a valuable tool to address uncertainties through identification of important model input parameters and to quantify the corresponding uncertainty in model output (Satelli et al., 2004). The results of sensitivity analysis are also important with regard to allocation of model sampling sites, better understanding of the modeled system, improvement of the calibration process, and thus, model validation and reduction of uncertainties (Lenhart et al. 2002; Hamby, 1994). Sensitivity analysis without utilization of automated techniques (i.e. manual variation of different input parameters one by one while keeping all other parameters unchanged) cannot truly reflect the real system behavior. This approach exhibits model responses under non-calibrated conditions because changes in only one parameter at a time while keeping other parameters fixed can bring the model to non-calibrated state. This dilemma is well tackled by the use of automated calibration approaches. Automated techniques perform the sensitivity analysis of different model input parameters one by one while keeping the model in the calibrated state (Doherty, 2002; Black and Black, 2012).

In the current study, the inverse parameter estimation tool PEST (Doherty, 2002) was used for the automated calibration and sensitivity analysis of a regional groundwater flow modeling in the irrigated agricultural region of Lower Chenab Canal (LCC), Rechna Doab, Punjab, Pakistan. This study aims to compare different model calibration techniques. Moreover, the use of some advanced regularization techniques for automated calibration methods is investigated. Detailed analyses about the sensitivity of model parameters are performed and areas of particular modeling importance are identified. Sensitivities of model results to different locations of observation points are also investigated and results are spatially presented for easy understanding. The arrangement of this manuscript is that the general information of the model region is described first; secondly, it presents the conceptual model and the theory of modeling approaches encountered and, finally, the presentation of results and necessary discussion on them is done.

2. Description of the study area

LCC, Punjab, Pakistan has been chosen as the study region (Fig. 1). The LCC irrigation system originates at the *Khanki* headworks which distribute water to its eastern and western parts through seven branch canals. This irrigation system was designed in 1892-1898 and its command area lies in Rechna Doab which comprises of the land mass between rivers Ravi and Chenab. The location of the area is between latitude 30° 36' and 32° 09' N and longitude 72° 14' and 77° 44’ E. The present study mainly focuses on the eastern part of LCC. Two link canals namely Qadirabad-Balloki (QB) and Trimu-Sidhnai (TS) flow from north to south and fall into river Ravi. Major part of LCC east lies in the districts of Faisalabad and

Toba Tek Singh. Administratively, the entire study area is split into 9 irrigation subdivisions: Chuharkana, Paccadala, Mohlan, Buchiana, Tandlianwala, Kanya, Tarkhani, Bhagat and Sultanpur. Irrigation subdivision is considered as the smallest management unit of the irrigation system in LCC. The structuring of these irrigation subdivisions ensures the equitable distribution of canal water among different consumers.

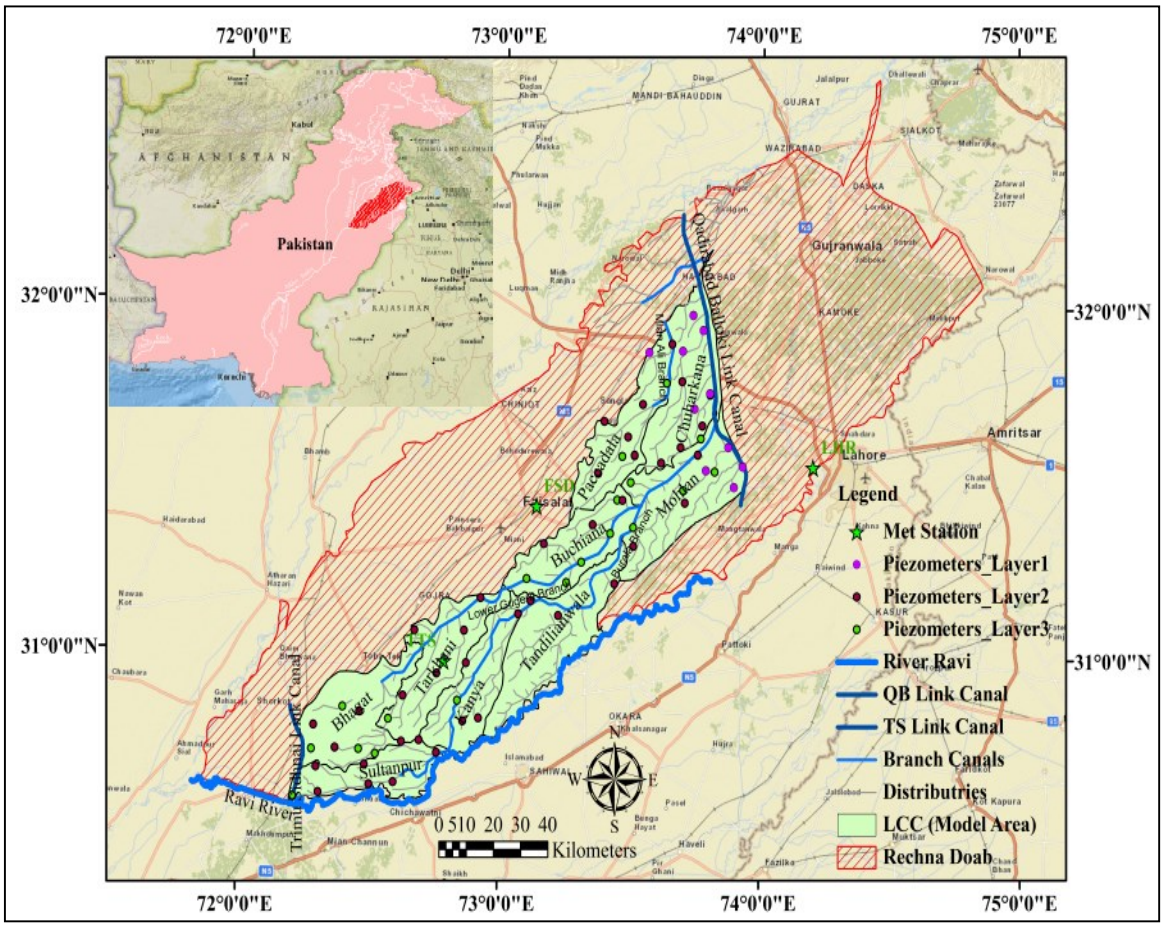

Fig. 1 Location and details of the study area

LCC is mainly categorized as agricultural area with a comprehensive irrigation canal network. Many different types of crops are grown throughout the year including rice, wheat, sugarcane, cotton, rabi fodder, kharif fodder etc. The whole cropping year can be subdivided into two seasons called kharif and rabi. The kharif season generally starts form May and ends in October, while the rabi season prevails from November to April. Rice and wheat are the two major crops during kharif and rabi seasons, respectively. The other crops cultivated during rabi season are rabi fodders (mainly barseem and oat), while cotton and kharif fodders (mainly sorghum, maize and millet) are grown in kharif season. Sugarcane is the annual crop which is cultivated in the months of September and February (Usman et al. 2012).

The climate of the area is arid to semi-arid. Four types of weather seasons are witnessed which include summer, winter, spring and autumn. The summers are hot and long

lasting with temperatures fluctuating between 21 and 50 ºC. During winters, daytime temperature ranges between 10 and 27 ºC, whereas night temperature may drop to zero. The average annual precipitation in Rechna Doab varies from 290 mm in the south-west to 1,046 mm in the north-east. Highest rainfalls occur during the monsoon period from July to September and account for about 60 % of average annual rainfall (Usman et al. 2012). There are three main weather stations in/near to the current study area operated by Pakistan Meteorological Department (PMD), which include Lahore (LHR), Faisalabad (FSD) and Toba Tek Singh (TTS).

3. Development of conceptual model

3.1. Processes

The conceptual model of LCC is shown in Figure 2. The model region is bound by two link canals on the eastern and western sides and along most of the southern side by river Ravi. The transport of water from river Chenab to river Ravi is necessary as water rights of river Ravi are provided to India under Indus Water Treaty signed between the two countries in 1960 and therefore it cannot cater irrigation needs of the region. The northern boundary of the model domain acts like inflow/outflow at different sections, which was generally identified and lateral flows were estimated by Darcy's law using piezometric data (Usman et al. 2015). Overall, the groundwater flow is parallel to this model boundary from north-east to south-west. LCC is comprised of a wide irrigation network which consists of main canals, branch canals, major distributaries and minor distributaries. The irrigation water to LCC is mainly supplied from Khanki headworks at river Chenab through the lower Chenab canal irrigation network. The transport of water through this irrigation network contributes a major recharge to groundwater at different stages of the system. The elevation of the region drops smoothly from north-east to south-west direction and causes regional groundwater flow movement along this elevation drop. A large area of LCC is sown under different crops which are irrigated by canal water along with the support of groundwater. As the cropping intensity in the model region is quite high and less rainfall is observed except during monsoon season, the share of groundwater to irrigation needs is quite high. The major share to groundwater recharge takes place from monsoon rainfalls and also from field percolation losses. The climate of the study area is mainly regarded as semi-arid with higher air temperatures which cause a major loss of irrigation water to atmosphere in form of evapotranspiration.

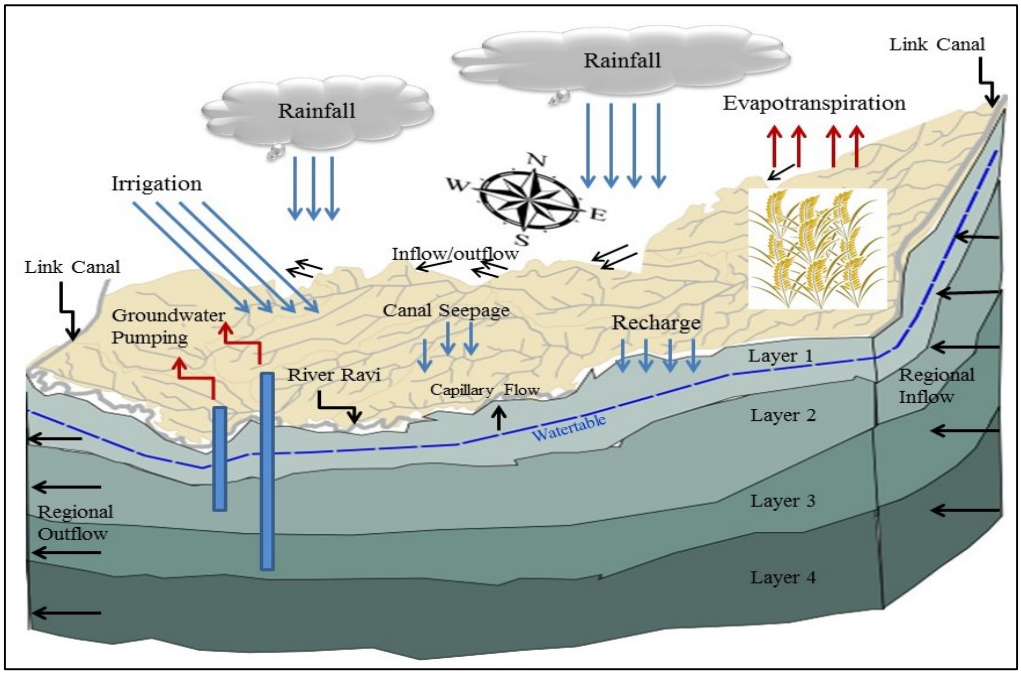

Fig. 2 Schematic diagram of the conceptual model

3.2. Hydraulic properties and geological scheme

The study area is part of an abandoned flood plain. The deeper part is formed by the underlying metamorphic and igneous rocks of Precambrian age. The area is underlain by highly stratified unconsolidated alluvial material composed of sands of various grades interbedded with discontinuous lenses of silt, clay and nodules of kanker, a calcium carbonate structure of secondary origin deposited by present and ancestral tributaries of the Indus River (Sarwar and Eggers, 2006). This forms the only one continuously interconnected aquifer and sediments at top mainly comprise of medium to fine sand, silt and clay. Soils of some area are fairly homogeneous containing high percentage of silt and fine to very fine sand whereas clay contents are higher in depression areas (Rehman et al. 1997). The origins of clay have not been identified specifically, but they are presumed to be the repeatedly reworked loess deposits of the hills at the north and northwest. Hydrogeological investigations in Rechna Doab were carried out during the 1957–1960 period wherein test holes were drilled throughout the Doab. Maximum thickness of alluvium is not accurately known although the logs of test wells show that thickness is over 150 m nearly everywhere (Fig. 3a). The alluvial complex is of heterogeneous nature and forms a fairly transmissive aquifer system.

Figure 3b illustrates the location of well logs in LCC, while Figure 3c indicates lithological details of selected well logs at different locations. They indicate that the thickness of the alluvium complex is relatively higher in lower parts compared with upper parts which contain small lenses of clay and gravel throughout the area. It shows that the aquifer is mainly composed of sand with deposits of clay, gravel and silt at different depths. However, there is no typical pattern in the arrangement of these materials. The material is highly porous and

is capable of readily storing and transmitting water. The horizontal permeability is an order of magnitude larger than the vertical (Bennett et al. 1967). The porosity of the water bearing material ranges from 35 to 45 % with an average specific yield of around 14 %. Khan (1978) has summarized the results of pumping tests and the lithological and mechanical analyses of test holes, according to which hydraulic conductivity varies from 24 to 264 m/day and specific yield values vary from 1 to 33 % in Rechna Doab.

(a)

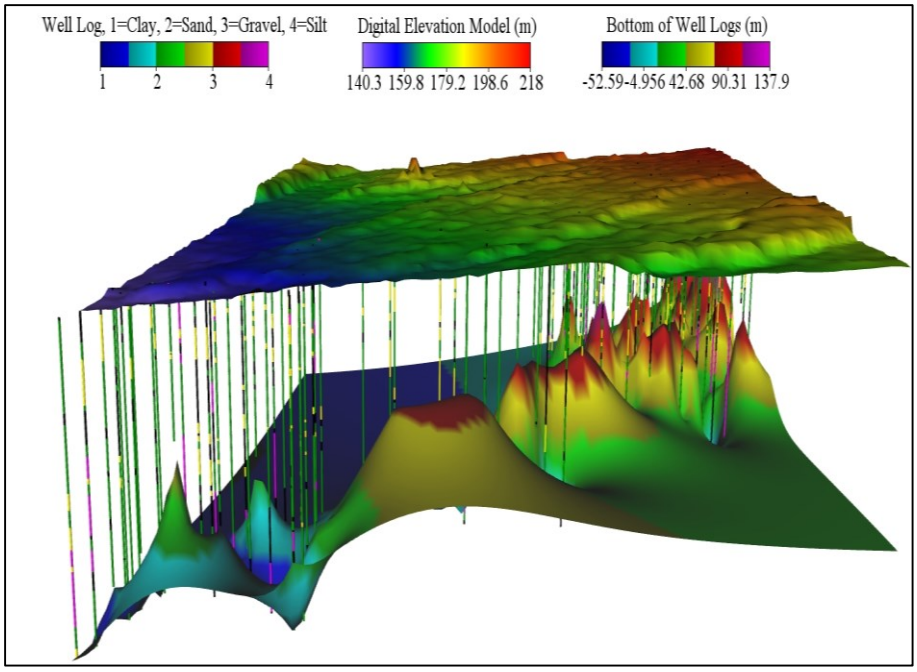

(b)

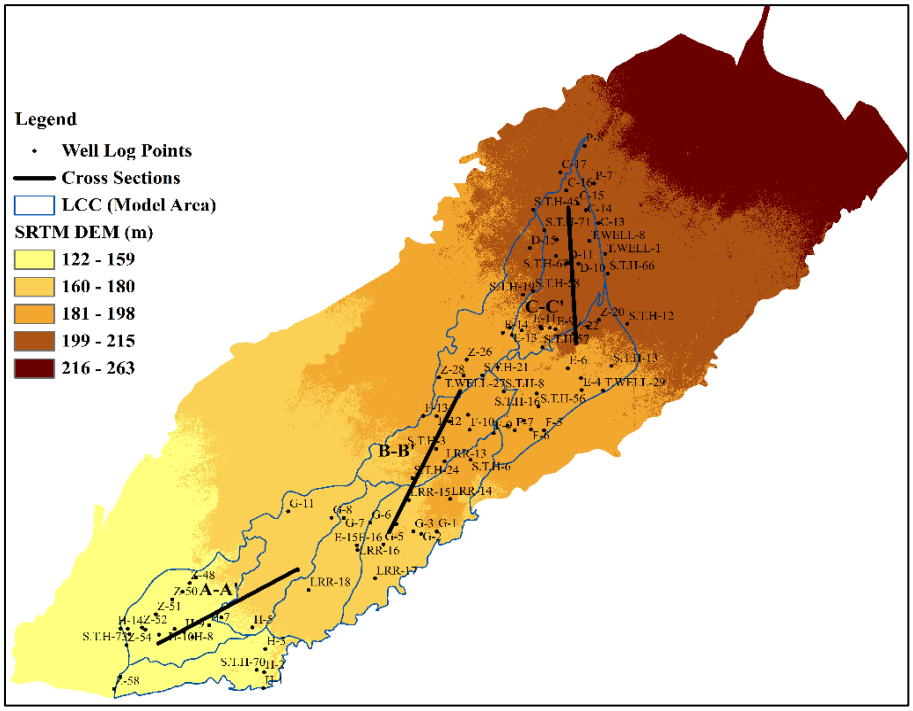

(c)

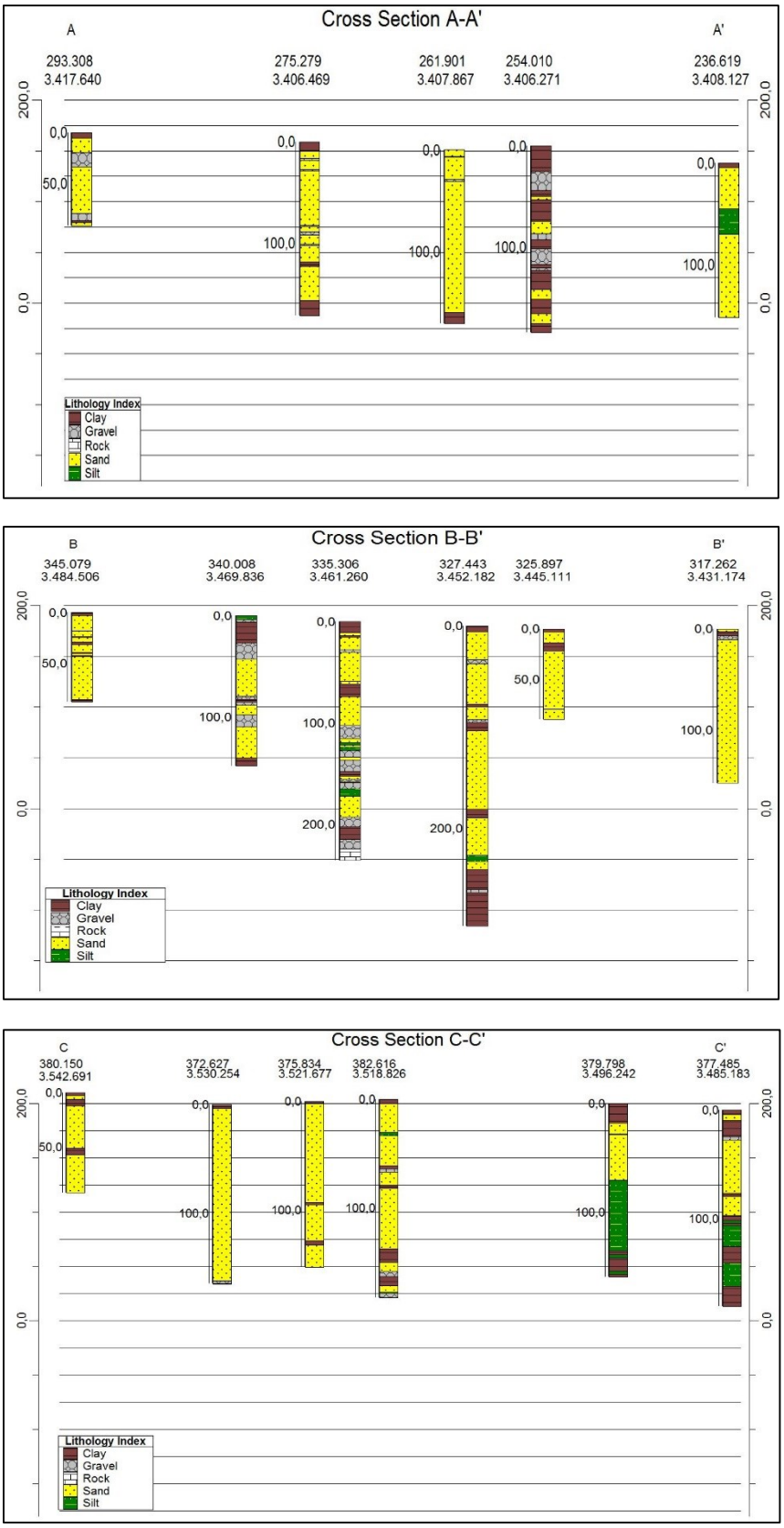

Fig. 3 (a) 3-D view of well logs (b) location of well logs and (c) lithological details of selected well logs at each X-section of LCC (Usman et al. 2015)

3.3. Data collection

3.3.1. Maps, shape files of natural features

The information about location and boundary of the model area is fundamental in the setup of any numerical model. The information regarding geometric features like boundaries of model area, rivers, canals, pumping wells etc., is generally required in form of shape files. These shape files were obtained from Punjab Irrigation Department (PID), Pakistan.

3.3.2. Elevation and well log data

For describing the geometry of the 3-D groundwater model, elevation data are required which were derived from a Digital Elevation Model (DEM) and from well log information. The Shuttle Radar Topography Mission (SRTM) digital elevation data of 90 m spatial resolution were retrieved cost free from the website of the Consultative Group for International Agricultural Research (CGIAR) Consortium for Spatial Information (CGIAR-CSI) (http:\\srtm.csi.cgiar.org) and well log data were collected from Salinity Monitoring Organization (SMO), Pakistan.

3.3.3. Material properties and model parameters

Piezometric water levels and river/canal gauges were attained from SMO and PID, respectively. The data of groundwater pumping and recharge were not readily available from any source and, hence, were estimated indirectly by utilizing different techniques described in detail by Usman et al. (2015). The major information about material properties in the saturated zone includes hydraulic conductivity, transmissivity, storativity, drain/fillable porosity etc. Soil texture details for different depth profiles were available from well-logs which were utilized to manipulate different hydraulic parameters against each material class (Freeze and Cherry, 1979).

4. Development of mathematical model

4.1. Theory of groundwater flow

The groundwater modeling system FEFLOW v6.1 (DHI-WASY, 2012) was used for the modeling procedure. FEFLOW has been successfully tested and applied in a number of benchmark studies around the world (Diersch, 2002). A 3-D finite element groundwater flow model is set up for the current study. The fundamental basis of FEFLOW is that it introduces the Darcy equation in the mass conservation equation to represent the mass conservation of any phase (Diersch, 2002):

$$\frac{\partial}{\partial t}(\varepsilon_\alpha \rho^\alpha) + \frac{\partial}{\partial X_i}(\varepsilon_\alpha \rho^\alpha V_i^\alpha) = \varepsilon_\alpha \rho^\alpha Q_\rho^\alpha \qquad (1)$$

where t is time [T], ε_α is volume fraction of α-phase [-], ρ^α is density of α-phase [ML^{-3}], X_i is Eulerian spatial coordinate vector [-], V_i^α is velocity vector of α-phase [LT^{-1}], Q_ρ^α is mass supply of α-phase [T^{-1}].

Further, the equation was modified for mass conservation of fluid:

$$\frac{\partial}{\partial t}\left(\varepsilon_f \rho^f\right) + \frac{\partial}{\partial X_i}\left(\rho^f q_i^f\right) = \rho^f Q_\rho^f \qquad (2)$$

The term q_i^f is known as the Darcy flux, and FEFLOW uses the following density-dependent formulation of the Darcy law (Diersch, 2002) to calculate this flux:

$$q_i^f = -K_{ij} f_u \left(\frac{\partial h}{\partial X_j} + \frac{\rho^f - \rho_o^f}{\rho_o^f} e_j\right) \qquad (3)$$

where K_{ij} is tensor of hydraulic conductivity of fluid phase [LT^{-1}], f_u is viscosity relation function [–], ρ_o^f is reference density of fluid phase [ML^{-3}], ρ^f is fluid density [ML^{-3}], and e_j is gravitational unit vector [-].

4.2. Setup of numerical model using FEFLOW

4.2.1. Mesh generation and setting of modeling problem

FEFLOW involves a number of steps to set up a groundwater model which includes designing of super-element-mesh, generation of mesh and setting of modeling problem. In super-element-mesh design, conceptual definition of geometry features of lines and points are included which is followed by mesh generation. For the current problem, the triangular mesh algorithm (Shewchuk, 2005) was selected owing to its fast speed and its capability to accommodate complex setups of polygons, lines and points. After refinement of triangular meshes, they were tested by Delaunay criteria for ensuring maximum stability of the model. Saturation case with projection of 3-D phreatic aquifer was selected as the problem class. Each mesh of the model domain contains three dimensions with six nodes per element. The total number of elements per layer and nodes per slice were 24,137 and 12,674, respectively. The whole aquifer was subdivided into 4 layers and 5 slices. The upper-most layer is set as phreatic which means a fixed slice topping an unconfined layer. The other slices are set as dependent and the bottom slice is declared fixed. Both steady and transient models were prepared and head results of the steady state model were utilized as initial conditions for the transient model. Constant and Adams-Bashforth time stepping schemes were used for steady and transient models, respectively. The Adams-Bashforth scheme is an automatic time step control scheme which gives easy convergence and stability to model runs. The PARDISO - Parallel Direct Solver (Schenk and Gärtner, 2004) was chosen for solving the equation system.

4.2.2. Regionalization of hydraulic properties

As there is no definite pattern in the arrangement of aquifer materials, the selection of a suitable regionalization method was crucial. The Akima interpolation algorithm (Akima,

1970) with linear interpolation type, with five neighbours and zero over/undershooting criteria was used for interpolation of parameters for the whole modeling domain. Interpolation was performed on presumably logarithmized values as this can lead to better regionalization results in case of log-distributed parameters such as hydraulic conductivity and drain/fillable porosity. Figure 4 depicts the distributed hydraulic conductivity in different layers along with information of maximum interior angles of mesh triangles and Delaunay criteria for the final model setup. Smaller angles of triangles are always considered better as they do not result in violation of Delaunay criteria. A triangular finite element violates the Delaunay criterion if the circumcircle of the triangle includes a node not belonging to the finite element. Delaunay-compliant triangulations maximize the minimum angle of all the triangles in the mesh; elements with large angles that are potentially leading to instabilities are avoided. Elements violating the criterion get a value of 1 in this parameter; triangles being consistent with the criterion have a value of 0.

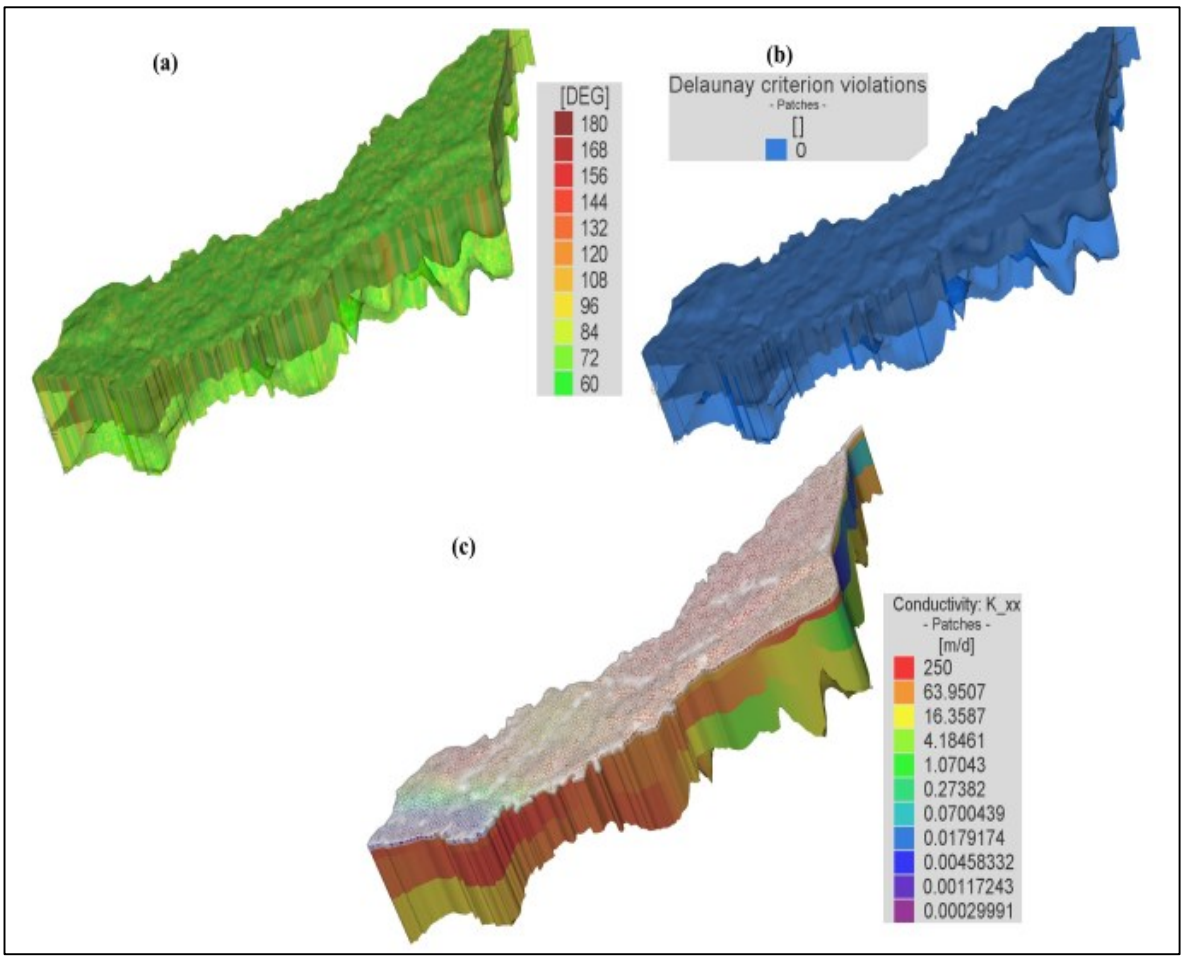

Fig. 4 (a) Representation of triangular mesh angles, (b) Delaunay criteria, and (c) distribution of interpolated hydraulic conductivity

4.2.3. Setting up different boundary conditions

Recharge is generally considered as a boundary condition for groundwater models but in case of FEFLOW, it is treated as a material property. As described earlier, recharge information was not available from any source. It was therefore estimated for a period from 2005 to 2012 by using different water balance approaches and by utilizing remotely sensed data. The prominent feature of such recharge is its estimation at a spatial resolution of 1 km x 1 km scale. The detail of each component of the water balance model and estimation of recharge can be read from Usman et al. (2015). The recharge is assigned as a time variant material property to the transient FEFLOW problem.

Prescribed head boundary conditions were assigned along the QB and TS link canals based on their historical water level record (Sarwar and Eggers, 2006). The gauge data for river Ravi were available only at headworks of Balloki and Sidhnai, however, the distance between them is quite long. Therefore, water levels in the course of the river were carefully worked out with DEM before their assignment to the model. First kind or Dirichlet type, time varying boundary condition was applied to river instead of Cauchy type boundary condition. The Cauchy boundary condition requires hydraulic conductance of river bed material and its geometry which was inaccessible from any source. Nevertheless, the flow in the river is not dynamically variable and it is also flowing at lower elevation in comparison to the model domain which could minimize the effects of this boundary condition along the lower model boundary. The other boundary conditions applied include Neumann boundary conditions mainly to the northern boundaries of the model and also to parts of the southern boundary which were not in contact with river Ravi. The inflow and outflow sections and flow to the model domain were identified using contours of piezometric water levels and by application of Darcy's law. The detailed methodology is accessible from Usman et al. (2015). The final boundary condition assigned to the model domain was for groundwater pumping which was assigned as nodal source/sink type boundary condition.

4.3. Model calibration and parameter estimation

4.3.1. Functionality of PEST for model calibration and parameters sensitivities

PEST (which is an acronym for Parameter ESTimation) software (Doherty et al. 1994; Doherty, 2002) is a model independent software for inverse parameter estimation and was used as a primary tool for optimization of the numerical model. The purpose of PEST is to assist in data interpretation, model calibration and predictive analysis (Doherty, 2002). PEST applies the Gauss-Marquart-Levenberg algorithm, which combines the advantages of the steepest descent method and the inverse Hessian method. This algorithm provides more efficient and faster convergence towards the objective function minimum (Doherty and Johnston, 2003).

The goodness of fit of model results to the observed data can be estimated and presented in form of residuals between measurements and simulated results. The sum of squares of these residuals is known as the objective function.

$$\Phi = \Sigma \left(h_i^{obs} - h_i^{sim}\right)^2 \quad (4)$$

where h^{obs} denotes an observation from field measurement and h^{sim} denotes its related simulation result.

Φ in groundwater models typically comprises of many different types of data, for instance, hydraulic heads, leakage rates or gauged flows (Brooks et al. 2014; Black and Black, 2012). The search algorithm used in PEST changes the model parameters until a minimum Φ is achieved. During PEST execution, the user observes two steps per iteration which include the derivative calculation and the adjustment of parameter values aiming to reduce the objective function. The parameter estimation process requires a set of model runs to calculate the sensitivity of the simulated values to changes in each variable parameter (Gallagher and Doherty, 2007). The details of these sensitivities are recorded in form of a matrix, known as Jacobian matrix. PEST carries out a number of optimization iterations by which it attempts to vary the parameter values to reduce the value of the objective function. The trialed changes made to any parameter are proportional to the respective sensitivity of the model results. Model runs are repeated with continuously updated parameters until no further improvement in model results can be obtained. The sensitivity matrix is recalculated at the start of each optimization iteration utilizing the former 'best' parameter set (Moore and Doherty, 2005). This process continues until it reaches either the user specified targeted objective function, the maximum number of optimization iterations allowed, or execution fails.

4.3.2. Pilot point calibration technique

The pilot point technique (de Marsily et al. 1984; Certes and de Marsily, 1991) defines parameters as a spatially variable distribution. In classical optimization approaches, the common assumption to each geologic formation is that it has spatially constant values, which is rarely true. To overcome this problem, the distribution of hydraulic properties within the model domain is described by a set of points at particular locations (the pilot points). A number of these pilot points are introduced to the model domain and PEST is asked to estimate the hydraulic properties of the aquifer at each such point by minimizing the objective function. These 'point-hydraulic-properties' are spatially interpolated in all active cells/elements within the model domain using kriging.

Individual pilot points can be assigned to different zones within the model domain. Only those points assigned to a particular zone can be used in calculating hydraulic property values throughout that zone by interpolation. Furthermore, the variogram can be different for each zone reflecting differences in the geology expected within each geological unit. Nevertheless, for the current problem each slice/layer of the model was treated as a single

zone for performing the interpolation. Figure 5 shows the location of each pilot point used in the present inverse model calibration, which was set up according to Doherty (2002; 2003).

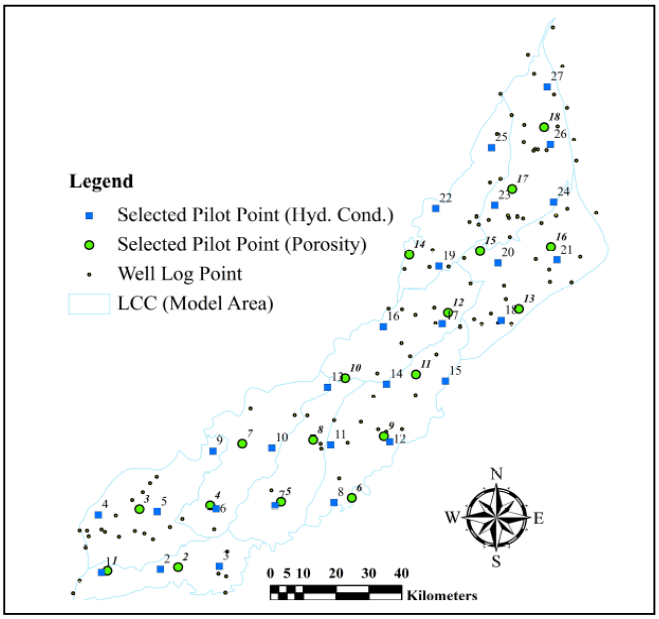

Fig. 5 Location of selected pilot points at different locations of LCC. Please note different locations of pilot points for hydraulic conductivity and drain/fillable porosity in a given layer but similar for each model layer

Conventional wisdom and the principle of parsimony dictate that the numbers of parameters involved in a parameter estimation process should be kept to a minimum. However, when using pilot points in conjunction with PEST's 'regularisation' mode, the opposite is often true. The use of pilot points in characterizing the spatial distribution of a hydraulic property must be accompanied by a mechanism whereby hydraulic property values assigned to pilot points are spatially interpolated. Kriging was used to accomplish the spatial interpolation. One of the benefits of kriging is that the factors by which hydraulic properties at pilot points are multiplied before summation to obtain the hydraulic property value are independent of the actual hydraulic property values at the pilot points. Hence a set of 'kriging factors' pertaining to each of the cells/elements can be calculated in advance of the actual interpolation process. The latter is undertaken again and again as the model is run repeatedly by PEST and it is therefore not necessary to repeat the calculation of the kriging factors within each model run. This can result in large saving of model run times to complete the overall parameter estimation process (Doherty and Hunt, 2010). The added advantage of using kriging is its further use for the regularization processes based on the same variogram as that to undertake kriging (Doherty, 2003).

4.3.3. Tikhonov regularization

Application of regularization helps to reduce non-uniqueness. For the current study, Tikhonov regularization is implemented in PEST as the numbers of estimation parameters are quite large (360 pilot points in total). The Tikhonov regularization involves a number of 'information' equations to define the initial values of the parameters; these equations can be defined by the user as prior information. The calibration process with Tikhonov regularization is formulated as constrained minimization process which minimizes the objective function to some user specified target. If this condition is not met, PEST minimizes the objective function without considering conditions specified by the user and in the meantime it adjusts weights to prior information. The use of prior information in PEST is quite sensitive especially for non-linear models (most models fall into this category), because specifying prior information usually results in parameter estimates that are close to values specified in the prior information (Liu et al. 2006).

4.4. Statistical analysis

In order to evaluate the performance of the FEFLOW model, statistical measures can be used to quantify the differences in the measured and calculated groundwater heads (Helweig et al. 2002). In the present study, coefficient of determination (R^2), root mean square error (RMSE), percent bias (PBIAS), and Nash Sutcliffe/model efficiency (ME) were used (Santhi et al. 2001; Usman et al. 2015; Nash and Sutcliffe, 1970).

$$R^2 = \frac{\Sigma(O-O_m)(S-S_m)}{[\Sigma(O-O_m)^2]^{0.5}[\Sigma(\mathrm{S}-\mathrm{S_m})^2]^{0.5}} \quad (5)$$

$$RMSE = \sqrt{\frac{1}{N}\sum_{\mathrm{i}=1}^{\mathrm{N}}(O_i - S_i)^2} \quad (6)$$

$$PBIAS = \frac{\sum_{i=1}^{N}(S_i-O_i)}{\Sigma O_i} * 100 \quad (7)$$

$$ME = 1 - \frac{\Sigma(O-S)^2}{\Sigma(O-O_m)^2} \quad (8)$$

where O is measured (observed) data; O_m is the mean of measured data; S is simulated data and S_m is the mean of the simulated data.

5. Results and discussion

5.1. Selection of calibration parameters and their initial values

The purpose of reliable calibration process is to develop a model which reasonably represents groundwater flow, recharge, and discharge, and reasonably matches observed water levels (Brooks et al. 2014). The specifications of the optimization algorithm in PEST include model parameterization, the selection of parameters and defining their feasible range, assigning prior information to parameter groups and assigning weights to observation groups (Bahremand and De Smedt, 2007). There is no rule of thumb about decision on parameters for performing calibration, and finalization of calibration parameters is purely dependent on

the modeling situation and available data. For example, according to Kim et al. (2004), potential primary calibration parameters include hydraulic conductivity and storativity for groundwater flow modeling, whereas for Sarwar (1999), the adjustment parameters include drainage depths and recharge rates for areas similar to LCC.

Model calibration in limited meanings is the adjustment of model parameters for the purpose to bring observed and simulated heads close enough. But in broader meanings, parameter modification is only one aspect of model calibration and key aspects, such as the conceptualization of the flow system that influence the model capability to attain the problem objective function, also are evaluated during the calibration (Reilly and Harbaugh, 2004). Principally, there is no limit for the number of calibration parameter types but it is noticed that if some parameters are used with wrong limitations then it may still result in the best match to observations. This indicates potential deficiency in model conceptualization (Reilly and Harbaugh, 2004). Therefore, both the closeness between the observed and simulated conditions and the extent to which important aspects of simulation are incorporated in the model are important in evaluation of model calibration. For the same reason, the number of calibration parameter types in the current modeling study is kept low. Some dynamically spatio-temporally variables like groundwater recharge, and groundwater pumping along with lateral inflow/outflow were estimated through separate approaches with fair reliability (Usman et al. 2015; Article IV), and they were not considered as calibration parameters. Hydraulic conductivity and drain/fillable porosity were only selected as primary calibration parameters. According to Reilly and Harbaugh (2004), most models that are used to understand the past, understand the present, or to forecast the future are calibrated by matching observed heads. Both of the hydraulic conductivity and drain/fillable porosity were log transformed in accordance with the fact that most studies cited in the groundwater literature, which treat these parameters as regionalized variables, indicate that their distribution is better described by a log variogram (Awan et al. 2015).

Any initial model parameter values can be used for automated optimization operation, nevertheless model fitting may be performed under untrue parameter values as compared to real situation and thus it can affect both optimization and sensitivity analysis. Therefore, for both automated and manual calibration processes, site characterization information was used as described by Young et al. (2010). In the first phase, the model was calibrated manually in steady state. The groundwater levels of October 2005 were used as initial condition for executing steady state calibration. The values of hydraulic conductivity are adjusted to bring calculated heads close to observed heads. Different statistical indicators show reasonable agreement between calculated and observed heads as R^2, ME, RMSE and correlation coefficient are 0.99, 0.98, 1.58 m and 0.98, respectively. For automated calibration, parameter values from manual calibration (modeler's pre-calibration expert judgment) were used as initial conditions in transient simulations as suggested by Reilly and Harbaugh

(2004). Figure 6 (upper half) shows the distributed initial hydraulic conductivity and drain/fillable porosity utilized in the pilot point optimization at head, middle and tail reaches of the 3-D groundwater model. For zone-based parameterization, separate zones were demarked for each model layer and distributions of initial hydraulic conductivity and drain/fillable porosity for this case at three model locations can be seen from Figure 6 (lower half). The parameter bounds were set for both hydraulic conductivity and drain/fillable porosity for all pilot points and zones. The values for horizontal hydraulic conductivity ranged between 10^{-6} m.day^{-1} and 300 m.day^{-1}, and for vertical hydraulic conductivity between 10^{-7} m.day^{-1} and 30 m.day^{-1}. Similarly, the values for drain/fillable porosity ranged from 0.009 to 0.250.

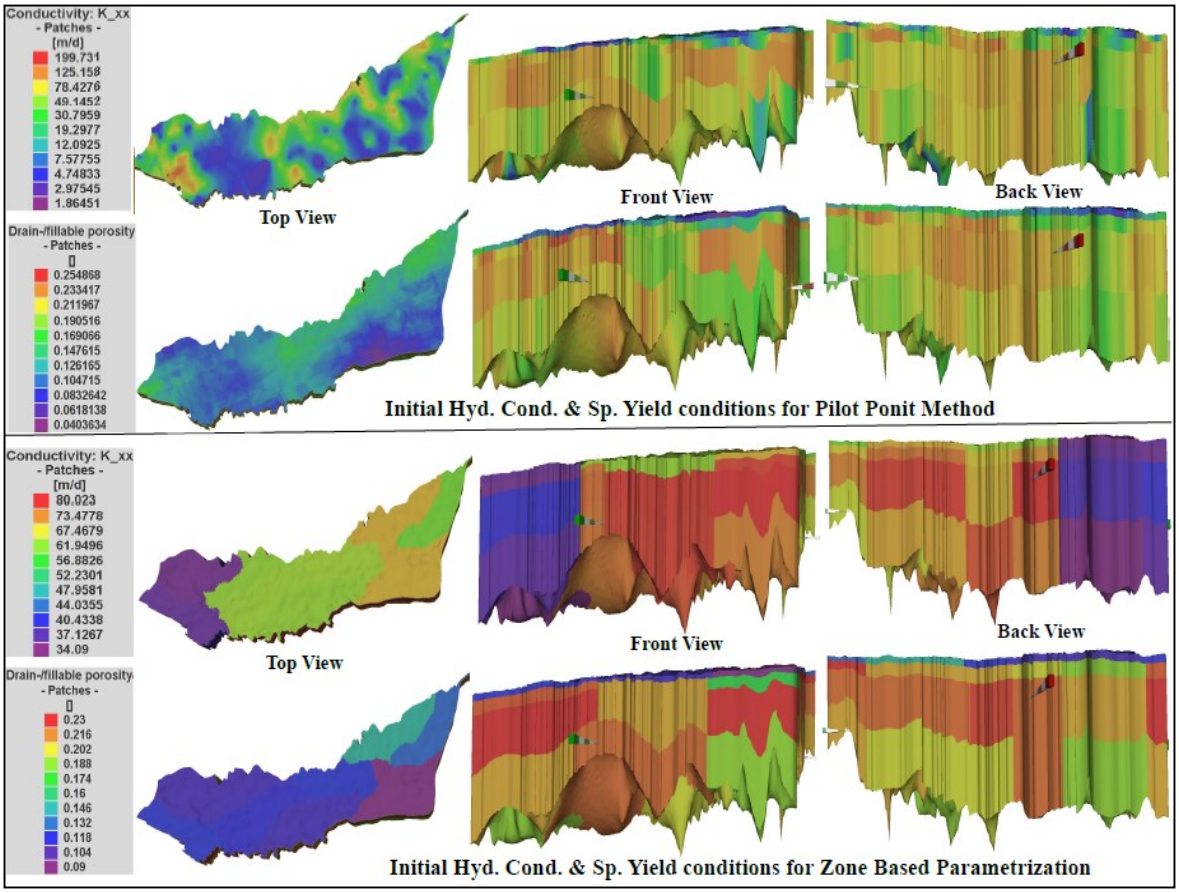

Fig. 6 Representation of initial parameter values for hydraulic conductivity (top) and drain/fillable porosity (bottom) for Pilot Point and Zone Based parameterization for different model views

A Parameter List Processor (PLPROC) (Doherty, 2015) was used for undertaking kriging interpolation of pilot points. This processor serves as a parameter preprocessor for complex numerical models, which do not necessarily use rectangular grids.

5.2. Calibration and validation results for transient model

Figure 7 demonstrates the development of the objective function with each iteration of automated optimization. About 585 observations of groundwater head were used for controlling the calibration process of the transient model. The objective function, which is here explained by the elements containing heads with equal weights, was decreased from 30932 m^2 to 1837 m^2 for pilot point optimization. In the initial phase, the decrease in objective function was greater but as the optimization process advanced, lower changes were observed. PEST estimates the best parameter values by minimizing the sum of squares of the differences between measured and simulated heads.

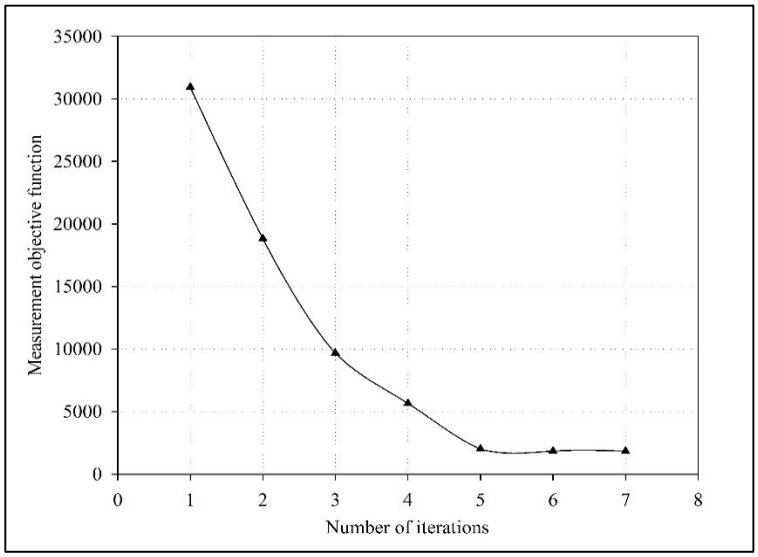

Fig. 7 Development of measurement objective function (m^2) with each PEST iteration

The performance of the groundwater model was evaluated by comparing the groundwater heads simulated by FEFLOW with measured heads. The data of the cropping seasons from winter 2005 (post monsoon) to winter 2008 (post monsoon) were utilized for model calibration. Both simulated and measured heads were calculated from the mean sea level (requirement of FEFLOW- 3D model). The simulated and measured heads were drawn on a scatter plot (Figure 8(a)). The majority of the points fall on/near to the main diagonal which indicates that the model was calibrated successfully. Figure 8(b) represents the spatial comparison between simulated and measured heads for two different simulation times. At most of the locations the two heads are quite close except for some regions in the northern parts of the study area. The possible reason for this relatively high difference could be due to the large number of tubewells in this region, which extensively pump groundwater especially for rice cropping. Therefore, the possibility of occasional partial inflow through boundaries of the study area could not be well represented by the inflow/outflow boundary conditions. Similar types of modeling results were also reported by Sarwar and Eggers (2006) in similar areas. Different error parameters including R^2, ME, PBIAS and RMSE indicate reliable calibration results. The value of R^2 for model calibration is 0.99. Similarly, ME, which is an

indicator of efficiency of calibration, is 0.976. This value indicates that deviation of simulated heads from measured heads is only 2.2 %. The value of PBIAS is only 0.026 whereas the RMSE of the simulated heads from measured ones is 1.23 m.

Following successful calibration, the model was validated for the groundwater data set for cropping years from summer, 2009 (pre monsoon) to winter, 2011 (post monsoon). The 1:1 chart for model validation is presented in Figure 8(c). Same statistical measures as used for calibration were employed for validation of simulated results. The value of ME is 0.969 which indicates that deviation of simulated heads from measured heads is only 3.0 %. The values of PBIAS and RMSE are -0.205 and 1.31 m, respectively, pointing towards reasonable results from the initially calibrated transient model. It is to note that all of the comparison results presented herein were achieved by pilot point optimization.

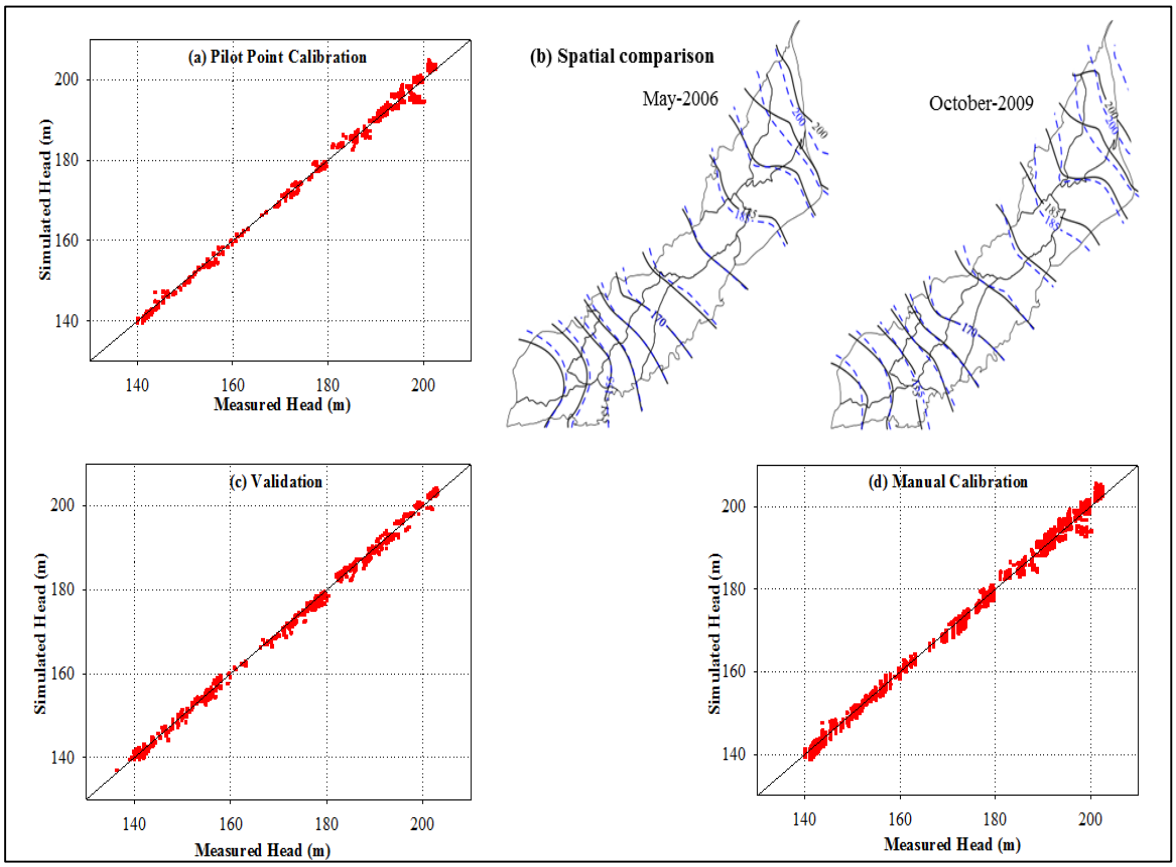

Fig. 8 (a) Scatter plot for pilot point calibration, (b) spatial comparison between simulated and measured heads, (c) validation of model results, and (d) manual comparison between simulated and measured heads

5.3. Comparison of calibration results from different methods

Apart from the calibration of the groundwater model by the pilot point method, comparisons with conventional manual calibration and automated zone-based calibration were also performed. For zone-based calibration, the whole model domain was distributed into nine zones (Fig. 6, model top view) based on localized knowledge of hydraulic material properties. The

decision about the number of zones for this approach is more or less subjective and based on the modeler's experience about the studied problem. Similar zones were demarked for each model layer which summed up to 36 zones in total for the current modeling problem.

The results of the manual calibration for the steady state model have been presented in the previous sections and the same model was extended to transient state for both manual and automated optimizations. Both manual calibrated, steady and transient, models showed relatively weak results in comparison to automated optimizations (Fig. 8d) as relatively higher error is observed for them. The statistical indicators, R^2, ME, PBIAS and RMSE, yielded values of 0.98, 0.964, 0.73 and 1.68 m, respectively, for manual calibration of the transient model. It is also to be noted that the manual calibration process of the transient model proved to be very subjective and cumbersome which resulted in poor calibration of some model regions. For example, the simulations were run for about 45 times before the model was considered calibrated. Awan et al. (2015) reported that they had to run the groundwater model for about 80 times to bring the difference between simulated and measured heads within 0.5 %. According to Sarwar (1999), it is common to make model runs from 20 to 50 times before an acceptable calibration is reached. It is also found that model calibration in one particular model region could have brought major changes between measured and simulated heads in other regions, which resulted in difficulties in calibration. Nevertheless, manual calibration was necessary to perform in advance of automated calibration because of the reason that local minima could be located due to non-uniqueness of non-linear models by automated calibration and also the number of iterations could be reduced remarkably to find minimum measureable objective function (Bahremand and Smedt, 2007).

The comparison of different calibration methods is also presented for a number of piezometers at different locations of the modeling domain in order to investigate their performance spatially. Hydrographs of 6 different piezometers, two each at head, middle and tail reaches of the modeling domain are presented in Figure 9. These piezometers are selected in a way to represent the whole model behavior as locations of different piezometers are near to different boundaries of the modeling system like link canals, river, inflow and outflow boundaries. From the trends of these hydrographs, it is clear that pilot point calibration always yields better results than both manual and zone based calibration. The differences of heads between manual calibration and pilot point calibration were relatively higher in upper model regions as compared to lower model regions. This could be mainly due to the possibility of occasional partial inflow/outflow from this region due to more pumping as described earlier. The descent of residuals of piezometric heads was quicker in lower model regions as compared to upper regions, which is another indication of previous statement. This also indicates that the model was well constructed especially for these regions. Similarly, the differences between hydrographs of measured and zone based calibration were relatively larger

at upper model locations. The possible reason for this could be that the use of zones of uniform hydraulic property values can be unsatisfying. Geological maps were utilized for this purpose, but there are many instances where these maps rarely help, as geological boundaries are approximately known (Doherty, 2003). Furthermore, the areas colored same on these geological maps do not necessarily possess similar hydraulic properties. For instance, in the current problem the zones are mainly described based on the irrigation subdivisions which were redefined frequently for different model trials but, due to larger heterogeneity of aquifer material especially in upper model regions, no final combination with best results was achieved. The best calibration of the model could have been possible if the hydraulic parameter bounds especially for hydraulic conductivity were set even higher as the values of present upper bounds. Nevertheless, it would have been far away from reality.

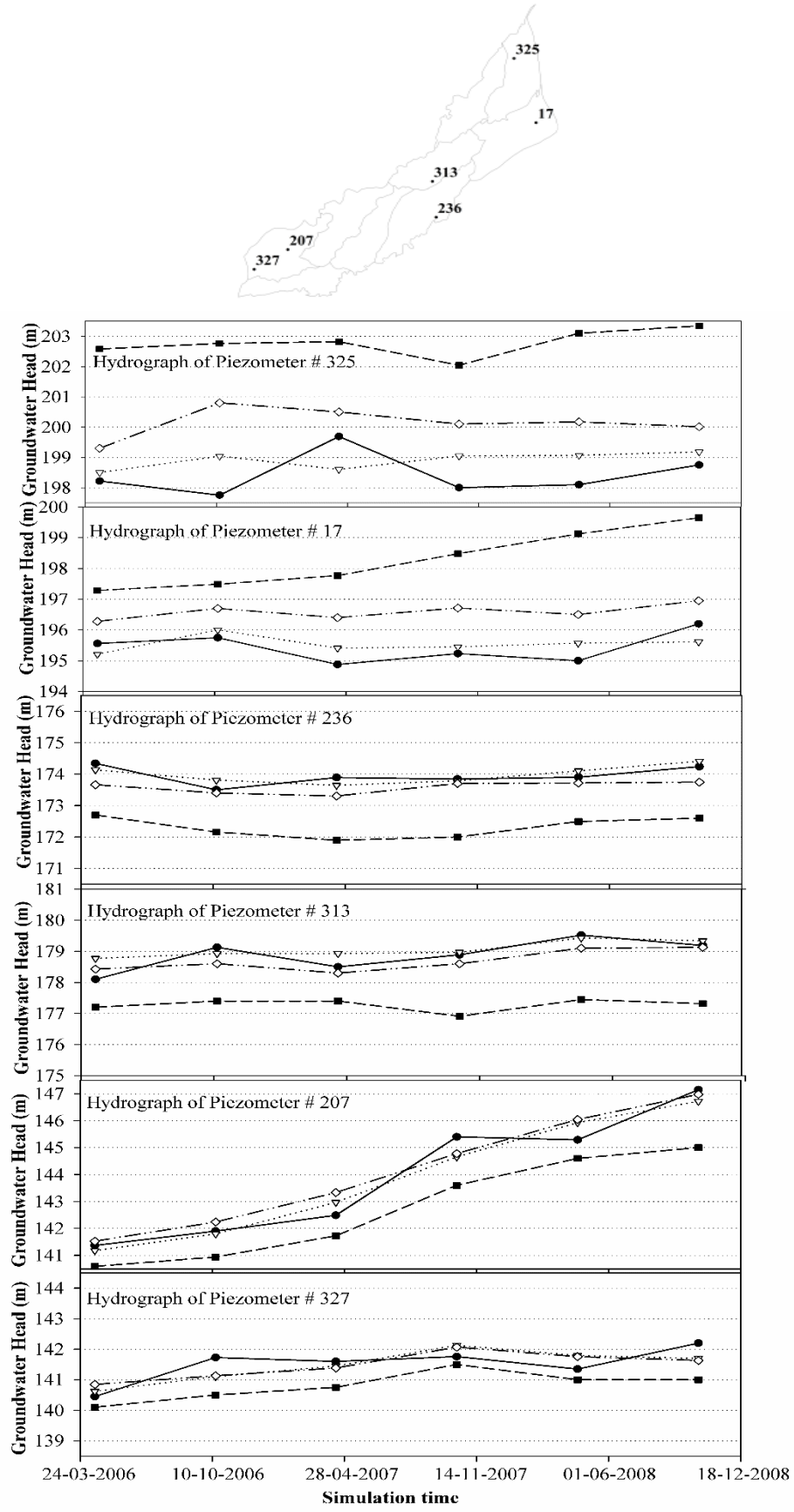

Fig. 9 Hydrographs of selected piezometers at different model locations for comparison of different calibration techniques

The calibration at model locations near to the river (i.e. piezometer #236, Fig. 9) was difficult by the manual approach but better calibration results were achieved by both automated techniques. It is reported by Usman et al. (2015) that the current study area receives its major recharge during summer seasons due to more monsoon rainfalls. In winter seasons, both rainfall and canal flows decrease yielding low recharge in major parts of LCC. This phenomenon is well represented from the trend lines of measured heads which show an increase in height after the summer seasons and falling trends after winter seasons. Both the pilot point and zone based automated calibration depicted this increasing/decreasing trends which is found missing in case of manual calibration. The difference between automated pilot point and zone based calibration techniques is observed relatively less in lower to middle reaches of the model domain.

5.4. Model parameter sensitivities and parameter error

A very useful feature of PEST optimization is automatic robust sensitivity analysis. This sensitivity analysis is useful for user intervention to optimization as it helps the modeler to understand which model parameters are more influential and which are less influential and can be set to fixed values. The sensitivity outputs are easily available from PEST output files and are useful for guiding the calibration process through exclusion of non-influential parameter and thus to avoid failing of PEST.

The PEST sensitivity analysis facilitates the modeler by allowing him to automate the tedious task of adjusting certain model inputs, running the model, reading the output of interest, recording their values, and then commencing the whole cycle again. According to Bahremand and Smedt (2007), the results of PEST sensitivity analysis should be carefully interpreted, as the dimensionless scaled sensitivities depend on the parameter values and different initial parameter value sets lead to different model results (Hill, 1998). Moreover, some parameters, which seem to have rather low influence, may be correlated with some other parameters and are not properly evaluated by sensitivity statistics (Madsen et al. 2002). PEST calculates a figure related to the sensitivity of each parameter with respect to all observations and lists the composite sensitivity to each parameter of all observation groups, as well as of each individual observation group. The composite parameter sensitivity of each observation group can be evaluated by calculating the magnitude of the respective column of the weighted Jacobian matrix with the summation confined to members of that particular observation group. The magnitude is then divided by the number of members of that observation group which have non-zero weights (Doherty, 2002).

The sensitivities of all pilot points in different model layers were estimated for all parameters. Figure 10 shows only the results for selected pilot points to facilitate visibility and representation of the results. However, the complete results are submitted as a supplemental material in Annex B. Overall, sensitivity with respect to hydraulic conductivity is higher than for drain/fillable porosity. The sensitivity of model output to model parameters

is found higher in most of the north-eastern parts in comparison to other model regions. It is even higher in 1st and 4th layer of the model domain. For lower model regions, sensitivity with respect to hydraulic conductivity is higher for 3rd and 4th model layer. In case of drain/fillable porosity there is no significant variation in sensitivity for different regions of the model domain, especially for 2nd and 4th model layer. Nevertheless, sensitivity is relatively higher for upper regions in the 1st model layer and for lower regions of the 4th model layer. The spatial information of sensitivity of model output could be useful for further decision about conducting data collection campaigns and to investigate impacts of abstraction in these areas (Black and Black, 2012). It might also be an indication of problems with model setup for such areas if parameter values have reached their upper bounds. Nevertheless, this is not a case for the current modeling setup.

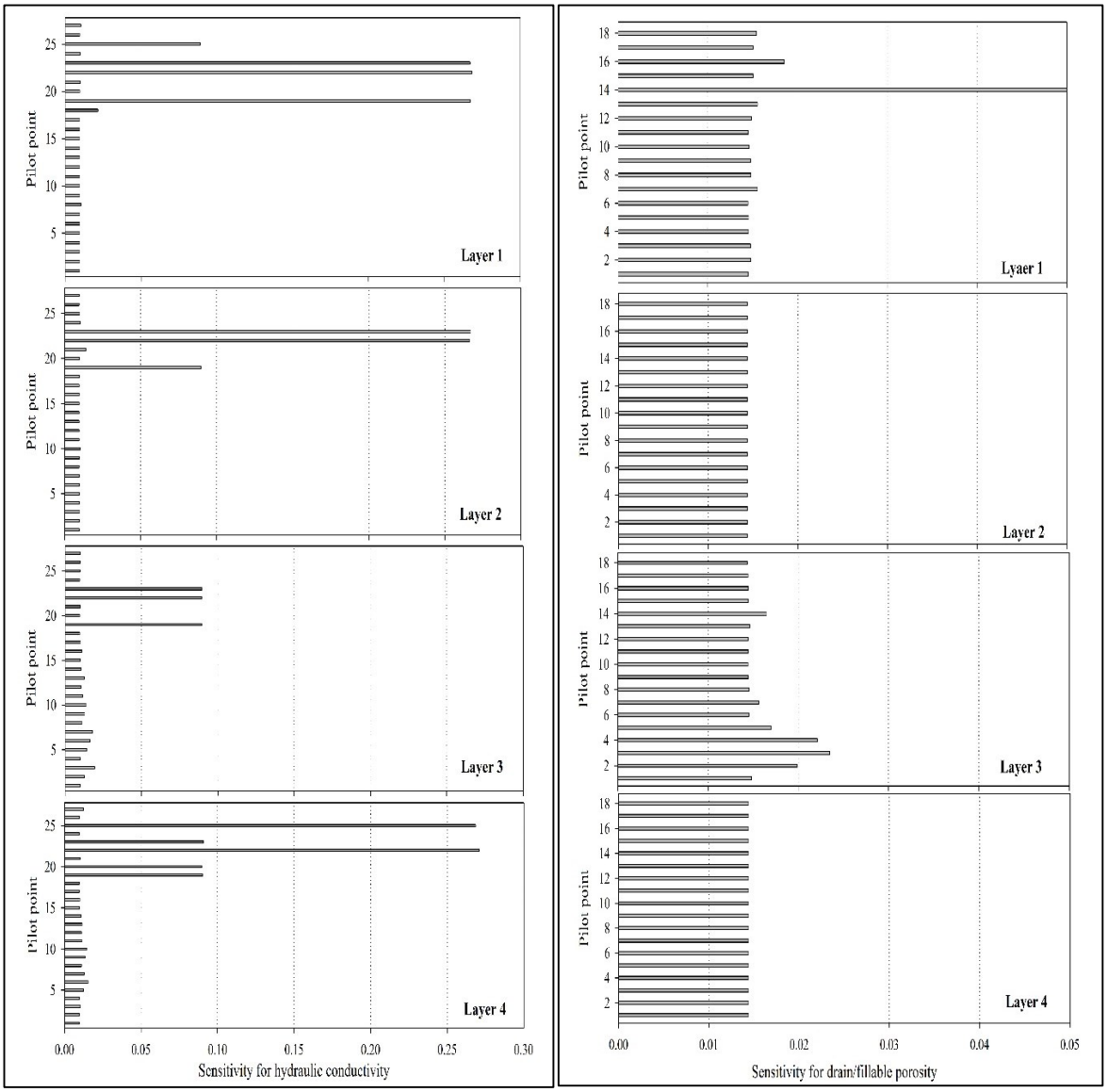

Fig. 10 Sensitivity with regard to hydraulic conductivity and drain/fillable porosity for selected pilot points in different model layers. (Please note different scales for both plots)

It is also imperative to investigate the sensitivity results in accordance with parameter error results as the understanding of parameter influence is also critical to identify which parameters are not well defined by the observation data and user knowledge input to PEST (Black and Black, 2012). Such analysis can help the modeler to identify regions where current field information is not sufficient and where future data assessment should take place in order to have better parameter data. The parameter error is calculated as the difference between initial and optimized parameter values divided by the initial value. For the current modeling problem, parameter error for hydraulic conductivity and drain/fillable porosity were estimated for all model layers which are provided as supplemental material in Annex B. Figure 11 shows the parameter error only for selected layer. The evaluation for hydraulic conductivity showed that both sensitivity and parameter error are found higher in model layers 1 and 2 for pilot points in regions A, B and C (Fig. 11 for parameter error of hydraulic conductivity in first model layer). When this information is incorporated with model layer thickness at such locations then it can guide researchers to assess whether further field investigations need to be performed (e.g. preferred pumping test site, drilled well logs etc.). Figure 11 is also marked with another region 'D' where the parameter error is high but the sensitivity of model output is not. This suggests that, as the model is not very sensitive to parameter changes in such regions, there is very less potential of improvement in model results with further field investigations. Contrary to this, there are some regions in the 4th layer (upper model locations) where model sensitivity is quite high but for this case the parameter error is low. This also guides researchers to expect less improvement in current modeling results with further field investigations at these locations. Another case is about moderate values of parameter error and model sensitivity for model layers 3 and 4. In this case, improvement in model results is possible but the decision about further field data collection is all about the purpose for which the model is constructed and of course on availability of sufficient funds.

The higher sensitivity of parameters for upper model regions is attributed to the nature of groundwater flow through the model domain. As described earlier, the sensitivity with regard to porosity is generally not very high and less variable throughout the model domain which is also accompanied by lower parameter errors. From the results of automated optimizations, it is obvious that equally good calibration of the model could be achieved from different parameter values due to model nonlinearity, model uncertainty and higher correlation between model parameters (Doherty et al. 1994). The problem is more pronounced for distributed models alike. However, this issue was tried to be countered by carefully applying available field knowledge in selection of suitable initial parameter values. In many real modeling studies, it is quite usual that no evidence of initial parameter values is available for such situations. Consequently, it is a duty of the modeler to present multiple models which exhibit equally good results to predict scenarios related to decision making

about aquifer management. The right conceptualization of modeling environment would also be valuable in this regard.

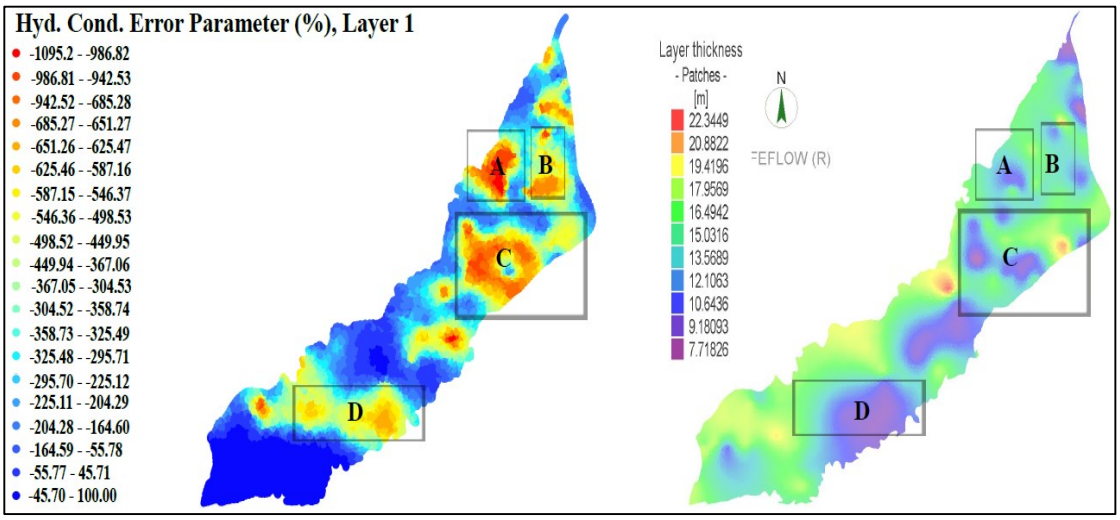

Fig. 11 Distribution of parameter error for hydraulic conductivity and thickness of first model layer

5.5. Sensitivities at selected observation points

In the last section, we have demonstrated the results for parameter sensitivity analysis and demarked the regions where changes in the parameters have strong/weak effects on the model optimization. We have also evaluated the deficiencies of given field information by utilizing sensitivity and parameter error to support future data assessments for further model improvements. However, in many cases engineers need information on some local scales which demand construction of local models with finer spatial discretization. For such models, generally, there is a need of more detailed field data which results in additional hydraulic tests. The decision about locations of such tests is crucial, both because of required time and money. The knowledge gained form sensitivity analysis performed from this particular study could help researchers to decide about important sites for conducting field assessments and to establish a successful model.

PEST estimates and keeps record of the sensitivities for different observation points in the Jacobian matrix. An independent utility named 'JROW2VEC' is utilized to extract this information from the Jacobian matrix for different individual observation points. According to Doherty (2002), observation sensitivity is generally of less use. But if the general flow behavior is not drastically variable in time and / or space then this information could be quite useful. In principle, sensitivity for all observation points could be deduced from the Jacobian matrix but for the simplicity of the results it is presented only for few observation points (22, 238, 242, 211 and 303), which are located at different parts of the model region. Corresponding plots are quite informative due to their spatial representation of sensitivity

results. Positive sensitivity values in such maps reflect the tendency of an increasing hydraulic head with decrease in values of hydraulic parameters and vice versa.

For instance, Figure 12(a) shows the sensitivity for observation point 22, which depicts that major regions of the model domain are not very sensitive to hydraulic head at this point but there are fragmented locations which show strong sensitivity either positive or negative at this observation point at all three different simulation times. Similarly, sensitivity distribution for observation point 242 can be observed from Figure 12(c). This shows a very clear trend of sensitivity distribution as majority of the model parts upstream of this location show positive sensitivity. It means if any hydraulic activity is to be performed at/near to this point; it should contain very good data about hydraulic properties in high sensitivity zones. The sensitivity distribution for observation point 211 (Fig. 12d) has very clear information as two different behaviors of sensitivity can be observed both upstream and downstream of this location. Majority of the nearby downstream locations exhibit very high negative sensitivity and majority of upstream location have weak to normal positive sensitivity. This suggests that downstream areas need to be properly investigated for hydraulic properties if any hydraulic activity is to be conducted at this location. The sensitivity distribution for observation point 238 does not show consistent results for all simulation times which means that flow trends at this location are variable from time to time and such locations can be identified by opposite arrow directions in Figure 12(b). For such locations, the information of observation sensitivity is not very useful. The sensitivity distribution and demarcation of important location for each particular region for rest of the selected observation points can be seen from Figure 12.

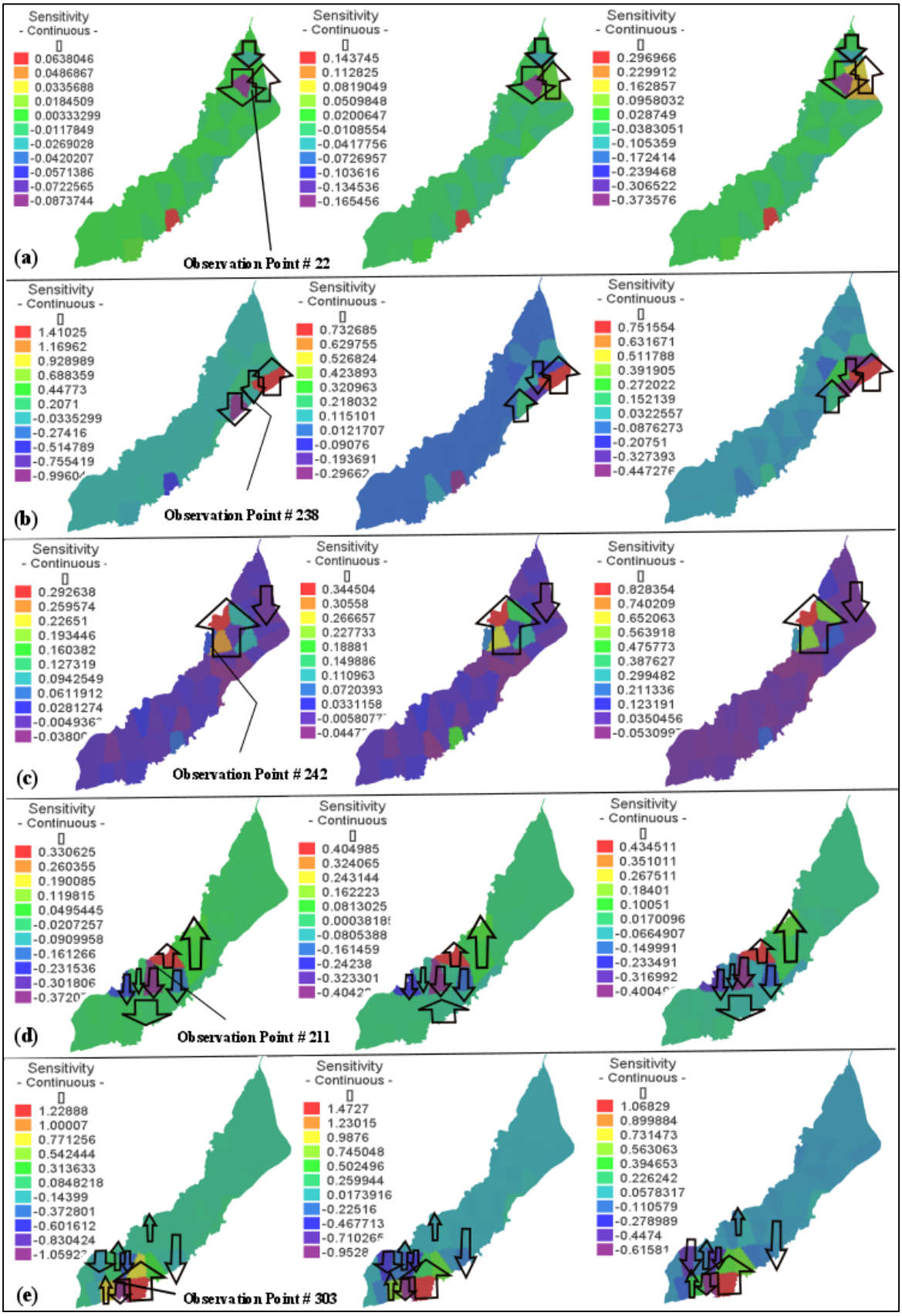

Fig. 12 Distribution of observation sensitivity for selected piezometric points. Note that the upper and lower arrow heads indicate increase and decrease in sensitivity

2. Conclusions and outlook

Quality data are a prerequisite to corroborate model calibration and validation leading to reliable predictions. Frequently unavoidable simplifications may cause larger uncertainties in model outcomes. Model calibration methods range from manual to automated techniques. The application of automated techniques exhibits growing popularity and its properties need to be addressed. Therefore, the current study was conducted in Pakistan on a large scale groundwater flow model to compare both techniques. A comparison of manual, zone-based and state-of-the-art pilot point calibration technique along with Tikhonov algorithm was performed. The following major conclusions can be drawn from the comparative study:

- It is found that the pilot point calibration method is more flexible and robust in comparison to both zone based parameterization and manual approaches due to its lesser subjectivity on part of the modeler's experience.
- Pilot point calibration results in a reliable model calibration and validation for a majority of model regions as different statistical indicators show reasonable values. For calibration, the values of R^2, Nash Sutcliffe Efficiency, % BIAS and RMSE are 0.99, 0.978, 0.026 and 1.23 m, respectively. Their values for validation of the model are 0.987, 0.962, -0.205 and 1.31 m, respectively.
- Manual calibration of the transient model shows worse results as compared to other approaches with higher value of RMSE (i.e. 1.69 m). It is also observed that model calibration by this approach proved cumbersome as the model had to be rerun 45 times before comparatively reliable model calibration was reached. The model calibration in some particular model regions resulted in major differences between measured and simulated heads.
- The spatial comparison of model calibrations shows that the pilot point approach yields overall better results at different locations with some higher differences at upper locations as compared to both zone based and manual calibration. The descent of measurement objective function is quicker in lower model regions as compared to upper regions.
- The possible reasons of higher differences between measured and simulated heads for some upper model regions could be due to the possibility of occasional partial inflow/outflow of groundwater owing to more pumping for rice crop and poor representation of this phenomenon in the current model definition due to simplification of boundary conditions for such regions. In case of zone-based parameterization this may also be possible due to poor representation of aquifer material heterogeneity for current parameter zones. In fact, no combination of final parameter zones was attained with best model results. This further indicates the limitation of such approaches due to their subjectivity.

- Parameter sensitivity analysis of the transient groundwater flow model shows that overall hydraulic conductivity is more influential as compared to drain/fillable porosity. However, this sensitivity is quite variable for different model locations and model layers.
- Sensitivities and error parameter results also address limitations/deficiencies of current hydraulic field data and help to identify regions where further field investigations could be performed.
- Sensitivities of different observation points demark different regions of particular importance for each such point and may guide engineers to concentrate there if any site specific activity is planned to be performed in the future.
- Present sensitivity analysis was performed by a local approach employed in PEST. For such methods, there is always a possibility that the entire parameter space might not be well represented. This issue can be addressed by some global sensitivity approach.
- Predictive analysis is another way to explore uncertainties of model results. For the current study, it was attempted; however, the use of such analysis is only limited to well posed problem which was not the case for the current model. If a problem is ill-posed, then it does not work because pertinent matrices become un-invertible. The only possibility then left is to explore non-linear uncertainty analysis options. PEST has provided utilities like PREDUNC and/or GENLINPRED for this purpose. Null space Monte Carlo and running model in 'Pareto' mode could be alternative solutions. Hence, it is recommended to explore these different approaches for further studies.

References

Abbaspour KC, Schulin R and Th. van Genuchten M (2001) Estimating unsaturated soil hydraulic properties using Ant-Colony-Optimization. Adv. in Water Resour. 24:827-841

Akima H (1970) A new method of interpolation and smooth curve fitting based on local procedures. Journal of the Association for Computing Machinery. 17(4):589-602

Awan U, Tischbein B, Martius C (2015) Simulating groundwater dynamics using FEFLOW-3D groundwater model under complex irrigation and drainage network of dryland ecosystems of central Asia. Irrigation and Drainage 64:283-296

Bahremand A, De Smedt F (2010) Predictive Analysis and Simulation Uncertainty of a Distributed Hydrological Model. Water Resources Management 24:2869–2880. doi: 10.1007/s11269-010-9584-1

Bahremand a., De Smedt F (2007) Distributed Hydrological Modeling and Sensitivity Analysis in Torysa Watershed, Slovakia. Water Resources Management 22:393–408. doi: 10.1007/s11269-007-9168-x

Barlow PM (2005) Use of simulation optimization modeling to assess regional groundwater systems: U.S. Geological Survey Fact Sheet 2005-3095, 4p

Bennett GD, Greenman DW, Swarzenski WV (1967) Groundwater hydrology of the Punjab, West Pakistan with special emphasis on problem caused by canal irrigation, United States Geological Survey (USGS). In: Water Supply Paper 608-H, US Geological Survey. Reston, VA

Black GE, Black AD (2012) PEST controlled: responsible application of inverse techniques on UK groundwater models. Geological Society, London, Special Publications 364:353–373. doi: 10.1144/SP364.22

Blasone R-S, Madsen H, Rosbjerg D (2007) Parameter estimation in distributed hydrological modelling: comparison of global and local optimisation techniques. Nordic Hydrology 38:451. doi: 10.2166/nh.2007.024

Brakefield LK, White JT (2015) Uncertainty of groundwater movement in the brackish water zone of the Edwards Aquifer during drought conditions. Proceeding of Modflow and More 2015: Modeling complex world – IGWMC Maxwell, Hill, Zheng and Tokin

Brooks LE, Masbruch MD, Sweetkind DS, Buto SG (2014) Steady-state numerical groundwater flow model of the Great Basin carbonate and alluvial aquifer system: U.S. Geological Survey Scientific Investigation Report 2014-5213, 124p., 2 pl. http://http://dx.doi.org/10.3133/sir20145213

Certes C, and de Marsily G (1991) Application of the pilot point method to the identification of aquifer transmissivities, Adv. Water Resour., 14(5), 284–300, doi:10.1016/0309-1708(91)90040-U

Darcy H (1856) Les Fontaines Publiques de la Ville de Dijon, Dalmont, Paris

De Marsily G., Lavedan G, Boucher M, and Fasanino G (1984) Interpretation of interference tests in a well field using geo-statistical techniques to fit the permeability distribution in a reservoir model. Geostatics for Natural Resources Characterization (2):831-849

DHI-WASY (2012) Reference manual of FEFLOW – Finite element subsurface flow and transport simulation system. User manual/Reference manual/White paper release 6.1. WASY Ltd: Berlin

Diersch HJ (2002) Interactive, graphics based finite element simulation system FEFLOW for modeling groundwater flow, Contaminant Mass and Heat transport processes. WASY Ltd: Berlin

Doherty (2015) PLPROC: A parameter list processor. National Centre for Groundwater Research and Training, Australia and Water Numerical Computing

Doherty J (2002) Manual for PEST, 5th ed. Brisbane, Australia: Watermark Computing

Doherty J (2003) Groundwater model calibration using pilot points and regularization. Groundwater 41(2): 170-177

Doherty J, Brebber L, and Whyte P (1994) PEST: model independent parameter estimation, Watermark Computing Trademarks, Australian

Doherty J, Johnston JM (2003) Methodologies for calibration and predictive analysis of a watershed model. Journal of the American Water Resources Association 39(2):251–265

Doherty JE, and Hunt RJ (2010) Approaches to highly parameterized inversion—A guide to using PEST for groundwater-model calibration: U.S. Geological Survey Scientific Investigations Report 2010–5169, 59 p

Freeze RA, Cherry JA (1979) Groundwater. Prentice Hall Inc., New Jersey. 604 pp

Gallagher M, Doherty J (2007) Parameter estimation and uncertainty analysis for a watershed model. Environmental Modelling & Software 22:1000–1020. doi: 10.1016/j.envsoft.2006.06.007

Glinski J, Horabik J, Lipiec J (2011) Encyclopedia of Agrophysics. Springer 2011

Hamby DM (1994) A review of techniques for parameter sensitivity analysis of environmental models, Environmental Monitoring Assessment 32:135–154

Hill, M.C., 1998. Methods and guidelines for effective model calibration: U.S. Geological Survey, Water-Resources Investigations Report 98-4005

Holzbecher E, Sorek S (2005) Numerical models of groundwater flow list. Encyclopedia of Hydrological Sciences 2401–2414

Hunt RJ, D'Oria M, Westenbrock SM, Doherty J (2015) Beyond groundwater: Calibration and uncertainty analysis for large transient coupled models. Proceeding of Modflow and More 2015: Modeling complex world – IGWMC Maxwell, Hill, Zheng and Tokin

Kazmi SI, Ertsen MW, Asi MR (2012) The impact of conjunctive use of canal and tube well water in Lagar irrigated area, Pakistan. Physics and Chemistry of the Earth, Parts A/B/C 47-48:86–98. doi: 10.1016/j.pce.2012.01.001

Khan MA (1978) Hydrological data, Rechna Doab: lithology, mechanical analysis and water quality data of testholes/test- wells, vol I. Publication no. 25, Project Planning Organization (NZ), Pakistan Water and Power Development Authority (WAPDA), Lahore

Kim NW, Chung IM, Won YS (2004) The development of fully coupled SWAT-Modfow model (II) (in Korean). Journal of the Korean Water Resources Association 37(6):503-521

Lenhart T, Eckhardt K, Fohrer N, and Frede HG (2002) Comparison of two different approaches of sensitivity analysis, Phys. Chem. Earth 27: 645–654

Liu YB, Batelaan O, Smedt F De (2006) Automated calibration applied to a GIS based flood simulation model using PEST. Floods, from Defense to Management – Van Alphen, Van Beek & Taal (eds), Taylor and Francis Group, London, ISBN 0415391199

Madsen H, Wilson G, and Ammentorp HC (2002) Comparison of different automated strategies for calibration of rainfall-runoff models. J. Hydrol., 261, 48-59

Moore C, and Doherty J (2005) The role of the calibration process in reducing model predictive error. Water Resources Research, v. 41, no. 5, W05020

Mulete MK, and Nicklow JW (2005) Sensitivity and uncertainty analysis coupled with automatic calibration for a distributed watershed model. Journal of Hydrology 306:127-145

Nash JE, and Sutcliffe JV (1970) River flow forecasting through conceptual models. 1. A discussion of principles. J. Hydrol., 10(3), 282–290

Oreskes N, Shraderfrechette K, and Belitz K (1994) Verification, validation and confirmation of numerical models in the earth sciences. Science 263: 641–646

Qureshi AS, Gill M a., Sarwar A (2010) Sustainable groundwater management in Pakistan: Challenges and opportunities. Irrigation and Drainage 59:107–116. doi: 10.1002/ird.455

Qureshi AS, McCornick PG, Sarwar a., Sharma BR (2009) Challenges and Prospects of Sustainable Groundwater Management in the Indus Basin, Pakistan. Water Resources Management 24:1551–1569. doi: 10.1007/s11269-009-9513-3

Refsgaard JC (1997) Parameterization, calibration and validation of distributed hydrologic models. J Hydrol 198:69–97

Rehman G, Jehangir WA, Rehamn A, Aslam M, Skogerboe GV (1997) Salinity management alternatives for the Rechna doab, Punjab, Pakistan, IIMI-Pub. 1, Lahore, Pakistan

Reilly TE, Harbaugh W (2004) Guidelines for evaluating groundwater flow models. SGS Scientifc Investigation Report 2004-5038, 30 p

Santhi C, Arnold JG, Williams JR, Srinivasan R, Hauck LM (2001) Validation of the SWAT model on a large river basin with point and non-point sources. Journal of the American Water Resources Association 37(5): 1169–1188

Sarwar A (1999) Development of a conjunctive water use model. An integrated approach of surface and groundwater modeling using a geographical information system (GIS). Dissertation, University of Bonn, Germany

Sarwar A, Eggers H (2006) Development of a conjunctive use model to evaluate alternative management options for surface and groundwater resources. Hydrogeology Journal 14:1676–1687. doi: 10.1007/s10040-006-0066-8

Satelli A, Tarantola S, Campolongo F, and Ratto M (2004) Sensitivity analysis in practice: A guide to assessing scientific methods. John Wiley & Sons, Ltd

Schenk O, Gärtner K (2004) Solving unsymmetric sparse systems of linear equations with PARDISO. Future Generation Computer Systems 20:475-487

Schewchuk JR (2005) Triangle: A two dimensional quality mesh generator and Delaunay triangulator. Computer Science Division, University of California at Berkeley. Version 1.6

Senarath SUS, Ogden FL, Downer CW, Sharif HO (2000) On the calibration and verification of two- dimensional, distributed, Hortonian, continuous watershed models. Water Resources Research 36(6):1495–1510

Shah T, Debroy A, Qureshi AS, Wang J (2003) Sustaining Asia's groundwater boom: an overview of issues and evidence. Natural Resource Forum 27: 130–141

Tikhonov AN, Goncharsky AV, tepanov VV, Yagola AG (1995) Numerical methods for the solution of ill posed problems, Kluwer Academic Publishers

Tokin MJ, Doherty J (2005) A hybrid regularization inversion methodology for highly parameterized environmental models. Water Resources Research 41, W10412, doi: 10.1029/2005WR003995

Usman M, Kazmi I, Khaliq T (2012) Variability in water use, crop water productivity and profitability of rice wheat in Rechna Doab, Punjab, Pakistan. Journal of Animal and Plant Sciences 22:998–1003

Usman M, Liedl R, Kavousi A (2015) Estimation of distributed seasonal net recharge by modern satellite data in irrigated agricultural regions of Pakistan. Environmental Earth Sciences. doi: 10.1007/s12665-015-4139-7

Yeh JTC, Mock PA (1996) A structured approach for calibrating steady state groundwater flow models. Groundwater 34(3):444-450

Young SC, Doherty J, Budge T, Deeds N (2010) Application of PEST to re-calibrate the groundwater availability model for the Edwards-Trinity (Plateau) and Pecos Valley aquifers. Texas Water Development Board: Austin, TX 78711-3231

Zhou Y, Li W (2011) A review of regional groundwater flow modeling. Geoscience Frontiers 2:205–214. doi: 10.1016/j.gsf.2011.03.003

Article V

Assessing groundwater dynamics under future land use/land cover and climate change scenarios in irrigated Indus Basin, Pakistan

Muhammad Usman & Rudolf Liedl

Abstract

Success of agriculture in Pakistan depends heavily on both surface water and groundwater. The shrinking groundwater share due to decreased river flows and accelerated population is causing ecosystem imbalance which is further intensified by rapid changes in land use / land cover (LULC) and climate. The present study aims to investigate impacts of these changes on groundwater dynamics in the lower Chenab canal (LCC) region of Pakistan. For this, a novel approach is employed by incorporating remote sensing data in combination with actual patterns of LULC change and future scenarios are proposed based on these findings. A statistical approach is employed for downscaling of actual evapotranspiration and precipitation data under two emission scenarios (H3A2 and H3B2) leading to prediction of future climatic changes. Moreover, a 3-D numerical groundwater flow model is used for evaluating current patterns of groundwater use and its dynamics under future scenarios. This model can track spatio-temporal groundwater changes. The water budget for the calibration and validation period shows a total horizontal water inflow of 2844 Mm^3 to LCC and an outflow of 2720.2 Mm^3. The water outflow through pumping is about 17374.43 Mm^3 as compared to groundwater recharge of 19933.20 million m^3 (Mm^3). The comprising surplus of 2682.87 Mm^3 raises groundwater levels in major parts of LCC. Changes in rice cultivation show the highest impact on groundwater levels in upper irrigation subdivisions of LCC whereas higher negative changes are observed for lower parts of LCC when fodder is replaced by rice, cotton, and sugarcane. Fluctuations in groundwater level among different scenarios are within ±1 m range thus showing a limited potential for groundwater management due to LULC changes. For future climate scenarios, a rise in groundwater level is observed under the H3A2 emission regime for 2011 to 2025. Nevertheless, a drop in groundwater level is expected due to increased crop consumptive water use and decreased precipitation under the H3A2 scenario for the periods 2026-2035 and 2036-2045. Although no imminent threat of groundwater shortage is anticipated, there is an opportunity for developing groundwater resources in the lower LCC regions through water re-allocation that would help to deal with anticipated water shortages in the study region. The groundwater situation under the H3B2 emission regime is relatively complex as very little rise in groundwater level through precipitation is expected during 2011-2025. Any positive change in groundwater under such scenarios is mainly associated with changes in crop consumptive water uses. Consequently,

water management requires revisiting of current cropping patterns as well as augmenting water supply through additional surface water resources. Considering the limitations of the current study, it is recommended to update the model with modifications in river flow due to climatic changes. Moreover, it is regarded helpful to investigate groundwater dynamics under combined effects of LULC and climate change.

Keywords: Groundwater modeling, Statistical downscaling, Land use / land cover, Water budget, Climate change scenarios

1. Introduction

Groundwater constitutes one of the largest fresh water resources and plays a myriad of roles through supporting the hydrological cycle (Richard et al. 2013), supplying water for human consumption and helping to maintain ecological values of many regions in the world (IPCC, 2007; UN/WWAP, 2006). Other major beneficiaries of groundwater include industrial uses and irrigation application. Globally, the share of groundwater for domestic, agricultural and industrial purposes is estimated to be 31%, 42% and 27%, respectively (Richard et al., 2013). Agriculture is thus considered to be the major consumer of groundwater and this share is even greater in case of arid and semi-arid regions of the world including India, Pakistan, China and middle-eastern countries (Usman et al. 2012).

Utilization of water supplies for successful agriculture in Pakistan is dependent both on surface and groundwater resources. The decreased river water supplies in the recent years have put extra pressure on groundwater for irrigated agriculture which is depicted by the increase in groundwater pumping from 10 billion m^3 in 1965 to 68 billion m^3 in 2002 (Usman et al., 2014). As a result, this situation poses a big challenge for sustainable groundwater management in the country, implying that water resources need to be utilized for an indefinite time without causing unacceptable environmental, social and economic consequences (Gleeson et al., 2012; Alley et al., 1999). This is only possible if each single drop of water is used in the context of socio-economic development and protection of ecosystems (Constanza et al., 1997). However, despite the critical importance of groundwater in integrated water resources management, it is not duly considered (UNEP/CBD, 2010; Hetze et al. 2008). Similar concerns have been raised by the European Commission Groundwater Directive and Water Framework Directive according to which it is necessary to investigate how groundwater use may affect ecosystems and vice versa.

Land use/land cover (LULC) changes are mainly human-induced parameters altering the groundwater dynamics especially in agricultural areas (Calder, 1993). Nevertheless, impacts of these changes on groundwater systems and its behaviour have not been extensively investigated (Bronstert, 2004). Most studies of LULC impacts on hydrology are based on stream flow dynamics in some watershed. Many experimental studies have been conducted where effects of change in forest cover on the hydrological behaviour is investigated (e.g.,

Bosch and Hewlett 1982;, Brown et al. 2005; Robinson et al. 2003; Hornbeck et al. 1993; Dams et al. 2008). Apart from these experimental studies, substantial research has been performed where different modeling approaches are utilized for exploring hydrological effects of LULC change. For instance, Bultot et al. (1990) and Bahremand et al. (2006) assessed the impact of reforestation on the hydrology of a watershed. Similarly, Asaf and Eggers (2006) investigated the impact of LULC change on the groundwater behaviour in the Indus Basin. However, all of the afore-mentioned studies have utilized hypothetical scenarios without considering real patterns of LULC change in the studied regions. There are also many investigations where models of LULC change were employed to generate future LULC change scenarios. Niehoff et al. (2002), for instance, utilized land use change modeling kit (LUCK) in conjunction with a modified version of the physically-based hydrological model WaSiM-ETH for flood prediction. Similarly, Tang et al. (2005) employed the Land Transformation Model (LTM) in combination with the Long-Term Hydrologic Impact Assessment (LTHIA) model for similar purposes. Furthermore, Tong and Liu (2006), Tang et al. (2005), McColl and Aggett (2007) and Dams et al. (2008), among others, have combined hydrological models with land use change.

On the other hand, most of the above mentioned modeling studies only focus on the surface hydrological processes failing to consider spatial variability of groundwater recharge due to computational constraints, data availability and model complexity. Exceptions to this are Dams et al. (2008), Batelaan and De Smedt (2007), Klöcking and Haberlandt (2002) and Batelaan et al. (2003) who investigated impacts of LULC change on groundwater with a fully distributed modeling approach. They used WetSpass which estimates recharge by incorporating actual evapotranspiration and precipitation along with other parameters (Albhaisi et al., 2013). Nevertheless, this tool cannot utilize irrigation as input parameter for estimation of distributed recharge, which is an important input for current study region. Therefore, another approach was suggested and where distributed recharge was estimated by using a complex water balance model incorporating data of actual evapotranspiration, LULC classification and change from remote sensing techniques at higher spatial resolutions. The details of such data types and their utilization for recharge estimation is available from Usman et al. (2015a & 2015b).

Climate change is another potential variable which can induce changes in natural ecosystems apart from LULC changes as for example, human-induced warming which is taking place with ‘very high certainty’ (IPCC, 2007). Consequently, investigating dynamics related to water resources management by taking into account climate changes as well as ecological and bio-geographical changes (Buytaert et al. 2009: Wiens et al., 2009), oceanography (Good et al., 2009) and glaciology (Holland et al., 2010). Nevertheless, neglecting groundwater under climate change is certain as according to Taylor et al. (2012), groundwater and dependent ecosystem have received less attention from scientific and other concerned

communities. In another IPCC report, it is admitted that there has been very little research on the potential impacts of climate change on groundwater although its share in world's water use, particularly in rural areas of arid and semi-arid regions, is considerable (IPCC, 2008).

Effects of climate change on nature may exhibit complex patterns. For instance, Crosbie et al. (2010) show considerable variation in trend and magnitude of climate change in terms of temperature, rainfall, evapotranspiration, and vapour pressure. One may also question the rule that annual recharge is considerably affected by annual rainfall only (McCallum et al., 2010) as recharge can also be affected by rainfall seasonality, intensity, humidity, air temperature, and crop evapotranspiration under changing concentrations of CO_2. In arid and semi-arid regions, increased variability in rainfall may increase groundwater recharge due to more frequent intensive rainfalls. At the same time, although, higher temperature means higher crop evapotranspiration rates and hence, there is less net groundwater recharge (Hetze et al., 2008) and vice versa. Crosbie et al. (2009) have also reported that increase in rainfall does not always lead to an increase in recharge. It is therefore necessary to undertake local studies that assess the specific combination of parameters which could be affected by climate change. For irrigated regions such as the current study region, the potential parameters of interest may be rainfall and crop evapotranspiration as both of these can behave differently due to changes in climate. Therefore, the current study was designed to comprehensively evaluate groundwater resources and to study their dynamics under changing LULC and climate change scenarios. The specific objectives of the current study are:

1. Development of realistic LULC change scenarios and downscaling of precipitation and actual evapotranspiration for the synthesis of future climate change projections under IPCC emission scenarios including H3A2 and H3B2.
2. Assessment of the detailed water budget for LCC at different spatial scales.
3. Investigating the effects of LULC and climate changes on groundwater dynamics both temporally and spatially.

2. Material and methods

2.1. LULC change scenarios

LULC is amongst important environmental factors which are affected heavily by anthropogenic activities and therefore impact the hydrological cycle (Wu et al., 2014). Evapotranspiration is the single term that links land surface energy balance and surface water balances (Zhao et al., 2013). This forms a key process of the hydrological cycle and is regarded valuable in water balance modeling especially for irrigated areas (Usman et al., 2015a). Evapotranspiration is used in hydrological studies as a water balance term which varies spatially due to differences in water use for various land uses (Wegehenkel, 2009). As shown by Usman et al. (2015b), evapotranspiration in any agro-climatic region can be estimated by using the Surface Energy Balance Algorithm (SEBAL) designed by Bastiaanssen et al. (1998b).

The detailed methodology and application of SEBAL for the current study is accessible from Usman et al. (2015a) (Article II). The other important information about devising LULC change scenarios is the results of different areal coverage and its change detection which are discussed in Usman et al. (2015c) (Article III). These results are correlated with spatially distributed actual evapotranspiration for establishing patterns of crop water use within these LULC classes and to identify potential areas of different LULC change in different irrigation subdivisions of LCC employing the zonal statistics approach in ArcGIS.

The results of different areal coverage represent the overall information at LCC scale. In reality, the cultivated area under a particular LULC class is not uniform throughout LCC but specific classes are dominant in particular irrigation subdivisions of LCC. Similarly, LULC change is also not uniform throughout LCC but it is highly dependent on overall areal coverage of a particular class in a specific sub-region. Due to this fact, the total area under any LULC class is segregated at irrigation subdivision level to consider spatial variability of any LULC change. The estimated proportions take into consideration the overall suggested change in any LULC at LCC scale.

Subsequently, different LULC scenarios are generated in order to provide their results for future hydrological modeling and to explore their impacts on possible changes in groundwater levels in the study area. To this end, the following two conditions are followed while devising these scenarios:

1. Ensuring the realistic limits of the area of each LULC class while introducing changes in the area of a particular LULC class based on estimated results (Type I).
2. Maintaining the area of a particular LULC class within its realistic change limits with no consideration of cropped areas of other classes (Type II).

Along with meeting the above-stated conditions, the following points are considered to ensure maximum suitability of LULC scenarios to the study area:

a) Change in any LULC class is based on its spatial coverage in any particular sub-region of LCC.
b) Increase/decrease in LULC area of any particular class is based on its current status in LCC (i.e. year 2011, the latest study year).
c) LULC change scenarios are based only on classes in kharif cropping seasons (May to October) as options for change are limited during rabi seasons (November to April) and the difference in consumptive water use is also less among rabi crops (Usman et al., 2015a; Usman et al., 2014).

2.2. Statistical downscaling of climatic parameters and future scenarios

Global Circulation Models (GCMs) are considered as major tools to predict the changes and variability in climate variables on global and continental levels. These numerical-based models interpret sea-ice, the oceans, and atmosphere (Fowler et al., 2007) and their predictions

regarding future climate changes are very helpful. However, the outputs are based on a large grid scale (250 - 600 km) (Mahmood and Babel, 2013; Gebremeskel et al., 2005). Due to this limitation, the outputs of GCMs cannot be used directly to investigate the impact of climate change in environmental and hydrological studies on local/regional scale (Wilby et al., 2000). The most important solution in this regard is to build a bridge between GCM scales (a coarse scale) and local scale (0-50 km) by downscaling (Wetterhall et al., 2006; Xu, 1999).

2.2.1. Downscaling approaches and description of SDSM

Many downscaling methods have been developed and implemented throughout the world by utilizing the outputs of GCMs to downscale climate change impact at local/regional scales (Wilby and Wigley, 1997; Gellens and Roulin, 1998; Wilby et al., 1999, 2006; Huth 2002; Hay and Clark, 2003; Diaz-Nieto and Wilby, 2005; Salzmann et al., 2007; Akhtar et al., 2008; Elshamy et al., 2009; Yang et al., 2010; Sunyer et al., 2011; Huang et al., 2011; Sou-vignet and Heinrich, 2011; Rahid and Babel, 2013). Generally, there are two main types of downscaling approaches including dynamical downscaling (DD) and statistical downscaling (SD). In DD, a Regional Climate Model (RCM) is coupled with the GCM. The RCM receives the large scale boundary condition and generates detailed information at the local/regional scales. RCM is susceptible to any systematic error which belongs to the GCM as it is dependent on the boundary conditions from GCM. The performance of the RCM is strongly dependent both on the driving force of the GCM and information about local scale forcing (e.g. orography, LULC and land–sea contrast etc.), (Mahmood and Babel, 2013). This necessitates the importance of appropriate data availability by strong coordination between the global and the regional climate modeling groups. The RCMs are computationally intensive and confine the number of simulations for climate scenarios (Hay and Clark, 2003; Fowler et al., 2007). On the other hand, SD approaches establish statistical links among the local scale and large scale variables. Such methods are computationally inexpensive and fast and hence have been adopted by a wider community of researchers (Wilby et al., 2000). SD is applied for a wide range of climate applications apart from its usefulness for numerical weather predictions. According to Giorgi et al. (2001), SD provides local scale information for climate change impact assessment studies. Nevertheless, the main disadvantage of the approach is its requirement for long historical meteorological data.

Many statistical downscaling software tools have been developed to date. Statistical Downscaling Model (SDSM) is one of them and is widely used throughout the world to downscale important climatic variables like precipitation, temperature and evapotranspiration etc. for assessing the impacts of climate change on hydrologic responses (Chu et al., 2010). This model is a hybrid of multiple linear regression and stochastic weather generator (Wilby et al., 2002; Wilby et al., 2006). Multiple linear regression establishes a statistical relationship between gridded predictors (such as mean sea level pressure) and single site

predictands (such as precipitation), and produces some calibration parameters. These parameters are then used by the stochastic weather generator to simulate up to one hundred daily time series to create a better correlation with the observed data (Wilby et al., 2002).

Two types of optimization methods are generally used in SDSM: (1) ordinary least squares (OLS) and (2) dual simplex (DS). OLS is used for the current study because it is faster than DS and produces comparable results with DS (Huang et al., 2011). Multiple linear regression is used to identify and select some suitable predictors from the atmospheric predictors in SDSM by utilizing the combination of the correlation matrix, partial correlation, histograms, scatter plots and p-values (Wilby and Dawson, 2013). Multiple co-linearity is considered during the predictor selection. Three different types of sub-models can be constructed in SDSM including monthly, seasonal and annual, therefore comprising the statistical relationship between the large scale atmospheric variables and the local scale variables like precipitation and evaporation. The current study employs only the annual model which considers similar type of regression parameters for each month of year. The other category of model includes conditional and unconditional models. Any category of such models can be used depending on the local scale variables (Mahmood and Babel, 2013). The conditional sub-model is used for variables such as precipitation, while the unconditional sub-model is used for independent variables such as temperature (Chu et al., 2010; Wilby and Dawson, 2013). Generally, the precipitation data is not distributed normally like temperature; therefore, SDSM transform such data types to make it normal before its further use for regression equation. The fourth root transformation function is used for precipitation data to render it to normal before its further application for regression analysis (Huang et al., 2011; Mahmood and Babel, 2013).

2.2.2. SDSM data requirements

Two types of daily time series, namely daily historic weather station data and large scale variables (National Centers for Environmental Prediction (NCEP) daily predictors), are used to develop SDSM. There are mainly four weather stations located in or near to the study area including Faisalabad, Toba Tek Singh, Lahore and Pindi Bhattian. Daily based long period weather data are required for SDSM, which were only available for Lahore and Faisalabad stations. From these two stations, daily data regarding maximum temperature, minimum temperature, relative humidity, sunshine hours, wind speed and rainfall were collected from 1960-2014. The daily data for Toba Tek Singh were available only from 2009-2014, while data were available from 2005 to 2014 for Pindi Bhattian. All such data were collected from Pakistan Metrological Department (PMD).

SDSM produces output daily time series by forcing the NCEP or HadCM3 predictors (Mahmood and Babel, 2013; Huang et al. 2011), the data of which were obtained cost free from http://www.cics.uvic.ca/scenarios/index.cgi?Scenarios, for the period of 1961-2010 and 1996-2050, respectively. H3A2 and H3B2 are the IPCC emission scenarios A2 and B2

of HadCM3, respectively. HadCM3 is selected for SDSM because it showed better agreement during evaluation of various GCMs (Mahmood and Babel, 2013, Akhtar et al., 2008; Huang et al., 2011).

2.2.3. Selection of predictands and screening of predictors

Any kinds of predictands can be downscaled using SDSM including maximum and minimum temperature, rainfall, evapotranspiration etc., depending on the objectives of further application. Temperature and precipitation are considered to be most important factors for agricultural regions because the former directly controls crop water needs by affecting evapotranspiration and the latter causes major contribution to groundwater recharge (Usman et al., 2015b). There is no direct use of temperature for recharge estimation, but it is a major variable for estimation of crop evapotranspiration. Therefore, actual evapotranspiration is estimated using temperature data along with other necessary climatic parameters by employing the advection-aridity approach (Usman et al. 2014). Later, both actual evapotranspiration and precipitation are utilized to estimate groundwater recharge under future changes and corresponding applications in groundwater modeling.

Screening of predictors is key to statistical downscaling using SDSM (Wilby et al. 2002). There are about 26 predictors to be used in the downscaling process and the complete list with detailed descriptions is available from Mahmood and Babel (2013). The process of predictor screening adopted in the current study employs an approach combining partial correlation, correlation matrix and p-value as devised by Gagnon et al. (2005) and Mahmood & Babel (2013). This process of predictor selection is a quantitative procedure where the selection of the first and most suitable predictor is relatively straightforward and easy, but the selection of subsequent predictors is more subjective. In the first step of this quantitative approach, a correlation matrix between NCEP predictors and predictands is set up. Then only the predictors with high correlation coefficients are screened out and ranked in descending order. The first predictor, having the strongest correlation among all predictors, is selected as super-predictor. Following this, the regression of highly correlated predictors is performed individually in the presence of the super-predictor and the absolute correlation coefficient between the predictor and predictand (R_1), the absolute correlation coefficient between individual predictors (R_2), absolute partial correlation (P_r), and p-value are obtained. In the next step, predictors with p-value greater than α (0.05) are eliminated to render the statistically significant results, and the highly correlated predictors (above 0.5 in this case) are taken out in order to avoid any multi-co-linearity. According to Pallant (2007), R_2 up to 0.7 is acceptable. For each predictor, the percentage reduction in absolute partial correlation (PRP) is calculated with respect to absolute correlation via $\mathrm{PRP} = (\frac{P_r - R_1}{R_1})$. The predictor with minimum PRP is selected as the second suitable predictor because this predictor has very insignificant multi-co-linearity with the super-predictor. The subsequent predictors can be selected by following the same procedure but there will be two super-predictors in the second repetition.

According to Mahmood and Babel (2013), mostly one to three predictors are enough during calibration of predictands without multi-co-linearity. Table 1 shows the screening of potential predictors for precipitation at Lahore. The details of screened predictors for other variables and weather stations can be found in Annex C.

Table 1 Screening of potential predictors for precipitation at Lahore

No.	Predictor Description	Predictor	R_1 (%)	R_2 (%)	P_r (%)	p-value	PRP (%)
1	Surface specific humidity	ncep_shum*	**24.1**				
2	Mean sea level pressure	ncep_mslp	19.2	49.7	6.70	0.000	65.10
3	850 hPa geopotential height	ncep_p850	17.5	52.0	30.6	0.000	74.85
4	Mean temperature at 2 m height	ncep_temp	17.5	39.7	25.3	0.000	44.57
5	500 hPa zonal velocity	ncep_p5_u**	17.4	59.4	15.3	0.000	**12.06**
6	500 hPa airflow strength	ncep_p5_f	17.3	51.9	0.001	0.561	99.99
7	500 hPa geopotential height	ncep_p500	17.3	52.5	67.2	0.000	288.4
8	Surface meridional velocity	ncep_v	13.6	8.20	37.0	0.000	172.0
9	850 hPa vorticity	ncep_p8_z	12.8	27.7	39.8	0.000	210.9
10	Surface wind direction	ncep_p_th	12.4	36.5	22.8	0.000	83.87
11	500 hPa wind direction	ncep_p5th	11.9	39.9	3.40	0.023	71.42
12	Surface divergence	ncep_p_zh	10.9	18.6	23.2	0.000	112.8
*super predictor **second predictor							

2.3. Calibration, validation of SDSM results and bias correction

SDSMs are developed by utilizing NCEP predictors screened for different variables at different locations. Daily data of precipitation and actual evapotranspiration from 1961 to 1995 are used for calibration of SDSM. Annual sub-models are developed individually for each predictand. Unconditional sub-models with fourth root transformation and conditional sub-models without transformation are used for precipitation and actual evapotranspiration, respectively. OLS method is used for optimization of the best fit. The calibrated models are used for simulation of the predictands from 1996-2010 using NCEP, H3A2, and H3B2 predictors by generating 20 ensembles and the means of these ensembles are used. Different statistical indicators are used for comparison of SDSM results with observed data. The indicators include coefficient of determination (R^2), root mean square error (RMSE), mean (M), standard deviation (SD), relative error in mean (RE_M), and relative error in standard deviation (RE_SD) for the periods of calibration and validation.

Bias correction is applied to compensate for any tendency to over- or under-estimate the mean of conditional processes by SDSM (Wilby and Dawson, 2007). For this purpose, the mean monthly bias factors for different variables are obtained from the calibration period

of 1961-1995. Then, these biases are adjusted to downscaled data for the validated period from 1996-2010. The statistical comparison is performed between un-biased SDSM downscaled data of precipitation and actual evapotranspiration, and observed data. Following successful validation, adjusted bias factors are utilized to rectify the current and future downscaled data obtained from HadCM3 predictors to achieve a more realistic picture of future climate (Mahmood and Babel, 2013). The following relationship is used to de-bias the mean precipitation and actual evapotranspiration SDSM downscaled data:

$$X_{db} = X_F \cdot \left(\frac{X_{obs}}{X_P}\right) \quad (1)$$

where X_{db} is de-biased daily time series of precipitation or actual evapotranspiration for future periods, X_F is future data downscaled by SDSM, X_P is the long term mean monthly values for precipitation or actual evapotranspiration for the period of 1961-1995 simulated by SDSM and X_{obs} represents the long term mean monthly observed values of precipitation or actual evapotranspiration.

It is to be noted that the application of these bias corrections for precipitation are only valid to its intensity and also to remove any systematic error occurred by SDSM downscaling. It is assumed that precipitation frequency is accurately simulated by SDSM (Mahmood and Babel, 2013).

2.4 Baselines and utilization of scenarios for groundwater modeling

Utilization of LULC and climate change scenarios for groundwater modeling is accompanied by a complex procedure as both types of scenarios do affect groundwater recharge. Since raster based recharge is utilized for groundwater modeling in the current study as explained by Usman et al. (2015b), the same approach is adopted for the preparation of recharge data under different scenarios of LULC and climate change. The details of this process are explained in the next sections.

Since specific change is always relative to some baseline time or period, different baselines were selected for both LULC and climate change scenarios for this study. As mentioned above, construction of LULC scenarios is based on changes in cropping patterns prevailing in 2011. However, for climate change scenarios, a baseline period from 2002-2012 is selected and any change is worked out for future periods 2016-2025, 2026-2035 and 2036-2045 by using the following relationship:

$$\%\ \text{change} = \left(\frac{x-y}{y}\right).100 \quad (2)$$

where x is the mean for the future period e.g., 2016-2025, and y is the mean for the baseline period of 2002-2012.

There are different ways to deal with climate change data, depending on their further application and objective. For the current study, future climate change data is dealt by considering

a constant change because the objective is not to track the changes in groundwater behavior yearly; rather the general situation at the end of a particular time period is to be investigated. Another reason is to simplify the preparation of pixel based recharge data of more than 30 years for the regional groundwater flow model. Therefore, from the above equation, % change will be a constant value for any year during the considered period. For instance, a constant change (e.g., 10%) in 2016 (beginning of period) will be the change with respect to 2002. Similarly, 10% change in 2025 (end of period) will be with respect to 2012.

3. Results and discussion

3.1. LULC change scenarios and water utilization

The details of different LULC change scenarios and overall possible water saving or more water utilization relative to current water usage are presented for each scenario in Table 2. The water saving or more utilization is based on changes at pixel scales which will be fed to the groundwater model in form of updated recharge. However, the results in Table 2 provide details of variation for water saving or more utilization at each irrigation subdivision under changed LULC to further explain the spatial variability of each change. Many different combinations of LULC change are possible. The details of many of them are provided in Usman et al. (2015). Out of many possible scenarios, only seven LULC scenarios are selected for the current study which will be used for performing simulation of groundwater. The selection of these scenarios is based on their impact on water utilization in different parts of LCC. For instance, scenarios 1, 6, and 7 show greater change in water utilization in upper irrigation subdivisions, while scenarios 4, 5, and 7 target middle irrigation subdivisions, and scenarios 2, 4, and 7 have greater impact on water utilization in downstream irrigation subdivisions. The overall analysis of more water utilization/saving at LCC level indicate that only scenarios 1, 3 and 4 result in decrease of water consumption and rest of the scenarios show more demand for water under modified LULC. The negative values depict increased water demand under changed LULC scenarios. Very few scenarios show similar changes in consumptive water use at LCC scale. However, the variation of change for each irrigation subdivision is significant and leads to spatial variability of the water table which would be even prominent at 1 km^2 pixel scale.

Table 2 LULC change scenarios and water saving (ha.m) for each irrigation subdivision

No.	Scenario	Type	Chuharkana	Paccadala	Mohlan	Buchiana	Tandla.	Tar-khani	Kanya	Bhagat	Sultanpur
1	25% decrease in R area by re-placing it with K.F & S.C	Type-I	100% R to K.F		50% each to K.F & S.C	100% R to K.F	100% R to S.C	50% R each to K.F & S.C			
			1163.8	**524.3**	**600.7**	**37.5**	**15.9**	**47.1**	**32.7**	**280.2**	**170.5**
2	50% decrease in C area by its conversion to S.C & K.F	Type-I	100% C to S.C	50% C each to K.F and S.C						100% to K.F **722.8**	100% to S.C **-263.0**
			-151.7	**47.9**	**-53.8**	**189.0**	**-305.1**	**-43.5**	**-225.9**		
3	50% increase in K.F area by major replacement of C & R	Type-I	100% K.F from R	100% K.F from C						100% from R **790.7**	100% from R **48.6**
			217.5	**267.4**	**97.0**	**242.4**	**123.2**	**208.7**	**45.6**		
4	30% decrease in S.C area by its conversion to K.F, C & R	Type-II	50% S.C each to K.F and R **1.1**	100% to K.F **16.7**	50% each to K.F & R **53.2**	100% to K.F **162.0**	50% S.C each to C and K.F			50% S.C each to R and C	
							534.3	**358.6**	**341.1**	**146.8**	**236.6**
5	30% increase in S.C area by its major replacement from K.F	Type-I	100% K.F to S.C							100% R to S.C **-31.6**	100% R to S.C **21.8**
			-1.1	**-16.7**	**-80.1**	**-162.0**	**-326.5**	**-371.4**	**-142.9**		
6	25% increase in R area by re-placing it with K.F & S.C	Type-II	100% K.F to R		50% each to K.F & S.C	100% R to K.F	100% R to S.C	50% R each to K.F & S.C			
			1163.8	**524.3**	**600.7**	**37.5**	**15.9**	**47.1**	**32.7**	**280.2**	**170.5**
7	75% decrease in K.F by re-placing R, C and S.C	Type-II	100% K.F to R **-326.3**	50% each to R and C **-1077.5**	50% each to S.C and C					50% each to C & R **-1838.5**	50% each to C and R **-82.8**
					-480.9	**-892.7**	**-693.2**	**-975.8**	**-313.8**		

Note: Figures in bold show decrease/increase in water utilization under changing LULC scenarios (ha.m), K.F = Kharif fodder, S.C = Sugarcane, C = Cotton, R = Rice

As spatial variability is a major concern of this study, the water saving or more water utilization is treated at pixel scale instead of irrigation subdivision level. Figure 1 represents the method of preparing updated rasters of recharge due to changed LULC. For preparing such rasters of recharge, target areas of particular LULC change are identified from results of LULC change detection and each pixel is identified to be converted from a particular LULC to another LULC. The decrease/increase in cultivated area of a particular LULC under each scenario is not an abrupt change; instead, this change is based on a uniform gradual change from the base period to 2030.

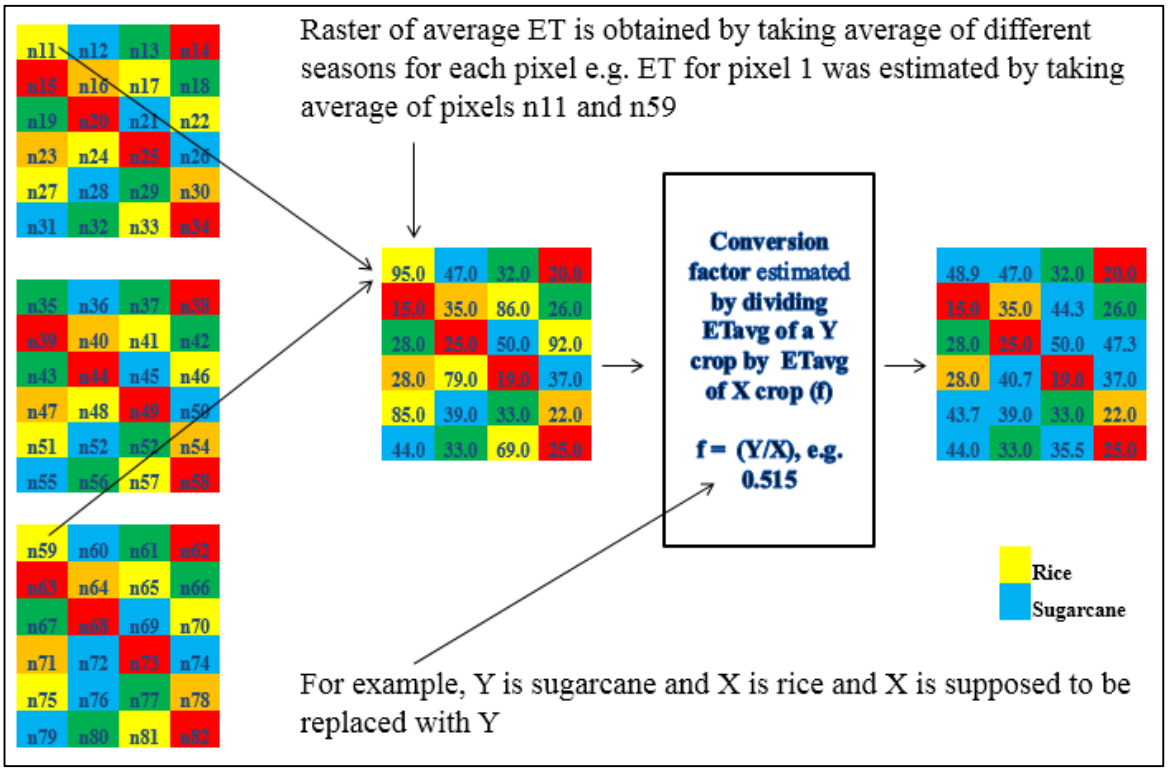

Fig. 1 Methodology for preparing updated recharge rasters for changing LULC

3.2. Results of climate change scenarios

3.2.1. Selecting predictors

It is observed that super-predictors for actual evapotranspiration at Lahore and Faisalabad stations are temperatures at 2 m height (temp). The other predictors for both stations include mean sea level pressure (mslp) and super-specific humidity (shum). Super-specific humidity is also a super-predictor for both stations in case of precipitation. The other predictors for precipitation at Lahore and Faisalabad are zonal velocity at 500 hPa and vorticity at 500 hPa, respectively. The results are quite consistent with Mahmood and Babel (2013), according to which shum is one of the major super-predictors for the majority of precipitation stations in Pakistan. Similarly temp is the main predictor for maximum and minimum temperatures. Along with wind velocity, temperature has a high effect on evapotranspiration and this behaviour is also seen in the current results. The predictors selected for the current study are

almost similar to those selected for other studies with similar predictands (Chu et al., 2010; Hashmi et al., 2011; Mahmood and Babel, 2013; Huang et al., 2011).

3.2.2. Calibration of SDSM

The calibration period for the current study was 35 years from 1961 to 1995. The daily precipitation and actual evapotranspiration data were simulated by SDSM using NCEP variables. The model performed reasonably well in the case of actual evapotranspiration which can be seen from the results in Table 3. The mean simulated values of actual evapotranspiration for both stations are comparable to observed data. However, the results for precipitation are relatively weak. For both stations, the difference between modeled and observed mean precipitation is large. Relative errors of mean and standard deviation are much greater for precipitation than actual evapotranspiration. Different researchers have evaluated SDSM for different variables including precipitation using different models and reported similar types of results. For instance, Huang et al. (2011) developed three different models for downscaling of precipitation and their results vary from weak to medium values for different performance indicators (e.g. R^2 ranges from 0.11 to 0.97). Whereas, Mahmood and Babel (2013) investigated SDSM for two models, monthly and annual, and according to them the monthly model performed better (R^2 is 0.992) as compared to the annual model (R^2 is 0.688). Overall, there is a consensus among different studies that temperature and evaporation performed better than precipitation in all cases (Wilby et al. 2002; Dibike and Coulibaly 2005; Khan et al. 2006; Mahmood and Babel, 2013; Wang et al. 2013). The possible reason is the heterogeneous nature of the precipitation occurrence/amounts, which is therefore difficult to simulate accurately (Wilby et al., 2002). Moreover, the calibration process of precipitation could be biased by the large number of zero values entered in the multiple regressions (Huang et al., 2011).

Table 3 Statistics of observed and downscaled mean monthly actual evapotranspiration and precipitation during calibration

Predictand	Station	Model	R^2	RMSE (mm)	M (mm)	SD (mm)	RE_M (%)	RE_SD (%)
Actual evapotranspiration	Lahore	Observed			128.52	51.92		
		NCEP	0.94	14.21	128.12	42.79	-0.31	-17.57
Precipitation		Observed			38.85	46.55		
		NCEP	0.88	24.12	21.45	30.68	-44.80	-34.08
Actual evapotranspiration	Faisalabad	Observed			132.72	53.75		
		NCEP	0.92	15.33	135.19	47.49	1.87	-11.64
Precipitation		Observed			26.88	30.87		
		NCEP	0.84	18.11	18.47	15.92	-31.30	-48.43

Figure 2 indicates the graphical comparison between observed data and monthly mean output of SDSM. In case of evapotranspiration, SDSM underestimates the results from March to May for Lahore and from March to June for Faisalabad. However, it overestimates the results for November, December, January and February for both stations. It also overestimates results during July to October, which is more prominent for Faisalabad in comparison to Lahore. With regard to precipitation, observed data are underestimated by SDSM in the majority of months especially in rainy months (July to August). There is only a small overestimation by SDSM results during October and November in comparison to observed precipitation.

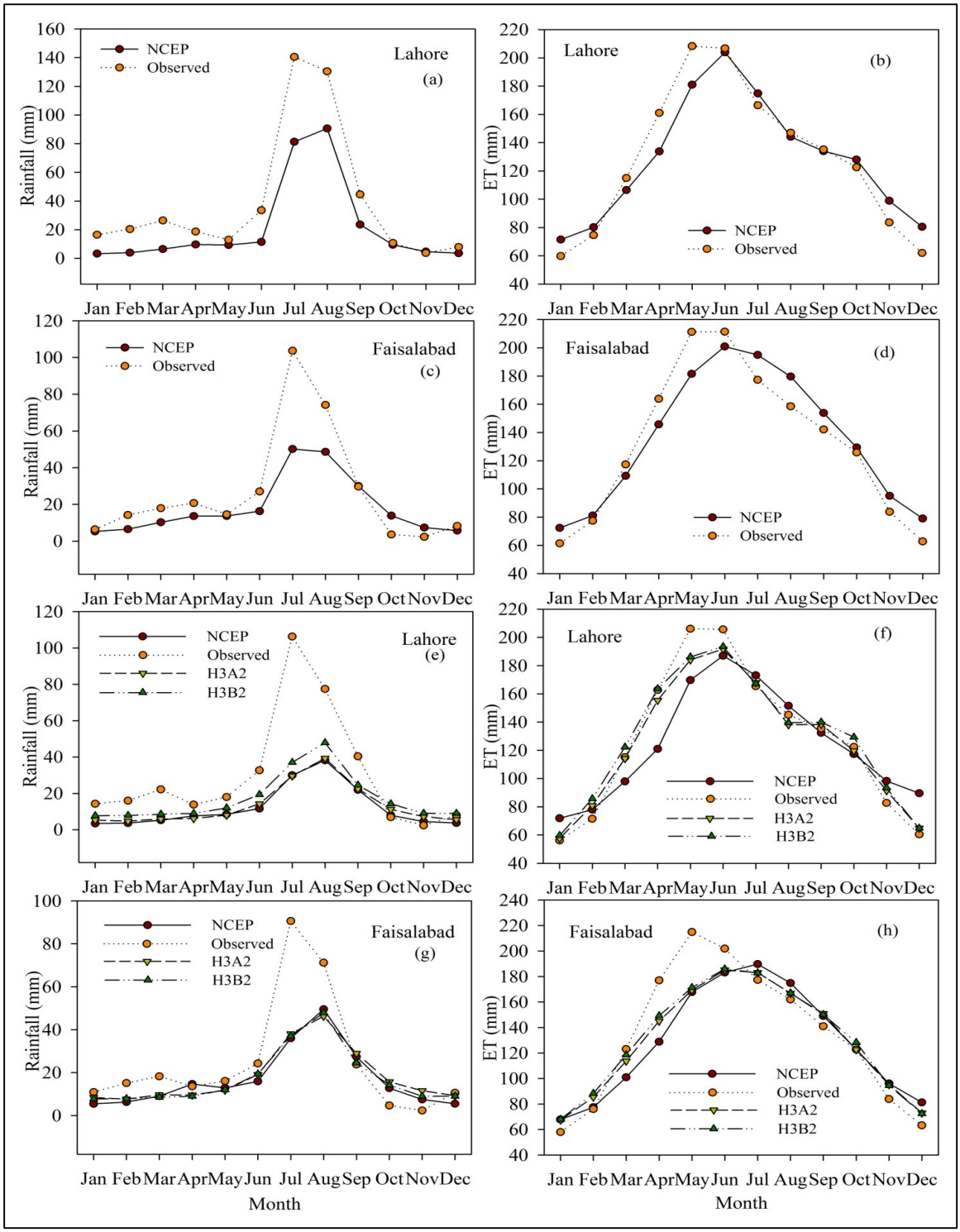

Fig. 2 Calibration (a, b, c & d) and prior biased corrected validation (e, f, g & h) results of SDSM

3.2.3. Validation of SDSM prior to bias correction

Three sets of data were used to validate the results from the SDSM model. These data include scenarios from NCEP as well as from HadCM3, namely H3A2 and H3B2. The same performance indicators as for calibration are used for validation of the SDSM. The validation period for evapotranspiration and precipitation was from 1996 to 2010.

Figure 2 depicts that the results are better for actual evapotranspiration than for precipitation. The R^2 values for evapotranspiration range from 0.89 to 0.98 and 0.83 to 0.92 for Lahore and Faisalabad, respectively. The relative errors in mean and standard deviation for Lahore range from 1.02 to 2.03% and from 13.87 to 20.64%, respectively. The corresponding values for Faisalabad range from 1.55 to 3.82% and from 19.35 to 21.59%, respectively. The values of different performance indicators for precipitation indicate that this variable is less correctly reproduced than evapotranspiration. For instance, values of R^2 range from 0.80 to 0.83 for Lahore and from 0.76 to 0.80 for Faisalabad. The other parameters including the relative error in mean and relative error in standard deviation also confirm the results as considerable higher values of these parameters are obtained for both stations in comparison to evapotranspiration (Table 4). Nevertheless, it is to be noted that the coefficients of determination and the predicted means are quite comparable with observed precipitation although variation for relative errors is more pronounced. This indicates that the models lack to predict the full variation in observed precipitation for both stations. However, the mean precipitation simulated by SDSM is comparable with observed data.

Table 4 Statistics of observed and downscaled mean monthly actual evapotranspiration and precipitation during validation (without bias correction)

Predictand	Station	Model	R^2	RMSE (mm)	M (mm)	SD (mm)	RE_M (%)	RE_SD (%)
Actual evapotranspiration	Lahore	Observed			127.41	52.42		
		NCEP	0.89	15.86	123.98	38.98	-2.03	-20.64
		H3A2	0.98	9.10	125.34	45.15	-1.63	-13.87
		H3B2	0.98	9.34	128.71	45.14	1.02	-13.89
Precipitation		Observed			29.18	31.45		
		NCEP	0.84	26.72	12.22	11.56	-58.13	-63.25
		H3A2	0.80	26.52	13.33	11.27	-54.34	-64.19
		H3B2	0.83	28.08	17.19	13.08	-41.09	-58.42
Actual evapotranspiration	Faisalabad	Observed			133.43	54.44		
		NCEP	0.83	22.97	128.32	43.90	-3.82	-19.35
		H3A2	0.91	18.33	129.77	42.74	-2.74	-21.49
		H3B2	0.92	17.22	131.35	42.69	-1.55	-21.59
Precipitation		Observed			25.14	27.17		
		NCEP	0.76	17.91	16.94	13.83	-32.59	-49.11
		H3A2	0.77	17.83	18.01	12.87	-28.34	-52.64
		H3B2	0.80	17.72	17.2	13.08	-31.59	-51.86

3.2.4. Validation of SDSM with bias correction

The results in the previous section indicate that there are large biases, especially for precipitation, which should be removed to further improve the validation results. The current study utilizes the bias correction method discussed in detail by Mahmood and Babel (2013) and

Salzmann et al. (2007). All SDSM models for both evapotranspiration and precipitation are corrected for biases. The detailed results in form of different statistical indicators are presented in Table 5.

Table 5 Statistics of observed and downscaled mean monthly actual evapotranspiration and precipitation during validation (bias corrected)

Predictand	Station	Model	R^2	RMSE (mm)	M (mm)	SD (mm)	RE_M (%)	RE_SD (%)
Actual evapotranspiration	Lahore	Observed			127.41	52.42		
		NCEP	0.98	7.30	124.15	47.13	-2.79	-8.09
		H3A2	0.99	4.04	127.19	49.76	-0.17	-5.06
		H3B2	0.99	5.96	129.47	49.41	2.39	-5.74
Precipitation		Observed			29.18	31.45		
		NCEP	0.99	11.16	32.72	36.97	10.01	8.07
		H3A2	0.99	15.04	34.36	38.68	20.12	11.51
		H3B2	0.99	19.87	38.08	41.14	22.47	14.79
Actual evapotranspiration	Faisalabad	Observed			133.43	54.44		
		NCEP	0.99	8.42	128.10	51.69	-2.99	-4.04
		H3A2	0.99	6.51	131.41	52.04	-1.51	-4.41
		H3B2	0.99	6.17	132.94	51.99	-0.36	-4.50
Precipitation		Observed			25.14	27.17		
		NCEP	0.99	6.18	28.32	31.83	6.67	7.14
		H3A2	0.98	9.82	29.7	34.76	11.13	8.91
		H3B2	0.98	10.72	32.8	41.43	13.34	11.54

Bias corrected downscaled mean results are also compared graphically with observed data as shown in Figure 3. From all the statistical indicators, it is obvious that both evapotranspiration and precipitation results improved. Especially, the precipitation results improved significantly as R^2 values increased from 0.80-0.84% to 0.98-0.99%, root mean square values decreased from 26.52-28.08 mm to 4.04-7.30 mm and relative errors in mean and standard deviation decreased from 41.09-58.13% and 58.42-64.19% to 10.01-22.47% and 8.07-14.79%, respectively, for Lahore. Similarly, the results for precipitation at Faisalabad also showed significant improvement as R^2 increased from 0.76-0.80% to 0.98-0.99%, root mean square values decreased from 17.72-17.91 mm to 6.18-10.72 mm, and relative errors in mean and standard deviation are decreased from 28.34-32.59% to 6.67-13.34% and 49.11-52.64% to 7.14-11.54%, respectively. The results from all variables including NCEP, H3A2, and H3B2 are satisfactory now and indicate strong applicability of SDSM to downscaling evapotranspiration and precipitation under emission scenarios (i.e. H3A2 and H3B2).

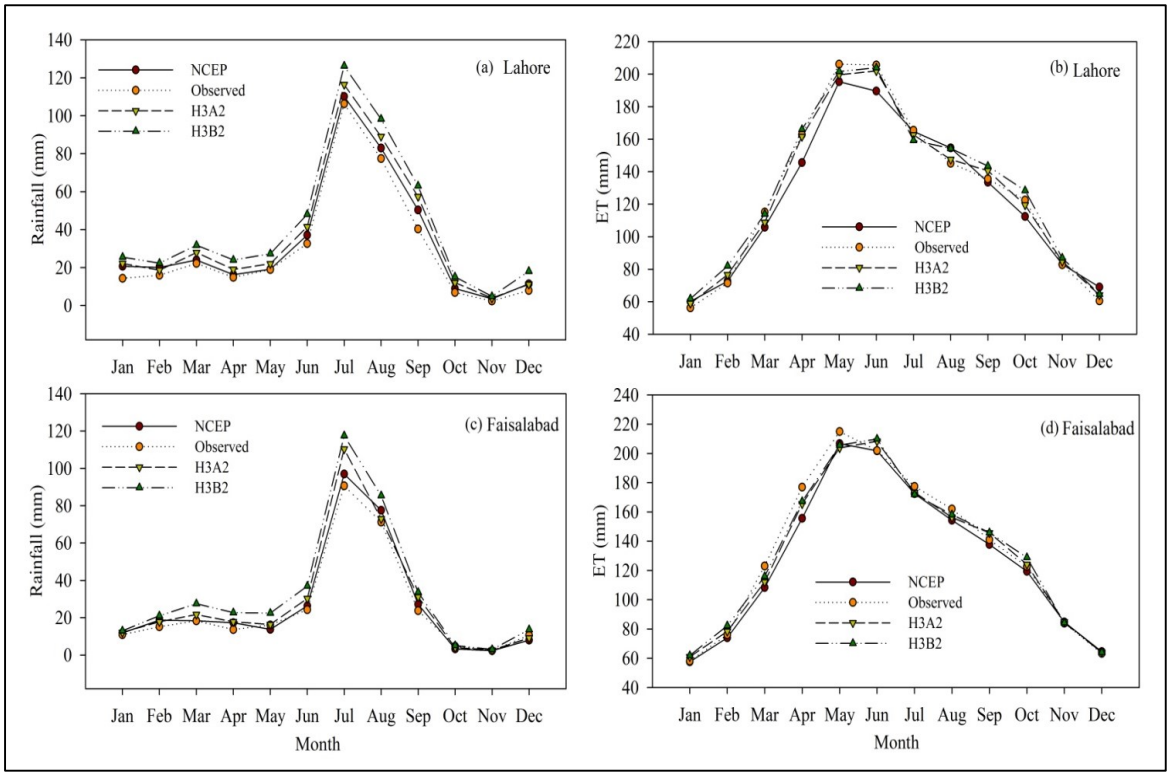

Fig. 3 Validation of SDSM results after bias correction

3.2.5. Downscaling evapotranspiration and precipitation under future emission scenarios

Table 6 presents the projected results of actual evapotranspiration and precipitation for different time durations (i.e. 2016-25, 2026-35 and 2036-45) with reference to the base line period (2002-2012) under emission scenarios H3A2 and H3B2. According to both emission scenarios, the change in evapotranspiration at both stations is consistent with differences during rabi seasons with increase at Faisalabad of 2.23% and 1.51% in 2016-25, 6.19% and 2.52% in 2026-35, and 5.87% and 7.29% in 2036-45. For Lahore, during the same season there is an increase in evapotranspiration of 2.20% and 1.18% in 2016-25, 9.46% and 2.59% in 2026-35, and 7.48% and 8.06% in 2036-45. The change during kharif seasons is also majorly consistent except during 2026-35, where the change in evapotranspiration is 2.22% and -0.95% at Faisalabad whereas at Lahore the change is 1.36% and -5.36% under H3A2 and H3B2, respectively. The detailed results of future change in evapotranspiration for other periods can be seen from Table 6.

With regard to precipitation, the future change during rabi seasons is more inconsistent for both emission scenarios. For instance, there is an increase of 1.68% in 2016-25 at Faisalabad, 4.67% and 5.79% at Lahore in 2016-25 and 2036-45 against a decrease of 4.57%, 32.19%, and 31.61%, respectively, under scenarios H3A2 and H3B2. Conversely, there is a decrease of 7.31% and 0.18% in 2026-35 and 2036-45 against an increase of 4.26% and 3.08% at Faisalabad. In case of kharif seasons, the change suggests that precipitation at both stations is generally increasing for all future periods and this is also mostly consistent except

for 2016-25 at Lahore where an increase of 33% for H3A2 and a decrease of 13.1% for H3B2 emission scenarios is expected. The groundwater recharge in this study region takes place majorly during kharif due to intensive monsoon rainfalls. Therefore, it is expected that rainfall recharge would increase in some future times. Similar kinds of results are presented by Awan et al. (2015). According to these authors an increase in recharge is expected from rainfall from 2012-20 under changing climate conditions.

Table 6 Future changes in actual evapotranspiration and precipitation (%) with reference to baseline period

Scenario	Predictor	Season	Faisalabad			Lahore		
			2016-25	2026-35	2036-45	2016-25	2026-35	2036-45
H3A2	Actual evapo-transpiration	Rabi	2.23	6.19	5.87	2.20	9.46	7.48
		Kharif	-2.29	2.22	1.58	-10.08	1.36	-0.59
		Annual	-0.67	3.64	3.12	-5.62	4.30	2.34
H3B2	Actual evapo-transpiration	Rabi	1.51	2.52	7.29	1.18	2.59	8.06
		Kharif	-0.14	-0.95	1.77	-1.45	-5.36	-2.05
		Annual	0.45	0.30	3.76	-0.49	-2.44	1.66
H3A2	Precipitation	Rabi	1.68	-7.31	-0.18	4.67	-6.81	5.79
		Kharif	27.86	7.61	11.99	33.52	11.05	13.98
		Annual	25.56	4.12	9.14	31.81	7.26	14.60
H3B2	Precipitation	Rabi	-4.57	4.26	3.08	-32.19	-29.72	-31.61
		Kharif	9.00	21.22	19.37	-13.1	2.12	1.34
		Annual	5.28	18.75	16.36	-19.73	-7.20	-6.99

Based on the changes of future climate variables, it is obvious that the degree of change is quite different at both stations particularly for the case of precipitation. The other point is that Lahore is located outside of the study area. The selection of Lahore and Faisalabad for downscaling of climatic data was done because long time series were available only for these two stations. The other two stations located inside the study region are Pindi Bhattian (upstream location) and Toba Tek Singh (downstream location). There is a need to investigate whether any significant relationship exists between different stations (i.e. between Lahore and Pindi Bhattian, and between Faisalabad and Toba Tek Singh). Owing to time series data, autocorrelations were worked out to see if there is any current time or lag time relationship between different stations. Figure 4 shows the autocorrelations of precipitation. This analysis is based on the daily precipitation data from 2005 to 2012 for Pindi Bhattian and from 2009 to 2012 for Toba Tek Singh. The highest correlation (0.72) is found between Lahore and Pindi Bhattian, followed by 0.50 for Faisalabad and Toba Tek Singh. The correlations between other stations were not very strong, for instance, correlations of 0.321, 0.30, 0.421, and 0.305 were found between Faisalabad and Lahore, Toba Tek Singh and Lahore, Faisalabad and Pindi Bhattian, and Pindi Bhattian and Toba Tek Singh, respectively. Generally, the lag time correlation relationship does not depict any strong relationship

for any case. Nevertheless, in the case of Faisalabad and Toba Tek Singh, it is seen that if there is precipitation at Faisalabad then there are fair chances of precipitation at Toba Tek Singh on next day.

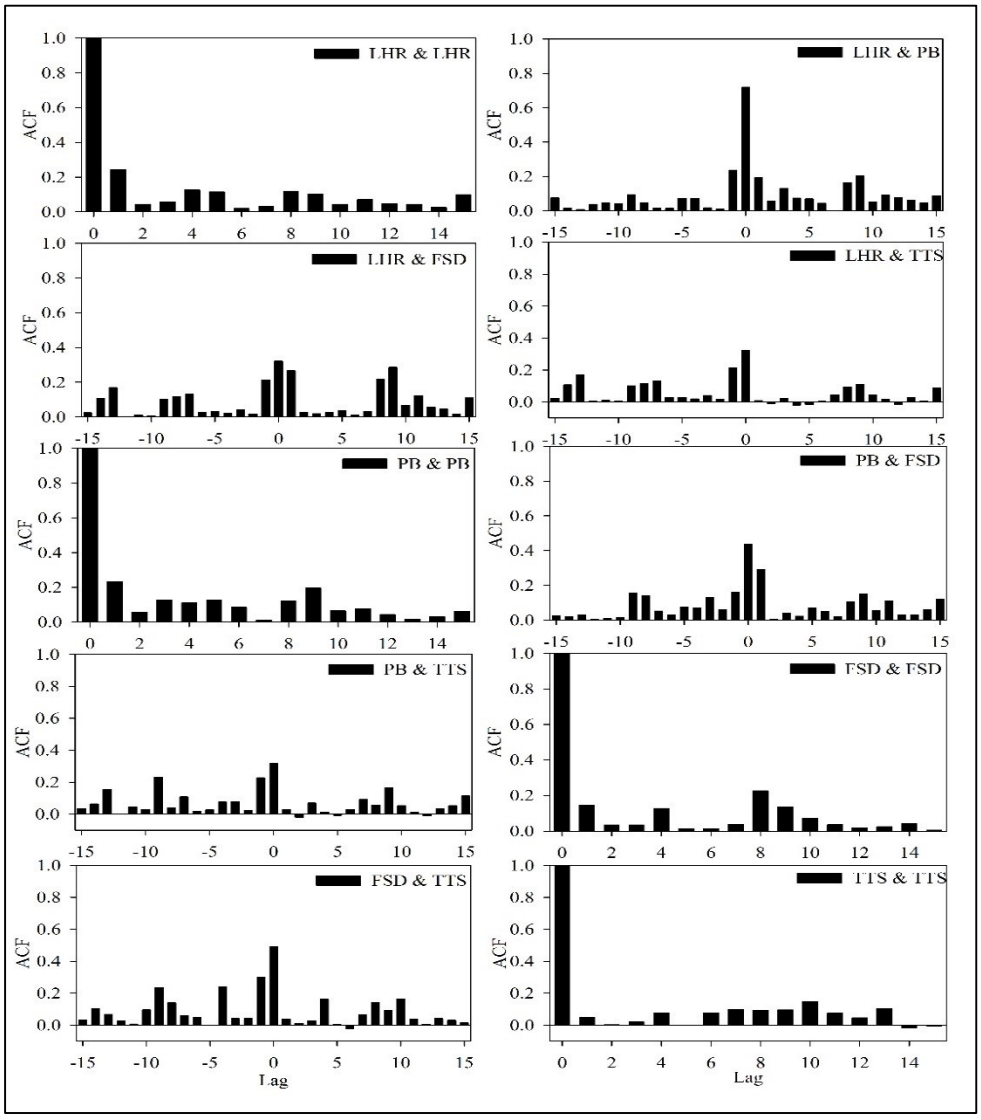

Fig. 4 Autocorrelation for precipitation at Lahore (LHR), Faisalabad (FSD), Pindi Bhattian (PB) and Toba Tek Singh (TTS) with lags in days and ACF = autocorrelation function

The autocorrelation results show that better correlation is found between Lahore and Pindi Bhattian and between Faisalabad and Toba Tek Singh. Also, Pindi Bhattian and Toba Tek Singh are located at the central locations of upper and lower irrigation subdivisions, respectively. Therefore, it is decided to utilize climate change results of Lahore for upper irrigation subdivisions including Chuharkana, Paccadala, Buchiana and Mohlan and results of Faisalabad for lower irrigation subdivisions including Tandlianwala, Tarkhani, Bhagat, Kanya and Sultanpur. Figure 5 represents the procedure of preparing raster of recharge under changing climate scenarios for feeding to the groundwater model. The rasters of changed

evapotranspiration are used directly for estimation of modified recharge while rasters of changed precipitation are first processed by excluding effective precipitation and other losses from total rainfall (as explained by Usman et al., 2015b) before their utilization for estimation of recharge.

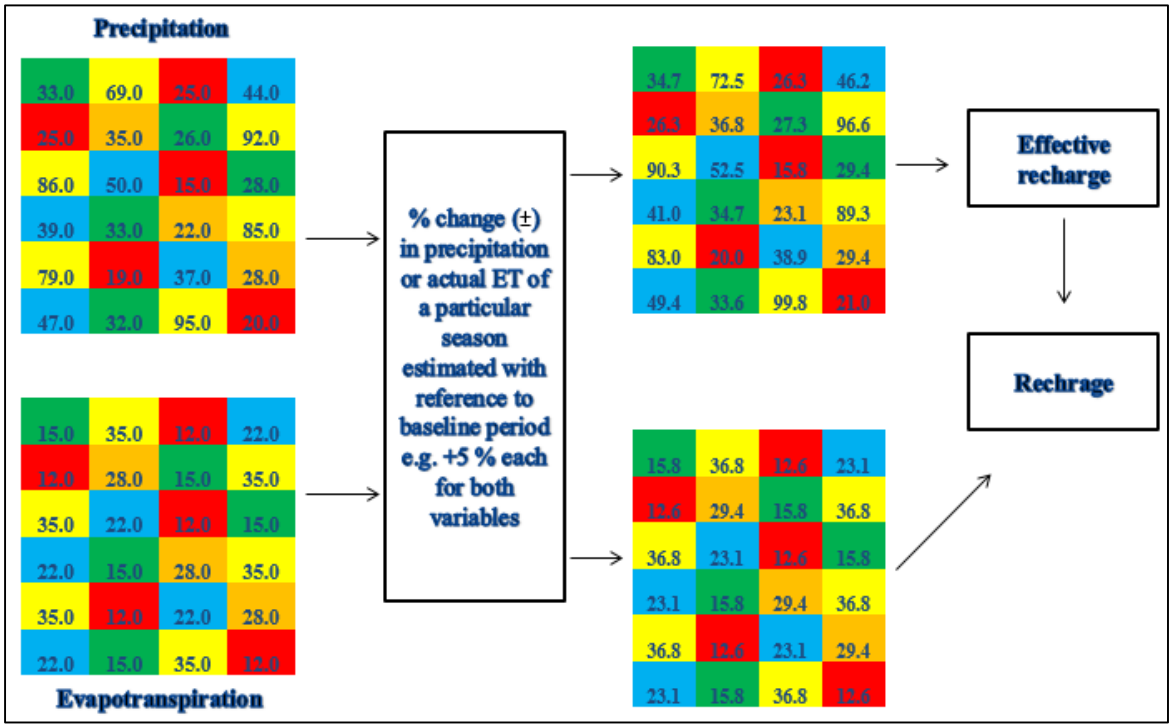

Fig. 5 Methodology for preparing updated recharge rasters under changing climate

3.3. Water budget and variation of Darcy flux in the study region

There are different ways to express numerical model results; one way is through water budget. The water budget provides detailed information about different components of model inflow and outflow along with providing clues to check whether the simulation remained stable or not. The water budget calculated by the groundwater model for the calibration and validation period (i.e. from Rabi 2005-06 to Kharif 2012) is presented in Table 7. The results are presented at whole LCC scale as well as for upper and lower LCC scales. These results show the detailed summary of flow for each boundary condition type, for sources and sinks, and for storage capture and release, whereas the imbalance term reflects the residual error.

Horizontal inflow and outflow calculated by the model refer to horizontal water flow rates which are generally less than the vertical exchange rates. The total period water budget of LCC shows a total horizontal water inflow of 2632 Mm^3 and 212 Mm^3 through Dirichlet and Neumann boundaries, respectively, whereas water outflow through these boundaries is 1156.4 Mm^3 and 1563.8 Mm^3, respectively. Water outflow through pumping from LCC is about 17374.4 Mm^3 while water inflow through groundwater recharge is about 19933.2 Mm^3. The difference between storage capture and release of 2682.4 Mm^3 for the whole LCC

indicates rising groundwater levels during the calibration and validation periods. The results are in concurrence with Usman et al. (2015b), who show an increasing trend in water level at the majority of LCC irrigation subdivisions. The results also show some discrepancies in the form of water imbalance which amounts to about 1.10 Mm^3 being negligible for LCC considering the magnitude of total water inflows and outflows.

Table 7 Water balance components (Mm^3) for calibration and validation period

Water Balance Component		**Spatial scale**		
Inflow	Outflow	Upper LCC	Lower LCC	Overall LCC
Dirichlet		275.5	2356.2	2632.0
	Dirichlet	25.9	1130.5	1156.4
Neumann		39.8	172.3	212.3
	Neumann	1120.7	443.1	1563.8
	Wells	8078.2	9296.4	17374.4
Distributed source (Recharge)		9997.7	9935.5	19933.2
Internal inflow		98.71	166.2	
Internal outflow		162.10	103.91	
Change in storage		1092.7	1589.7	2682.4
Note: Any difference in values could be due to round off error				

From Table 7 it is clear that Dirichlet inflow and outflow is quite low for upper LCC in relation to lower LCC. This difference arises due to the fact that the lower parts of lower LCC are connected to river Ravi and Trimu-Sidhnai link canal whereas upper LCC is only connected to Qadirabad-Balloki link canal. Horizontal inflow to upper LCC through Neumann boundaries is also less as compared to lower LCC, however the difference is larger for outflows where the outflow through Neumann boundaries (i.e. 1120.7 Mm^3) is quite large for upper LCC as compared to lower LCC (i.e. 443.1 Mm^3). The groundwater pumping from the upper and lower LCC is about 8078.2 Mm^3 and 9296.4 Mm^3 against recharges of 9997.7 Mm^3 and 9935.5 Mm^3, respectively.

Water budget for LCC shows an average total water inflow of about 1.11 x 10^6 m^3/day in the model domain through Dirichlet and Neumann boundaries with an average outflow of 1.06 x 10^6 m^3/day, respectively. Likewise, average total inflow in the model domain by areal recharge is about 7.80 x 10^6 m^3/day whereas average total outflow through pumping is about 6.80 x 10^6 m^3/day.

Darcy flux variations in four different model layers for different irrigation subdivisions are presented in Figure 6 whereas the spatial distribution of flux is given in Annex D for all four model layers. Results indicate relatively higher flux in lower parts of LCC in third and fourth model layers whereas higher values are observed in upper LCC in first and second model layers. The gradient of regional groundwater flow indicates potential aquifer zones in shallow depths of upper LCC and deeper depths of lower LCC. Overall average

flux for different model layers is highest for the third layer with a value of 0.0375 m/day, followed by 0.0343 m/day for the fourth model layer whereas it is 0.0171 and 0.0261 m/day for the first and second model layer, respectively.

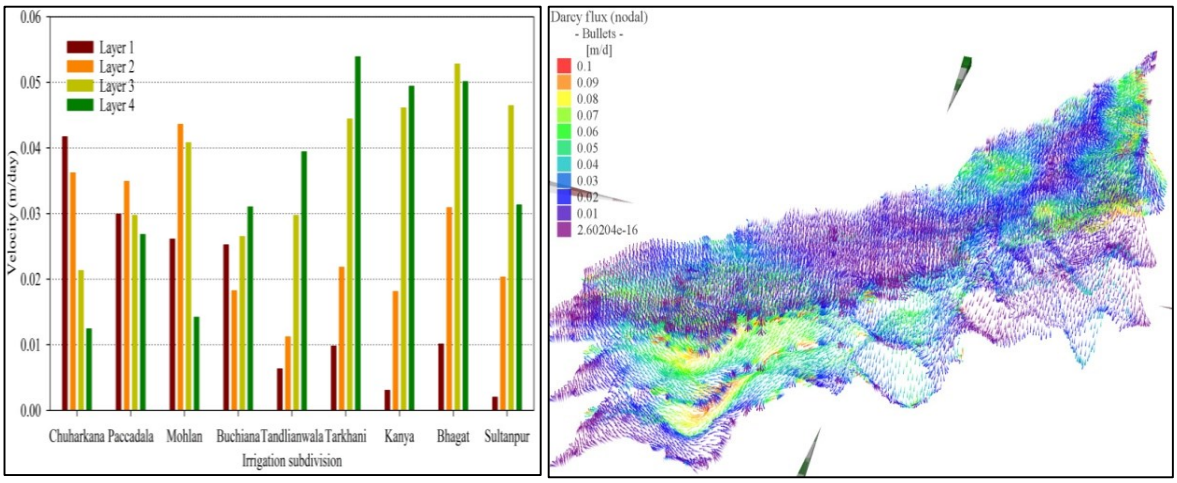

Fig. 6 (a) Average Darcy flux (i.e. Darcy velocity) for different model layers in different irrigation subdivisions and (b) Darcy fluxes distribution in different model layers

3.4. Status and management of groundwater under different future LULC and climate change scenarios

3.4.1. Groundwater under changing LULC

We performed groundwater simulations under the seven different LULC scenarios listed in Table 2. The temporal changes in average groundwater levels are presented for different irrigation subdivisions in Figure 7. The spatial distribution of these changes is given in Annex E to facilitate the identification of locations in LCC with groundwater level increase/decrease under different scenarios with the progress of simulation time.

Generally, two independent trends in groundwater dynamics are observed, i.e. increasing groundwater levels in upper irrigation subdivisions including Chuharkana, Paccadala and Mohlan, whereas decreasing levels prevail in middle and lower subdivisions of LCC. The highest individual positive change in groundwater level with respect to the base period is observed for Mohlan with a value of +3.88 m under the first scenario, while the highest negative change in groundwater level is observed for Tarkhani with a value of -3.23 m under the seventh scenario (Table 2). Detailed analysis for individual irrigation subdivisions shows that the decrease in rice area (i.e. scenario 1) has the highest positive impact on groundwater level change in the Chuharkana irrigation subdivision with a value of 2.07 m. The next major change is observed under the third scenario (1.53 m) where fodder cultivation increases up to 50% compared to its present cultivation from base time. The change observed under this scenario is almost similar to those arising under other scenarios, for example, second (1.37 m), fourth (1.41 m) and fifth (1.38 m). The change in groundwater level under the sixth scenario slightly increases from base time to April 2026 (i.e., 0.78 m), especially

from April 2021 to April 2026 (i.e., 0.04 m). Afterwards, a slight decreasing trend of 0.04 m between April 2026 and April 2030 is observed. This outcome possibly arises from the fact that LULC changes are not based on the whole year but are limited only to kharif season crops with no change during rabi seasons. Therefore, any temporal change in general trend of groundwater level may continue in the same direction with varying pace until a point when this trend would reverse. This becomes evident from the progression of trend lines under different scenarios against average condition (i.e., business as usual scenario).

Changes in groundwater head for the Paccadala and Mohlan irrigation subdivisions are also mainly affected by the first scenario. The change for Paccadala is mostly positive for all scenarios except the sixth scenario where there is a slowly decreasing trend in groundwater level from April 2016 onwards. The change for the Mohlan irrigation subdivision remains positive under all proposed scenarios. Considering the results of overall groundwater level changes, rice crop seems to exert most influence on any change in the upper LCC.

Changes in groundwater level for the rest of the irrigation subdivisions located at middle and lower reaches of LCC show decreasing trends for all scenarios. For these irrigation subdivisions, the largest decrease is observed under the seventh scenario (Table 2). However, the rate of change varies for different irrigation subdivisions, as for instance, the decrease in case of Tarkhani irrigation subdivision is maximum (i.e., 2.6 m) compared with 2.09 m, 1.81 m, 1.38 m, 1.35 m and 0.06 m for Buchiana, Kanya, Bhagat, Tandlianwala, and Paccadala irrigation subdivisions, respectively. This is generally due to a higher difference in crop water use between kharif fodder and rice as well as between kharif fodder and sugarcane mainly in Tarkhani and Buchiana irrigation subdivisions. There are some scenarios wherein groundwater shows a constant trend after April 2021 for the majority of the irrigation subdivisions (e.g., fourth scenario). These irrigation subdivisions include Buchiana, Bhagat, Kanya, and to some extent Tarkhani and Sultanpur. Under the third scenario, an increase in groundwater level is observed wherein there is initially a drop of 0.69 m in groundwater level from base time to April 2021 but later on it rises by 0.15 m till April 2030. The detailed increase/decrease in groundwater levels for various time periods under other scenarios is presented in Figure 7.

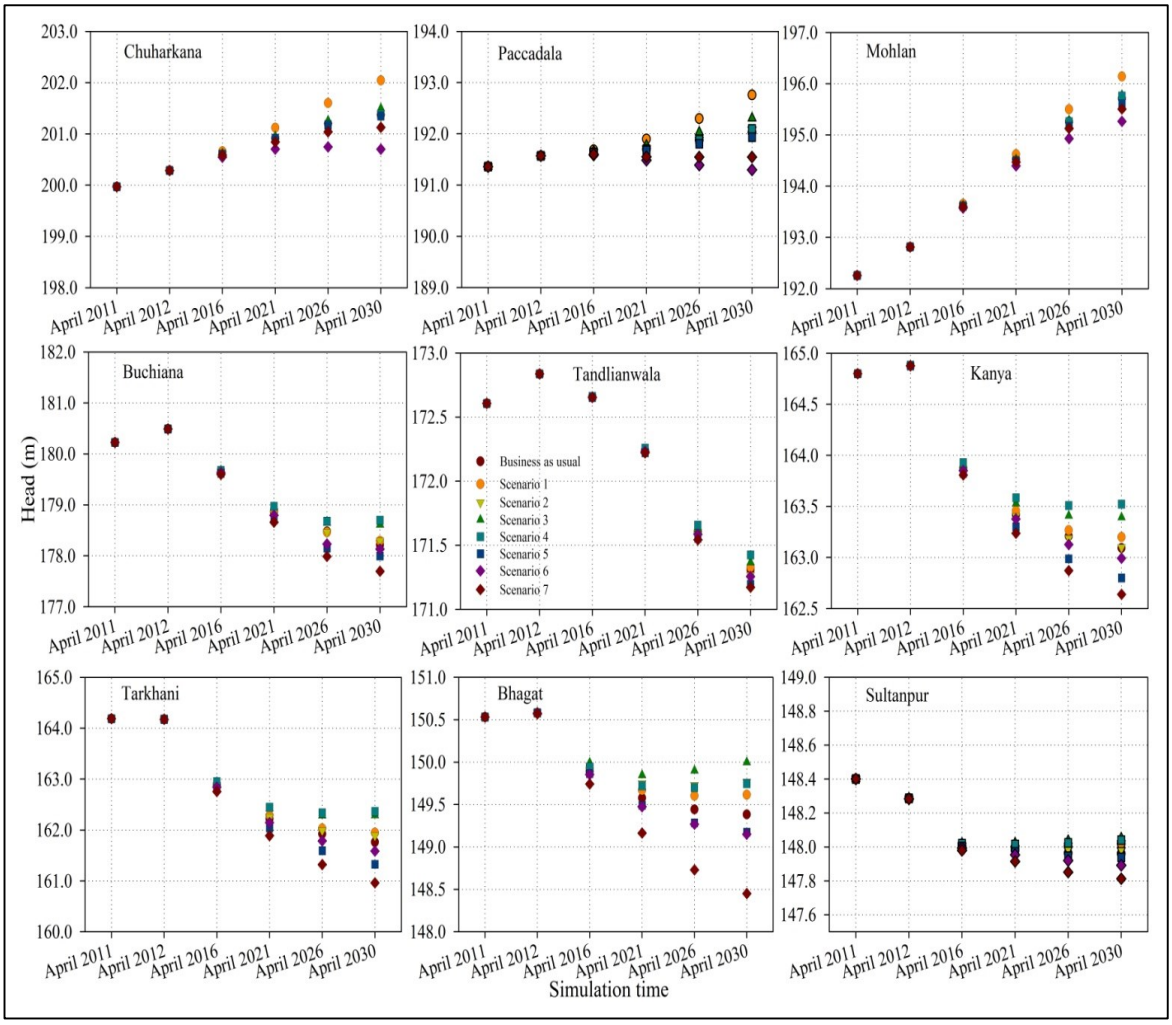

Fig. 7 Groundwater dynamics under changing LULC for different irrigation subdivisions (Please note different vertical scales for each plot)

The preceding discussion on groundwater level results referred to the base time without normalizing the effects under business as usual conditions. The analysis, therefore, is extended to evaluate real time changes through incorporation of these effects. The results so far depict the highest impact on groundwater level in upper irrigation subdivisions through change in rice cultivation (e.g., Scenario 1). The highest positive change is observed in Paccadala (+0.73 m) followed by 0.67 m and 0.43 m for Chuharkana and Mohlan irrigation subdivisions, respectively (Fig. 8). The highest negative change in groundwater level is found under the sixth scenario where an increase in rice area of 25% is proposed. The second major negative change is under the seventh scenario (i.e., 75% decrease in fodder area and its substitution by rice, cotton and sugarcane). Changes under this scenario are equal to -0.48 m, 0.24 m, 0.20 m, and -0.52 m for Paccadala, Chuharkana, Mohlan and Buchiana irrigation subdivisions, respectively. Variation in groundwater level under other scenarios is not so high in upper irrigation subdivisions except for Buchiana where simulated changes are +0.40 m and 0.50 m under third and fourth scenarios, respectively.

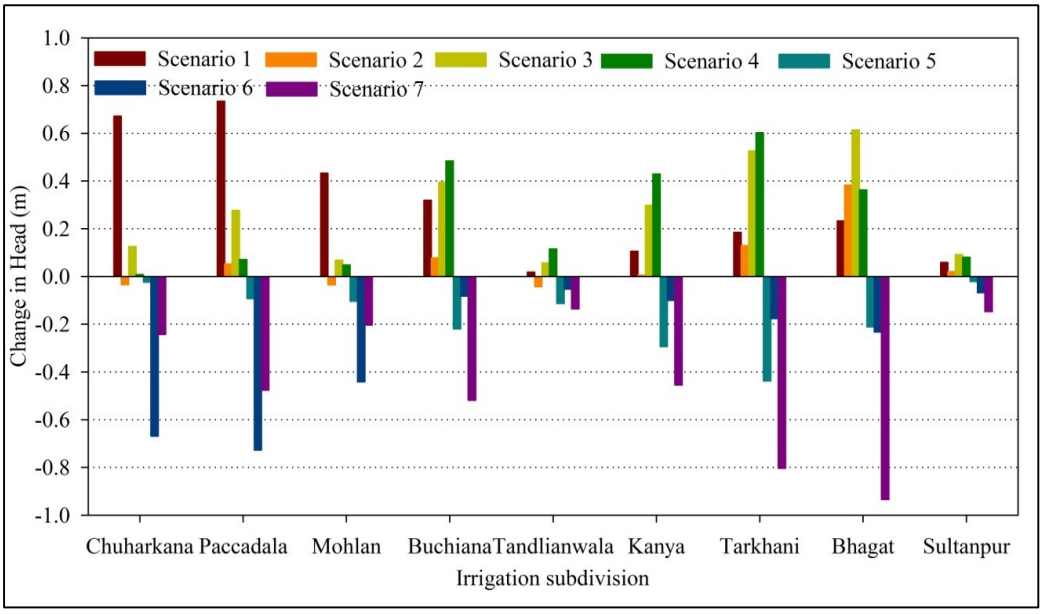

Fig. 8 Change in groundwater level at different irrigation subdivisions after normalizing with respect to business as usual conditions

Fluctuations in groundwater level for lower LCC clearly indicate higher negative changes under the seventh scenario with values of 0.93 m for Bhagat followed by 0.80 m, 0.50 m, 0.15 m and 0.14 m for Tarkhani, Kanya, Sultanpur, and Tandlianwala irrigation subdivisions, respectively. Moreover, a maximum positive change is observed for Bhagat under the third scenario with a value of 0.61 m followed by 0.60 m and 0.43 m for Tarkhani and Kanya, respectively, under fourth scenario.

The summary of results under present LULC scenarios indicates a fluctuation of only ±1 m depth for groundwater level which is almost negligible. It is noteworthy that the majority of proposed LULC changes under different scenarios are based on real trends of actual changes that occurred during last seven years. In order to effectively manage groundwater by changes in LULC, the current cropping patterns would not help achieve this goal. Nevertheless, this goal is achievable through policy intervention and persuasion of farmers to adopt new cropping plans.

3.4.2. Groundwater under changing climate conditions

Results presented in the previous section include groundwater dynamics under proposed LULC changes irrespective of looking at climate change impacts. Here we describe groundwater behaviour under future climate scenarios. For this, actual evapotranspiration and precipitation under H3A2 and H3B2 emission scenarios are used to simulate groundwater from the baseline period to 2045. The temporal and spatial changes in groundwater levels are presented in Figure 9 and in Annex E, respectively. Six different climate change scenarios

are evaluated separately considering actual evapotranspiration, precipitation and the combined effect of both under H3A2 and H3B2 emission scenarios. Table 8 depicts the summary of these scenarios utilized in this study.

Table 8 Detail summary of different climate change scenarios used for present study

No.	Scenario
8	Change in actual evapotranspiration under H3A2
9	Change in actual evapotranspiration under H3B2
10	Change in precipitation under H3A2
11	Change in precipitation under H3B2
12	combined change in precipitation and actual evapotranspiration under H3A2
13	combined change in precipitation and actual evapotranspiration under H3B2

Contrary to the outcomes under LULC scenarios, groundwater seems to be quite dynamic under future climate changes. Two distinct trends in groundwater levels are generally found, according to which groundwater is expected to increase for the majority of regions in/around Chuharkana, Mohlan and Paccadala irrigation subdivisions for all future scenarios. In contrast, there is generally a dropping trend in groundwater between the baseline time period and 2045 for the rest of the regions. Nevertheless, a varying positive or negative change in groundwater level is also observed spatio-temporally in different parts of LCC.

Analysis of groundwater levels for different irrigation subdivisions without normalizing the effects of general groundwater trends (i.e., behaviour under business as usual situations) shows that there is an increase of about 6.62 m for Mohlan followed by 3.95 m and 3.75 m for Paccadala and Chuharkana irrigation subdivisions, respectively, under H3A2 emission scenario. Anticipated changes under H3B2 are 3.36 m, 1.17 m, and -0.76 m for Mohlan, Chuharkana and Paccadala, respectively. The largest negative groundwater change is observed for Tarkhani with values of 7.19 m and 6.85 m under H3B2 and H3A2, respectively. Other prominent changes are in Kanya (-4.76 m and -4.65 m), Buchiana (-5.95 m, -4.18 m), and Bhagat (-3.91 m and -4.38 m) under H3B2 and H3A2 emission scenarios, respectively. Likewise, net changes in groundwater level (i.e., excluding trends for the business as usual case) under different scenarios are also worked out for the whole duration. Accordingly, net changes for Chuharkana (1.71 m), Mohlan (1.91 m) and Paccadala (2.50 m) irrigation subdivisions are positive but with varying amounts compared with those for H3A2. Similarly, changes in groundwater levels for the H3B2 emission scenario are -1.5 m, -2.0 m and -2.54 m for Chuharkana, Mohlan and Paccadala irrigation subdivisions, respectively. Projected changes in groundwater level at lower LCC are -4.27 m and -4.03 m for Tarkhani, -0.72 m and -0.50 m for Tandlianwala, -0.56 m and -0.59 m for Sultanpur, -2.84 m and -2.75 m for Kanya, -2.27 m and -3.54 m for Buchiana, and -3.18 m and -2.90 m for Bhagat under H3A2 and H3B2 emission scenarios, respectively.

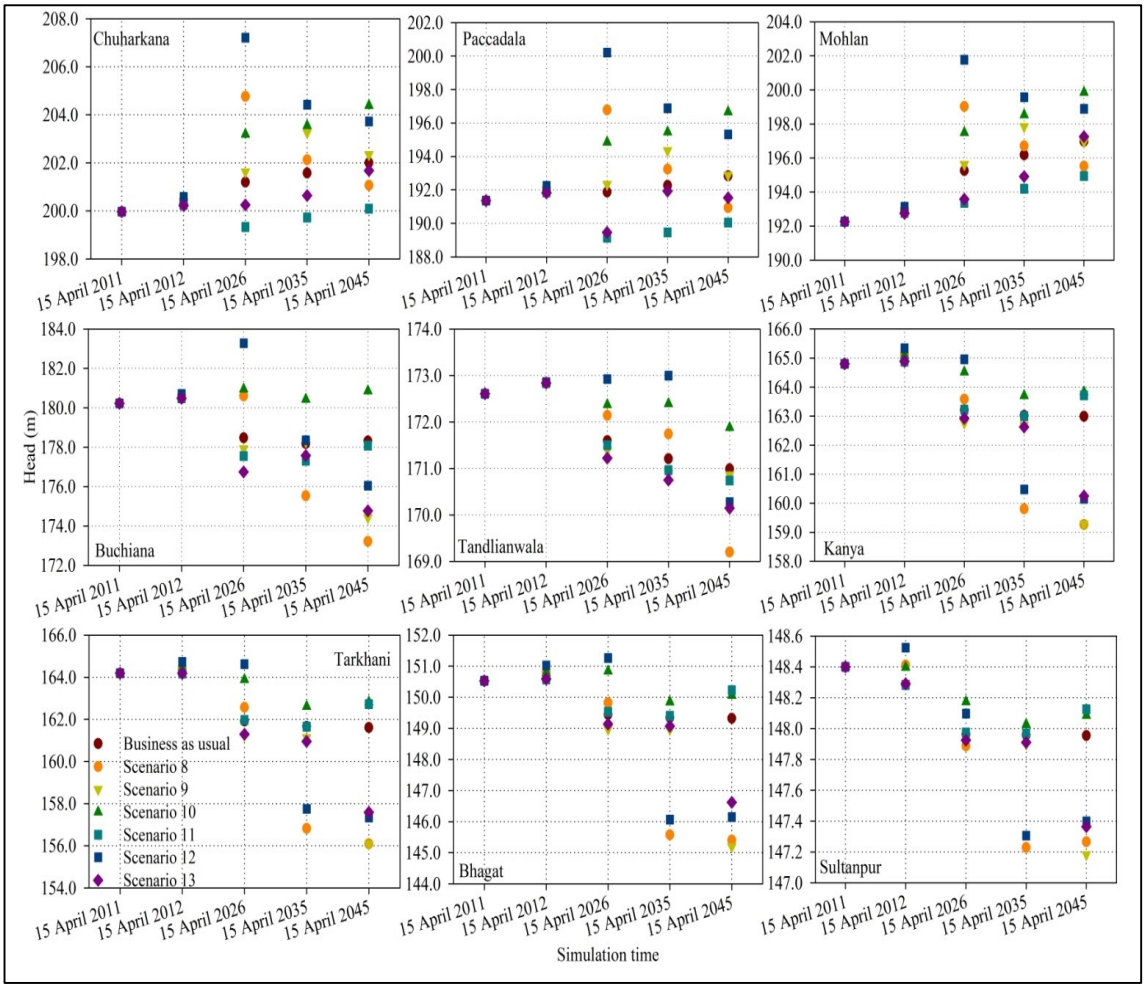

Fig. 9 Groundwater dynamics under future climate change scenarios (Table 8) for LCC irrigation subdivisions from 2011 to 2045 (Please note different vertical scales for each plot)

It is to be noted that the above results are based on the overall study period but these results deviate considerably for various simulation periods. To counter this, results are segregated into several time periods (i.e., 2011 to 2025; 2026 to 2035 and 2036 to 2045) as presented in Figure 10. We draw some valuable information from these results. For instance, groundwater levels in all irrigation subdivisions may rise between 2011 and 2025 under the H3A2 emission scenario. Expected changes in the upper parts would be even higher. These positive changes are due to both lower consumptive water use by crops and increased precipitation in various irrigation subdivisions. They are relatively high in upper parts due to reduced consumptive water use whereas in lower parts it is due to increased precipitation. Consequently, the threat of groundwater shortage is almost non-existent for these parts thus implying that water can be reallocated to surface water-deficit or lower regions. This would not only help to avoid possible water logging in some parts of Mohlan and Paccadala but also conserve groundwater at lower regions for future use where the groundwater table is deeper than in upper regions. This rationality in groundwater utilization during 2011-2025

is expected to facilitate water supply during the periods 2026-2035 and 2036-2045. Consequently, effective water management during 2011-2026 could safeguard against possible water shortages under projected conditions. Another option would be to alter current cropping patterns and grow crops with less water demand along with developing new crop breeds needing less water with no effect on yields.

A more complex groundwater situation is observed under the H3B2 emission scenario where the expected increase in groundwater levels due to future precipitation is almost negligible. Any positive change in groundwater is mainly associated with changes in crop consumptive water use. Such situation requires integrated management of water resources by emphasizing changes in current cropping patterns and creating options to acquire water from additional surface water resources. Nevertheless the situation of river water flow in the country is generally highly variable and uncertain (Bhatti, 1999).

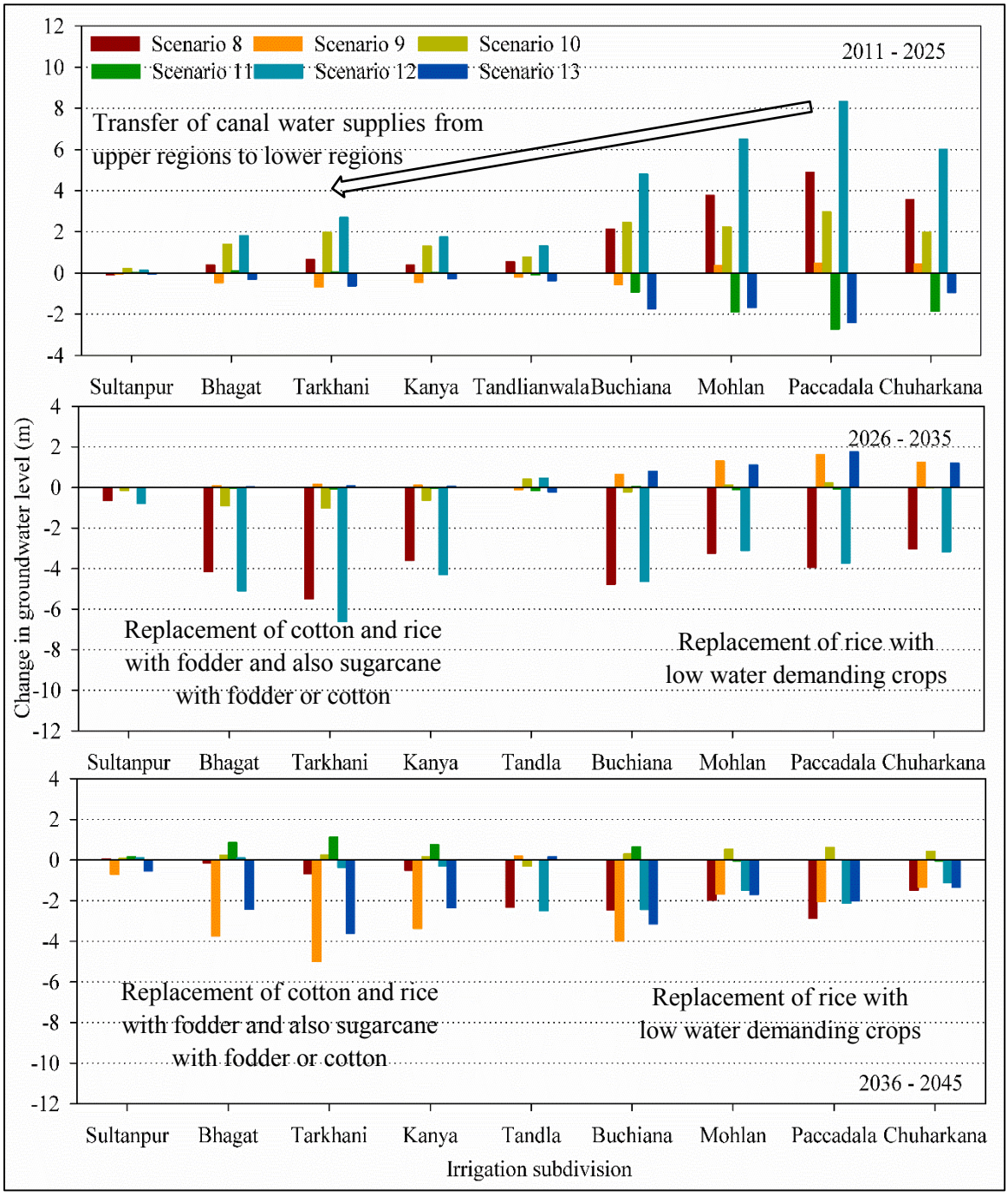

Fig. 10 Groundwater dynamics under future climate scenarios (Table 8) for LCC during specific time periods

4. Conclusions and outlook

Groundwater use constitutes a major input for sustained crop production in Pakistan as groundwater fulfils about half of the crop water requirements in Pakistan (Kazmi et al. 2012). This share continues to increase in the wake of continuously lowering surface water supplies and increasing population. This results in rapid fluctuations in watershed owing to human interferences and natural changes. These changes are even more rapidly happening in irrigated areas, mainly catalyzed by the altering natural environment and incompatible policies.

Such changes generally transpire in the form of changes in land use land cover and climate. There is always a challenge to ascertain their effect on water resources in the future, which is only possible by investigating current resources, establishing a reliable modeling approach and then extending its applicability to future scenarios.

The present study explores changes in land use and climate and their impacts on groundwater dynamics through modelling. For land use classification and change detection, remote sensing data at higher spatial resolutions are used while statistical downscaling techniques are applied for devising future climate change scenarios. Changes in land use / land cover and climate are translated in the form of modified groundwater recharge and this recharge is then utilized in the groundwater flow model in order to explore changes both temporally and spatially. The following conclusions are drawn based on our analysis:

- Downscaling of actual evapotranspiration and precipitation shows improved outcomes for actual evapotranspiration. Bias in SDSM predictions is higher for precipitation than in case of actual evapotranspiration although the bias correction improves results considerably.
- Projected and actual evapotranspiration results at different stations are generally consistent both for rabi and kharif seasons. The only inconsistency is observed for the period 2026-35, where the change at Faisalabad is 2.22% against -0.95%; and for Lahore it is 1.36% against -5.36% under H3A2 and H3B2 emission scenarios, respectively.
- With regard to precipitation, the future change during rabi seasons is inconsistent for both emission scenarios. In case of kharif seasons, the precipitation at both stations is generally increasing for all future periods while being mostly consistent except in 2016-25 at Lahore where there is an increase of 33% for H3A2 and decrease of 13.1% for H3B2 emission.
- The period water budget for LCC shows a total horizontal water inflow of 2844 Mm^3, while the water outflow is 2720.2 Mm^3. The water outflow through pumping from LCC is about 17374.43 Mm^3 while the water inflow through groundwater recharge is about 19933.20 Mm^3. There is a storage change of 2682.87 Mm^3 for whole LCC.
- The rate water budget of LCC shows an average total water inflow into the model domain of about 1.11 x 10^6 m^3/d while an outflow of 1.06 x 10^6 m^3/d is simulated. The average total inflow into the model domain by areal recharge is about 7.80 x 10^6 m^3/d and average total extraction due to pumping is about 6.80 x 10^6 m^3/d.
- Relatively higher Darcy fluxes are found in the third and fourth model layers in lower parts of LCC but in first and second model layers at upper parts of LCC, thus indicating potential zones for groundwater development.
- Change in rice cultivation has the highest impact on groundwater in upper irrigation subdivisions. The groundwater levels for lower LCC regions indicate high negative

changes under decreased fodder area replaced by rice, cotton and sugarcane. The highest positive change is observed for Bhagat under 50% increase in kharif fodder area by major replacement of cotton and rice followed by Tarkhani and Kanya under 30% decrease in sugarcane area by its conversion to kharif fodder, cotton and rice. Fluctuations in groundwater level among different scenarios are within ±1 m, which shows that proposed LULC changes only have limited groundwater management.

- Groundwater dynamics under future climate scenarios shows a rise in groundwater levels for whole LCC from 2011 to 2025 under the H3A2 emission scenario. The changes for upper irrigation subdivisions are relatively higher. These positive changes in different irrigation subdivisions are due to decreased consumptive water use by crops and also due to increased precipitation. However, the change due to consumptive water use is relatively higher in upper parts, and in lower parts it is relatively higher due to increased precipitation.
- Presently there is no threat of groundwater shortage. Rather, there is a need to reallocate surface water resources to supply more water to lower areas and thus to develop groundwater resources in these regions. This activity would also safeguard against any threat of water logging in some parts of upper LCC.
- Judicious utilization of groundwater resources during 2011-2025 is also important considering groundwater behavior for periods 2026-2035 and 2036-2045. During these periods, a drop in groundwater is expected under the H3A2 scenario due to increased consumptive water use by crops and decreased precipitation. Hence, proper water management during 2011-2025 could safeguard against possible water shortages. Another solution could include the alteration of current cropping patterns to grow crops with less water demand. There is also a need to breed similar crops which consume less water without affecting farmer's crop yield.
- Groundwater situation under the H3B2 emission scenario is more complex as compared to H3A2 because a lower rise of groundwater levels due to precipitation is expected. Any positive change in groundwater under this scenario is mainly associated to crop consumptive water use changes. Such situation requires integrated water resources management emphasizing on changes in current crop cultivation patterns and also on water transfer from some additional surface water resources.
- The current modeling setup does not consider any changes in river flow due to climate change effects which need to be further investigated. The climate change scenarios are only based on data from two weather stations. Data availability and quality needs to be improved in future by setting up more weather stations and also by employing dynamical approaches of downscaling. The current groundwater dynamics are studied under changing climate without considering the change in LULC. Further research should be directed to study the system under both climate change and LULC change together.

References

Akhtar M, Ahmad N, Booij MJ (2008) The impact of climate change on the water resources of Hindukush–Karakorum–Himalaya region under different glacier coverage scenarios. Journal Hydrology 355 (1–4):148–163. doi:10.1016/j.jhydrol.2008.03.015

Albhaisi M, Brendonck L, Batelaan O (2013) Predicted impacts of land use change on groundwater recharge of the upper Berg catchment, South Africa. Water SA (39): 211–220. doi:10.4314/wsa.v39i2.4

Alley WM, Reilly TE, Franke OL (1999) Sustainability of ground-water resources. 1186, 79 pp.. US GeolSurvCirc 1186, 79 pp

Awan UK, Ismaeel A (2014) A new technique to map groundwater recharge in irrigated areas using a SWAT model under changing climate. Journal of Hydrology, (519): 1368–1382. doi:10.1016/j.jhydrol.2014.08.049

Bahremand A, Smedt FDE (2006) Parameter sensitivity and uncertainty analysis of the WetSpa model using PEST 2006, 26–35

Bastiaanssen WGM, Menenti M, Feddes RA, et al (1998b) A remote sensing surface energy balance algorithm for land (SEBAL) formulation. J. Hydrol., (212/213): 198-212

Batelaan O, De Smedt F, Triest L (2003) Regional groundwater discharge: phreatophyte mapping, groundwater modelling and impact analysis of land-use change. Journal of Hydrology 275 (1–2): 86–108

Batelaan O, Desmedt F (2007) GIS-based recharge estimation by coupling surface–subsurface water balances. Journal of Hydrology (337): 337–355. doi:10.1016/j.jhydrol.2007.02.001

Bhatti MA (1999) Water resource system of Pakistan: status and issues. Pakistan Science Foundation, Islamabad, ISBN: 969-8040 -14 -5, 729

Bosch JM, Hewlett JA (1982) A review of catchment experiments to determine the effect of vegetation changes on water yield and evapotranspiration, Journal of Hydrology (55): 3-23

Bronstert A (2004) Rainfall-runoff modeling for assessing impacts of climate and land-use change. Hydrological Processes (18): 567–570

Brown AE, Zhang L, McMahon TA, Western AW, Vertessy RA (2005) A review of paired catchment studies for determining changes in water yield resulting from alterations in vegetation. Journal of Hydrology (310): 28–61

Bultot F, Dupriez GL, Gellens D (1990) Simulation of land use changes and impacts on the water balance: a case study for Belgium, J. Hydrol., (114): 327–348

Buytaert W, Celleri R, Timbe L (2009) Predicting climate change impacts on water resources in the tropical Andes: Effects of GCM uncertainty. Geophysical Research Letters (36): L07406

Calder IR (1993) Hydrologic effects of land-use change, in: Handbook of hydrology, edited by: Maidment, D. R., McGraw-Hill, New York, USA, 13.1-13.50, 1993

Chu JT, Xia J, Xu CY, Singh VP (2010) Statistical downscaling of daily mean temperature, pan evaporation and precipitation for climate change scenarios in Haihe River, China. Theor Appl Climatology (99): 149–161

Chu JT, Xia J, Xu CY, Singh VP (2010) Statistical downscaling of daily mean temperature, pan evaporation and precipitation for climate change scenarios in Haihe, China. Theoretical and Applied Climatology (99):149–161

Costanza R, d'Arge R, de Groot RS, et al (1997) The total value of the world's ecosystem services and natural capital. Nature (387): 253–260

Crosbie R, McCallum J, Harrington G (2009) Diffuse groundwater recharge modelling across northern Australia. Russell The Journal Of The Bertrand Russell Archives.

Dams J, Woldeamlak ST, Batelaan O (2008) Predicting land-use change and its impact on the groundwater system of the Kleine Nete catchment, Belgium. Hydrol. Earth Syst. Sci. (12): 1369–1385

Diaz-Nieto J, Wilby RL (2005) A comparison of statistical downscaling and climate change factor methods: impacts on low flows in the River Thames, United Kingdom. Clim Chang 69(2): 245–268. doi:10.1007/s10584-005-1157-6

Dibike YB, Coulibaly P (2005) Hydrologic impact of climate change in the Saguenay watershed: comparison of downscaling methods and hydrologic models. J Hydrol, 307(1–4): 145–163. doi:10.1016/ j.hydrol.2004.10.012

Elshamy ME, Seierstad IA, Sorteberg A (2009) Impacts of climate change on Blue Nile flows using bias-corrected GCM scenarios. Hydrol Earth Syst Sci (13): 551–565. doi:10.5194/hess-13-551- 2009

Fowler HJ, Blenkinsop S, Tebaldi C (2007) Linking climate change modelling to impacts studies: recent advances in downscaling techniques for hydrological modelling. International Journal of Climatology 27(12): 1547–1578

Gagnon S, Singh B, Rousselle J, Roy L (2005) An application of the statistical downscaling model (SDSM) to simulate climatic data for streamflow modelling in Québec. Canad Water Resour J, 30 (4): 297–314. doi:10.4296/cwrj3004297

Gebremeskel S, Liu YB, de Smedt F, Hoffmann L, Pfister L (2005) Analyzing the effect of climate changes on streamflow using statistically downscaled GCM scenarios. Int. J. River Basin Manag. 2(4):271–280. doi:10.1080/15715124.2004.9635237

Gellens D, Roulin E (1998) Stream flow response of Belgian catchments to IPCC climate change scenarios. J Hydrol, 210(1–4): 242– 258. doi:10.1016/s0022-1694(98)00192-9.

Giorgi F, Hewitson B, Christensen J, Hulme M, Von Storch H, Whetton P, Jones R, Mearns L, Fu C (2001) Regional Climate Information – Evaluation and Projections. In: Climate Change 2001: The Scientific Basis. Contribution of Working Group I to the Third Assessment Report of the Intergovernmental Panel on Climate Change [Houghton, J.T.,Y. Ding, D.J. Griggs, M. Noguer, P.J. van der Linden, X. Dai, K. Maskell, and C.A. Johnson (eds.)]. Cambridge University Press, Cambridge, United Kingdom and New York, NY, USA, 881pp

Gleeson T, Alley WM, Allen DM, Sophocleous MA, Zhou Y, Taniguchi M, Vander Steen J (2012) Towards sustainable groundwater use: setting long-term goals, back casting, and managing adaptively. Ground Water 50 (1): 19–26

Good P, Lowe JA, Rowell DP (2009) Understanding uncertainty in future projections for the tropical Atlantic: Relationships with the unforced climate. Climate Dynamics, (32): 205–218

Hashmi M, Shamseldin A, Melville B (2011) Comparison of SDSM and LARS-WG for simulation and downscaling of extreme precipitation events in a watershed. Stoch Env Res Risk A 25 (4):475–484. doi:10.1007/s00477-010-0416-x

Hay LE, Clark MP (2003) Use of statistically and dynamically downscaled atmospheric model output for hydrologic simulations in three mountainous basins in the western United States. J Hydrol, 282(1–4): 56–75. doi:10.1016/s0022-1694(03)00252-x

Hetze F, Vaessen V, Himmelsbach T, Struckmeier W, Villholth K (2008) Groundwater and climate change: Challenges and possibilities

Holland MM, Serreze MC, Stroeve J (2010) The sea ice mass budget of the Arctic and its future change as simulated by coupled climate models. Climate Dynamics (34): 185–200

Hornbeck JW, Adams MB, Corbett ES, Verry ES, Lynch JA (1993) Long-term impacts of forest treatments on water yield: A summary for north-eastern USA, Journal of Hydrology, 150(2–4): 323–344

Huang J, Zhang J, Zhang Z, Xu C,Wang B, Yao J (2011) Estimation of future precipitation change in the Yangtze River basin by using statistical downscaling method. Stoch Env Res Risk A 25(6):781– 792. doi:10.1007/s00477-010-0441-9

Huth R (2002) Statistical downscaling of daily temperature in Central Europe. J Clim 15(13): 1731–1742. doi:10.1175/1520-0442 (2002)015<1731:sdodti>2.0.co;2

IPCC (2007) Climate Change 2007: The Physical Science Basis. Contribution of Working Group I to the Fourth Assessment Report of the Intergovernmental Panel on Climate Change, Solomon, S., Qin, D., Manning, M., Chen, Z., Marquis, M., Averyt, K. B., Tignor, M. & Miller, H. L., (Eds.), Cambridge University Press, Cambridge, UK and NY, USA, 996 pp.

IPCC (2008) Climate Change and Water. IPCC Technical Paper VI. Available at: http://www.ipcc.ch/pdf/technical-papers/climate-change-water-en.pdf

Khan MS, Coulibaly P, Dibike Y (2006) Uncertainty analysis of statistical downscaling methods. J Hydrol, 319(1–4): 357–382. doi:10.1016/j.jhydrol.2005.06.035

Klöcking B, Haberlandt U (2002) Impact of land use changes on water dynamics – a case study in temperate meso and macroscale river basins. Phys. Chem. Earth (27): 619–629

Mahmood R, Babel MS (2013) Evaluation of SDSM developed by annual and monthly submodels for downscaling temperature and precipitation in the Jhelum basin, Pakistan

and India. Theoretical and Applied Climatology (113): 27–44. doi:10.1007/s00704-012-0765-0

McColl C, Aggett G (2007) Land-use forecasting and hydrologic model integration for improved land-use decision support, J. Environ. Management (84): 494–512.

Pallant J (2007) SPSS Survival Manual: a step by step guide to data analysis using the SPSS for windows

Robinson M, Cognard-Plancq AL, Cosandey C, David J, Du- rand P, Fuhrer HW, Hall R., Hendriques MO, Marc V, McCarthy R, McDonnell M, Martin C, Nisbet T, O'Dea TP, Rodgers M, Zollner A (2003) Studies of the impact of forests on peak flows and base flows: A European perspective, Forest Ecology (186): 85–97

Salzmann N, Frei C, Vidale PL, Hoelzle M (2007) The application of Regional Climate Model output for the simulation of high-mountain permafrost scenarios. Global Planet Chang 56(1–2): 188–202. doi:10.1016/j.gloplacha.2006.07.006

Sarwar A, Eggers H (2006) Development of a conjunctive use model to evaluate alternative management options for surface and groundwater resources. Hydrogeology Journal (14): 1676–1687. doi:10.1007/s10040-006-0066-8

Sunyer MA, Madsen H, Ang PH (2011) A comparison of different regional climate models and statistical downscaling methods for extreme rainfall estimation under climate change. Atmos Res. doi:10.1016/j.atmosres.2011.06.011

Tang Z, Engel BA, Pijanowski BC, Lim KJ (2005) Forecasting land use change and its environmental impact at a watershed scale, J. Environ. Management (76): 35–45

Taylor AB, Martin NA, Everard E, Kelly TJ (2012) Modelling the Vale of St Albans: parameter estimation and dual storage. In: Shepley, M. G., Whiteman, M. I., Hulme,P.J.& Grout,M. W. (eds) Groundwater Resources Modelling: A Case Study from the UK. Geological Society, London, Special Publications (364): 193–204

Taylor RG, Scanlon B, Doll P, Rodell M, van Beek R, Wada Y, Longuevergne L, Leblanc M, Famiglietti JS, Edmunds M, Konikow L, Green TR, Chen J, Taniguchi M, Bierkens MFP, MacDonald A, Fan Y, Maxwell RM, Yechieli Y, Gurdak JJ, Allen DM., Shamsudduha M, Hiscock K, Yeh PJF, Holman I, Treidel H (2013) Ground water and climate change. Nature Climate Change (3): 322–329. doi:10.1038/nclimate1744

Tong STY, Liu AJ (2006) Modelling the hydrologic effects of land-use and climate changes, Int J. Risk Assess. Management 6(4– 5): 344–368

UNEP/CBD (United Nations Environment Programme/Convention of Biological Diversity) (2010) In depth review of the program of the work on the biological diversity of inland water ecosystems. In: Prepared for 14th Meeting, Nairobi, 10–12 May 2010

Usman M, Kazmi I, Khaliq T (2012) Variability in water use, crop water productivity and profitability of rice and wheat in Rechna doab, Punjab, Pakistan. Journal of Plant and Animal Sciences (22): 998–1003

Usman M, Liedl R, Awan UK (2015a) Spatio-temporal estimation of consumptive water use for assessment of irrigation system performance and management of water resources in irrigated Indus Basin, Pakistan. Journal of Hydrology. doi:10.1016/j.jhydrol.2015.03.031.

Usman M, Liedl R, Kavousi A (2015b) Estimation of distributed seasonal net recharge by modern satellite data in irrigated agricultural regions of Pakistan. Environmental Earth Sciences. doi:10.1007/s12665-015-4139-7

Usman M, Liedl R, Shahid MA, Abbas A (2015c) Land use / land cover classification and its change detection using multi-temporal MODIS NDVI data. Journal of Geographical Sciences 25, 1479–1506. doi:10.1007/s11442-015-1247-y

Usman M, Liedl R, Shahid MA (2014) Managing Irrigation Water by Yield and Water Productivity Assessment of a Rice-Wheat System Using Remote Sensing. Journal of Irrigation and Drainage Engineering. doi:10.1061/(ASCE)IR.1943-4774.0000732

Wegehenkel M (2009) Modeling of vegetation dynamics in hydrological models for the assessment of the effects of climate change on evapotranspiration and groundwater recharge. Adv. Geosci. (21): 109–115. doi:10.5194/adgeo-21-109-2009

Wetterhall FA, Bárdossy D, Chen SH, Xu CY (2006) Daily precipitation-downscaling techniques in three Chinese regions. Water Resources Research, 42:W11423. doi:10.1029/2005WR004573

Wiens JA, Stralberg D, Jongsomjit D, Howell CA, Snyder MA (2009) Niches, models, and climate change: Assessing the assumptions and uncertainties. In: Biogeography, changing climates, and niche evolution. Proceedings of an Arthur M. Sackler Colloquium of the National Academy of Sciences, Irvine, California, USA, 11–13 December 2008. Washington, DC: National Academy of Sciences, 19729–19736

Wilby RL, Wigley TML (1997) Downscaling general circulation model output: a review of methods and limitations. Prog Phys Geog, (21): 530–548. doi:10.1177/030913339702100403

Wilby RL, Harris I (2006) A framework for assessing uncertainties in climate change impacts: low-flow scenarios. Water Resour Res, 42, W02419. doi:10.1029/2005WR004065

Wilby RL, Dawson CW (2013) The statistical downscaling model: Insights from one decade of application. International Journal of Climatology (33): 1707–1719. doi:10.1002/joc.3544

Wilby RL, Hay LE, Leavesley GH (1999) A comparison of downscaled and raw GCM output: implications for climate change scenarios in the San Juan River basin, Colorado. Journal of Hydrology (225): 67-91

Wilby RL, Hay LE, Gutowski WJ, Arritt RW, Takle ES, Pan Z, Leavesley GH, Martyn PC (2000) Hydrological responses to dynamically and statistically downscaled climate model output. Geophysical Research Letters 27(8): 1199. doi:10.1029/1999GL006078

Xu CY (1999) Climate change and hydrologic models: a review of existing gaps and recent research developments. Water Resources Management 13(5): 369–382. doi:10.1023/a:1008190900459

Yang W, Bárdossy A, Caspary HJ (2010) Downscaling daily precipitation time series using a combined circulation- and regression- based approach. Theor Appl Climatol, 102(3–4): 439–454. doi:10.1007/s00704-010-0272-0

Wu F, Zhan J, Su H, Yan H, Ma E (2014) Scenario-based impact assessment of land use / cover and climate changes on watershed hydrology in Heihe river basin of Northwest China. Advances in Meteorology, Article ID 410198

Zhao L, Xia J, Xu C, Wang Z, Sobkowiak L, Long C (2013) Evapotranspiration estimation methods in hydrological models. Journal of Geographical Sciences (23): 359–369. doi:10.1007/s11442-013-1015-9

Annex B

Model output sensitivities and parameter error

Annex B-1 Output sensitivity for hydraulic conductivity and drain/fillable porosity

Coordinates		For hydraulic conductivity				
X	Y	Layer 1	Layer 2	Layer 3	Layer 4	Pilot Point ID
385837.0000	3535973.0000	0.011	0.010	0.010	0.016	C-14
379119.0000	3519310.0000	0.018	0.010	0.010	0.038	D-11
360731.0000	3496813.0000	0.218	0.199	0.074	0.121	E-13
309050.0000	3431319.0000	0.010	0.010	0.012	0.012	E-15
381390.7000	3477821.1000	0.011	0.013	0.010	0.021	E-4
374314.7000	3497970.2000	0.110	0.111	0.041	0.053	E-9
368972.8000	3465441.9000	0.021	0.010	0.010	0.012	F-5
357769.1000	3467472.7000	0.037	0.016	0.017	0.024	F-8
334029.6900	3434557.8900	0.010	0.010	0.010	0.011	G-1
326778.7400	3434895.6000	0.010	0.010	0.011	0.011	G-3
313568.9000	3438446.4000	0.010	0.010	0.012	0.011	G-6
277645.4800	3386566.6500	0.010	0.010	0.013	0.013	H-1
242063.2000	3407439.3000	0.010	0.010	0.010	0.010	H-12
278134.1000	3391658.4000	0.010	0.010	0.019	0.011	H-2
265783.4600	3410222.0400	0.010	0.010	0.015	0.013	H-6
256552.8000	3404326.9000	0.010	0.010	0.013	0.011	H-8
337716.6900	3457008.7600	0.010	0.010	0.010	0.010	LRR-13
314109.9600	3420251.0700	0.010	0.010	0.012	0.011	LRR-17
367411.7000	3477434.9600	0.031	0.016	0.015	0.061	S.T.H-16
350872.0800	3484310.5000	0.252	0.089	0.085	0.092	S.T.H-21
379969.5600	3519189.2000	0.016	0.010	0.010	0.029	S.T.H-34
367738.6300	3473217.9500	0.017	0.010	0.010	0.027	S.T.H-56
368119.9000	3510686.3000	0.156	0.130	0.047	0.133	S.T.H-58
240358.0588	3394934.4869	0.010	0.010	0.010	0.010	1
258299.9188	3394934.4869	0.010	0.010	0.013	0.010	2
276241.8188	3394934.4869	0.010	0.010	0.019	0.011	3
240358.0588	3412876.3269	0.010	0.010	0.010	0.010	4
258299.9188	3412876.3269	0.010	0.010	0.014	0.013	5
276241.8188	3412876.3269	0.010	0.010	0.016	0.015	6
294183.7188	3412876.3269	0.010	0.010	0.018	0.013	7
312125.5188	3412876.3269	0.011	0.010	0.011	0.011	8
276241.8188	3430818.2269	0.010	0.010	0.013	0.014	9
294183.7188	3430818.2269	0.010	0.010	0.014	0.015	10
312125.5188	3430818.2269	0.010	0.010	0.011	0.012	11
330067.4188	3430818.2269	0.010	0.010	0.010	0.011	12
312125.5188	3448760.1269	0.010	0.010	0.013	0.012	13

330067.4188	3448760.1269	0.010	0.010	0.011	0.011	14
348008.9188	3448760.1269	0.010	0.010	0.010	0.010	15
330067.4188	3466702.0269	0.010	0.010	0.011	0.010	16
348008.9188	3466702.0269	0.010	0.010	0.010	0.010	17
365950.9188	3466702.0269	0.022	0.010	0.010	0.010	18
348008.9188	3484643.8269	0.267	0.090	0.090	0.090	19
365950.9188	3484643.8269	0.010	0.010	0.010	0.090	20
383892.9188	3484643.8269	0.010	0.014	0.010	0.010	21
348008.9188	3502586.1269	0.268	0.266	0.090	0.271	22
365950.9188	3502586.1269	0.267	0.267	0.090	0.091	23
383892.9188	3502586.1269	0.010	0.010	0.010	0.010	24
365950.9188	3520528.1269	0.089	0.010	0.010	0.269	25
383892.9188	3520528.1269	0.010	0.010	0.010	0.010	26
383892.9188	3538469.1269	0.010	0.010	0.010	0.013	27

Output sensitivity for drain/fillable porosity

Coordinates		**For drain/fillable porosity**				
X	**Y**	**Layer 1**	**Layer 2**	**Layer 3**	**Layer 4**	**Pilot Point ID**
380150.000	3542691.000	0.0156	0.0144	0.0144	0.0144	C-16
379119.000	3519310.000	0.0155	0.0144	0.0144	0.0144	D-11
369775.000	3499135.000	0.0156	0.0144	0.0144	0.0144	E-11
360731.000	3496813.000	0.0357	0.0144	0.0146	0.0144	E-13
309050.000	3431319.000	0.0148	0.0144	0.0146	0.0144	E-15
374314.700	3497970.200	0.0161	0.0144	0.0144	0.0144	E-9
364981.700	3465936.060	0.0155	0.0144	0.0146	0.0144	F-6
353361.300	3465316.000	0.0149	0.0144	0.0144	0.0144	F-9
326778.740	3434895.600	0.0148	0.0144	0.0144	0.0144	G-3
313568.900	3438446.400	0.0147	0.0144	0.0145	0.0144	G-6
277645.480	3386566.650	0.0149	0.0144	0.0149	0.0144	H-1
278866.600	3399296.100	0.0146	0.0144	0.0206	0.0144	H-3
275279.300	3406469.090	0.0146	0.0144	0.0214	0.0144	H-5
256552.800	3404326.900	0.0147	0.0144	0.0208	0.0144	H-8
338673.200	3444797.600	0.0146	0.0144	0.0144	0.0144	LRR-14
314109.960	3420251.070	0.0146	0.0144	0.0147	0.0144	LRR-17
367411.700	3477434.960	0.0157	0.0144	0.0145	0.0144	S.T.H-16
350872.080	3484310.500	0.0896	0.0144	0.0150	0.0144	S.T.H-21
335306.200	3461259.670	0.0352	0.0144	0.0146	0.0144	S.T.H-3
372613.980	3498545.300	0.0159	0.0144	0.0144	0.0144	S.T.H-43
369975.000	3492369.550	0.0160	0.0144	0.0144	0.0144	S.T.H-57
376276.280	3526993.770	0.0155	0.0144	0.0144	0.0144	S.T.H-63
242164.819	3395297.347	0.0145	0.0144	0.0148	0.0144	1
263720.319	3395297.347	0.0148	0.0144	0.0199	0.0144	2
252942.619	3413964.927	0.0148	0.0144	0.0235	0.0144	3
274498.019	3413964.927	0.0145	0.0144	0.0221	0.0144	4
296053.519	3413964.927	0.0145	0.0144	0.0170	0.0144	5

317609.019	3413964.927	0.0145	0.0144	0.0145	0.0144	6
285275.819	3432632.527	0.0155	0.0144	0.0156	0.0144	7
306831.319	3432632.527	0.0148	0.0144	0.0146	0.0144	8
328386.719	3432632.527	0.0148	0.0144	0.0144	0.0144	9
317609.019	3451300.127	0.0146	0.0144	0.0144	0.0144	10
339164.919	3451300.127	0.0145	0.0144	0.0144	0.0144	11
349941.919	3469967.727	0.0148	0.0144	0.0144	0.0144	12
371497.919	3469967.727	0.0155	0.0144	0.0146	0.0144	13
339164.919	3488635.127	0.2674	0.0144	0.0165	0.0144	14
360719.919	3488635.127	0.0150	0.0144	0.0144	0.0144	15
382275.919	3488635.127	0.0185	0.0144	0.0144	0.0144	16
371497.919	3507303.127	0.0150	0.0144	0.0144	0.0144	17
382275.919	3525970.127	0.0154	0.0144	0.0144	0.0144	18

Annex B-2 Parameter error (%) for hydraulic conductivity and drain/fillable porosity

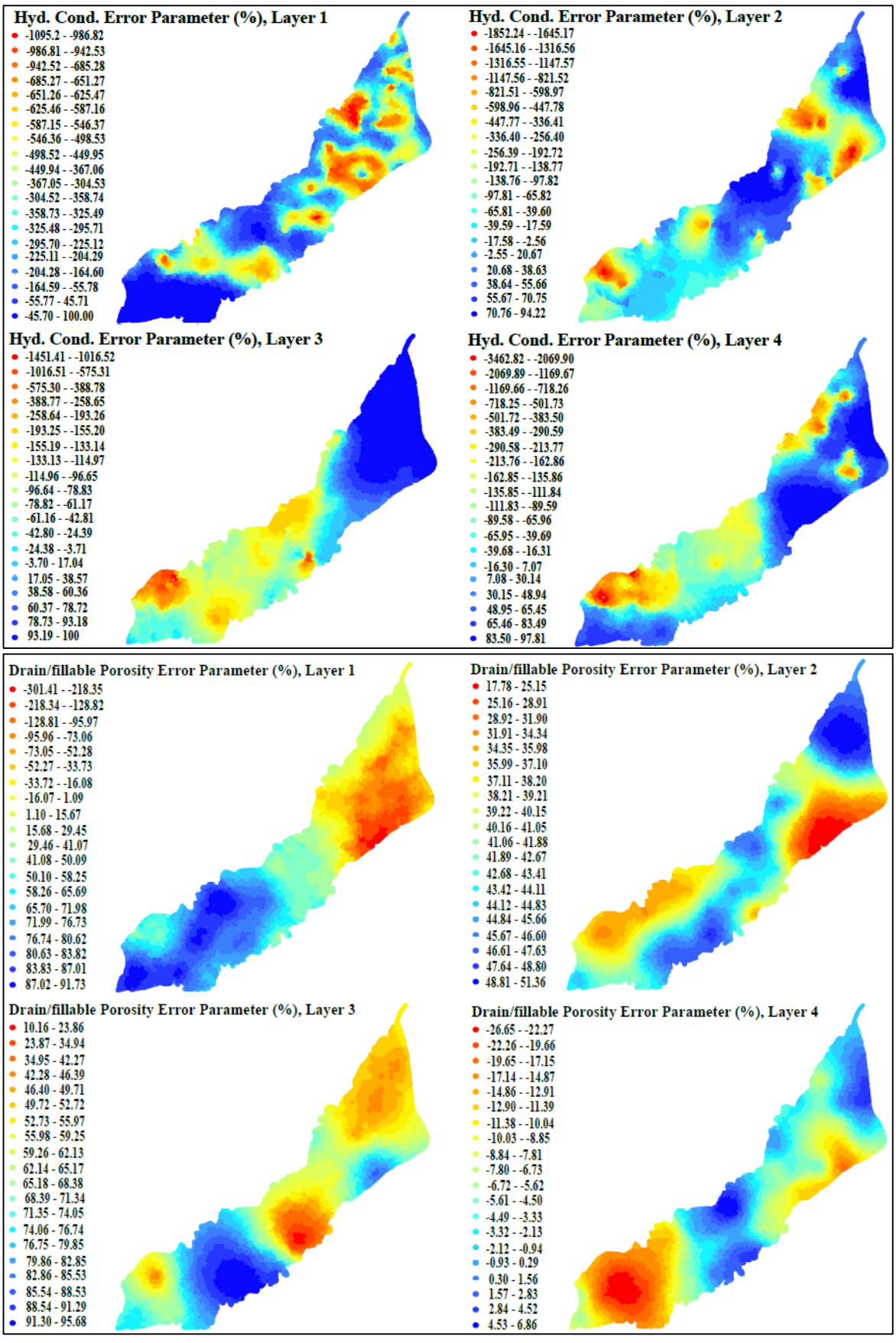

Annex C

Screening of predictors

Annex C-1 Precipitation at Faisalabad

No.	Predictor Name	R_1 (%)	R_2 (%)	P_r (%)	p-value	PRP (%)
1	ncep_shum*	**29.0**				
2	ncep_mslp	26.8	75.4	16.8	0.000	37.31
3	ncep_p850	25.2	61.5	6.00	0.000	76.19
4	ncep_temp	24.8	73.6	35.6	0.000	43.55
5	ncep_p500	23.9	72.2	56.3	0.000	135.5
6	ncep_p5_u	22.2	66.4	11.1	0.000	50.00
7	ncep_p_z	21.5	61.9	39.9	0.000	85.58
8	ncep_p5_f	18.9	65.2	9.30	0.000	50.79
9	ncep_p5_z**	15.3	39.5	21.0	0.000	**37.26**
10	ncep_p5th	14.4	41.3	5.70	0.000	60.42
11	ncep_p8_v	14.4	48.9	0.70	0.410	95.14
12	ncep_p_u	12.6	43.6	3.30	0.004	73.81
*super predictor **second predictor						

Annex C-2 Actual evapotranspiration at Lahore

No.	Predictor Name	R_1 (%)	R_2 (%)	P_r (%)	p-value	PRP (%)
1	ncep_temp*	**77.5**				
2	ncep_p_v	74.4	87.9	0.20	0.542	99.73
3	ncep_mslp	73.1	88.9	41.2	0.000	43.63
4	ncep_p_f	70.1	74.1	0.90	0.310	98.71
5	ncep_p_u	68.5	70.1	15.4	0.000	77.51
6	ncep_p500	60.6	85.4	15.4	0.000	74.58
7	ncep_p_th	58.2	69.4	3.40	0.0002	94.15
8	ncep_p_zh	54.4	69.3	4.40	0.000	91.91
9	ncep_p850	53.2	64.9	26.5	0.000	50.18
10	ncep_rhum	51.9	42.7	36.2	0.000	30.25
11	ncep_r850	51.5	37.4	27.2	0.000	47.18
12	ncep_shum**	46.3	79.4	51.3	0.000	**10.79**
*super predictor **second predictor						

Annex C-3 Actual evapotranspiration at Faisalabad

No.	Predictor Name	R_1 (%)	R_2 (%)	P_r (%)	P value	PRP (%)
1	ncep_temp*	**82.2**				
2	ncep_mslp**	78.1	91.9	75.1	0.000	**3.84**
3	ncep_p_z	72.2	83.5	62.8	0.000	13.02
4	ncep_p_u	71.6	75.1	1.80	0.060	97.49
5	ncep_p_f	70.2	72.8	10.3	0.000	85.33
6	ncep_p500	62.7	84.6	31.2	0.000	50.24
7	ncep_p850	60.3	69.5	53.8	0.000	10.78
8	ncep_shum	51.6	73.6	30.3	0.000	41.28
9	ncep_p8_f	49.5	53.8	3.70	0.0001	92.53
10	ncep_p5_f	47.1	62.9	0.20	0.547	99.58
11	ncep_r850	47.1	46.7	3.40	0.0002	92.78
12	ncep_p5_u	46.9	63.9	10.0	0.000	78.68
*super predictor **second predictor						

Annex D

Distribution of Darcy fluxes in different model layers

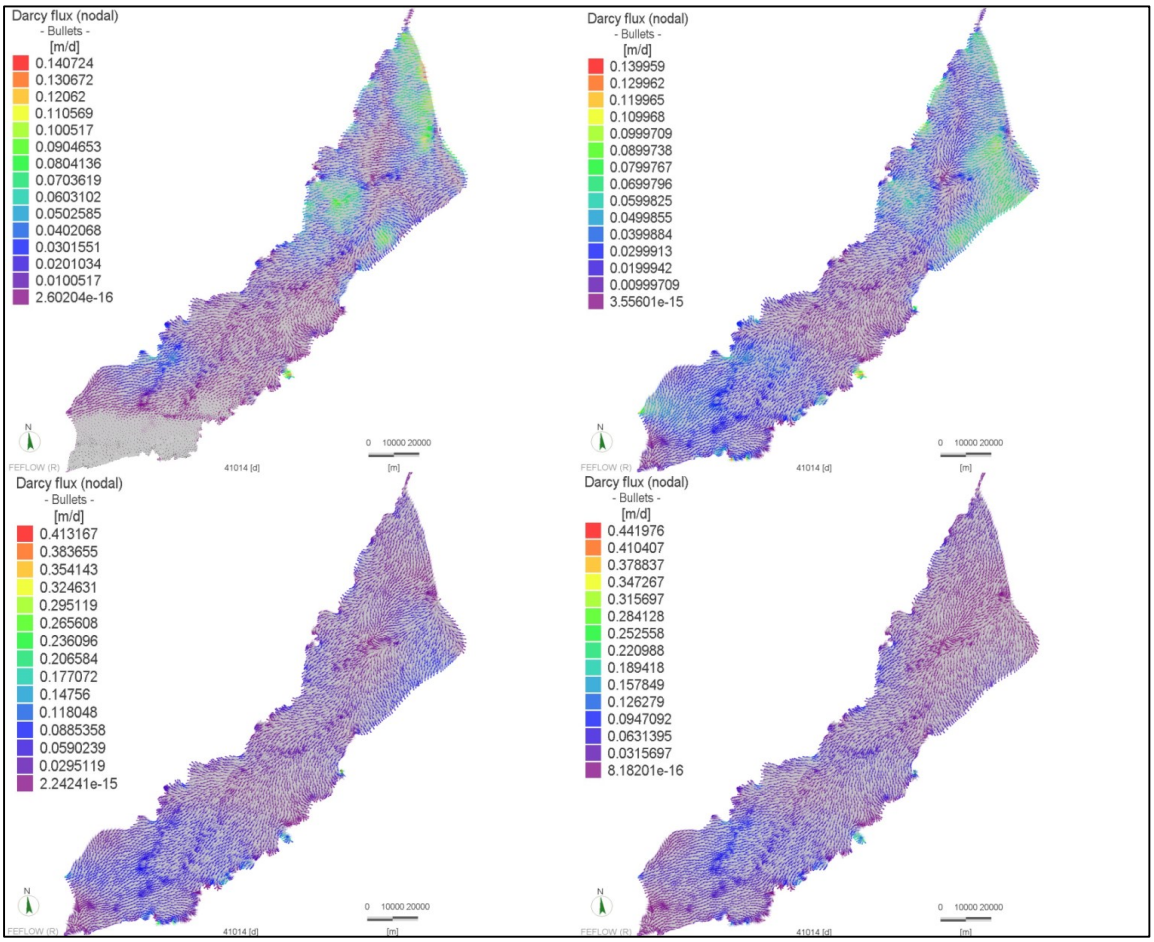

Annex E

Change in groundwater head (m) for different simulation times reference to baseline

Scenario 1

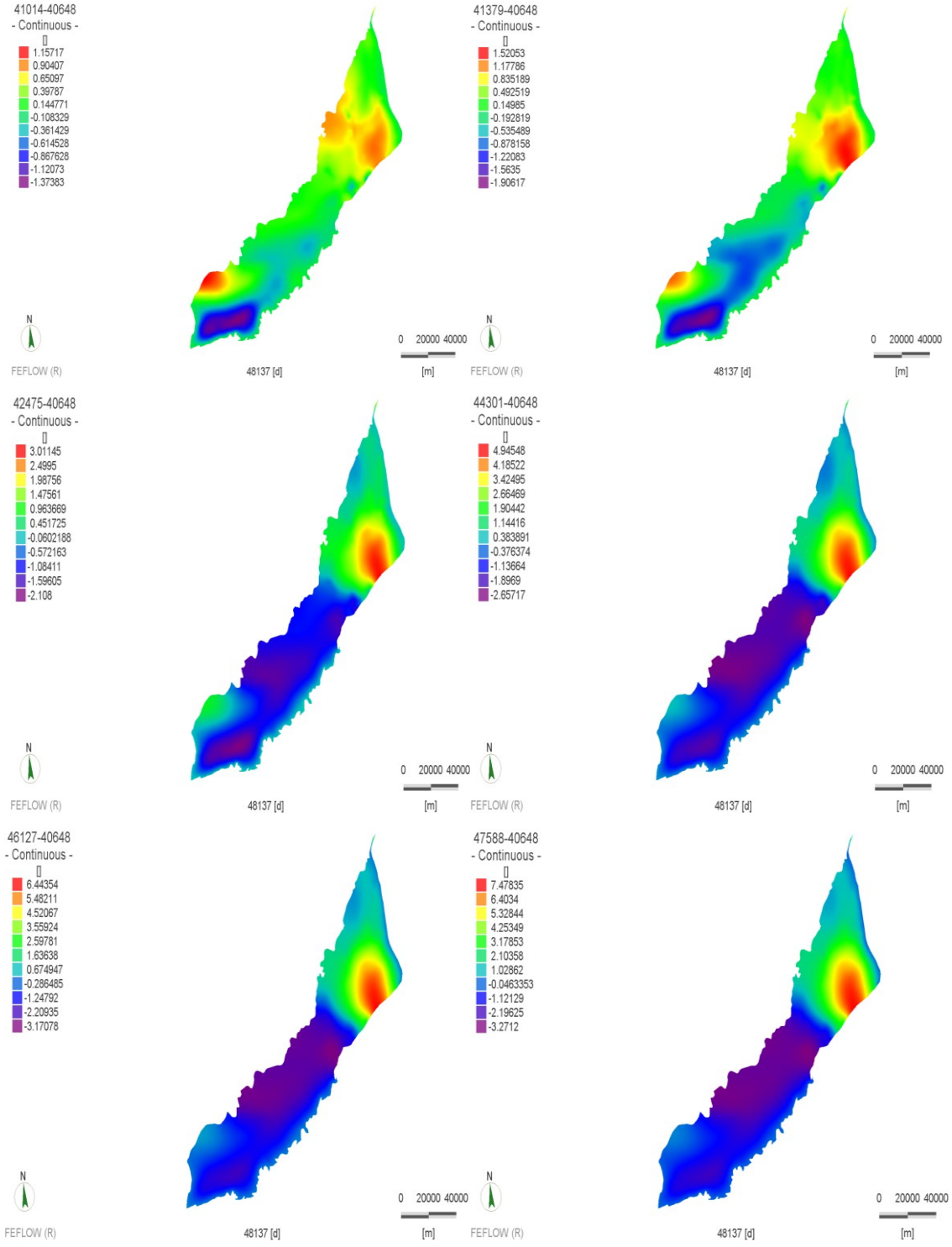

Scenario 2

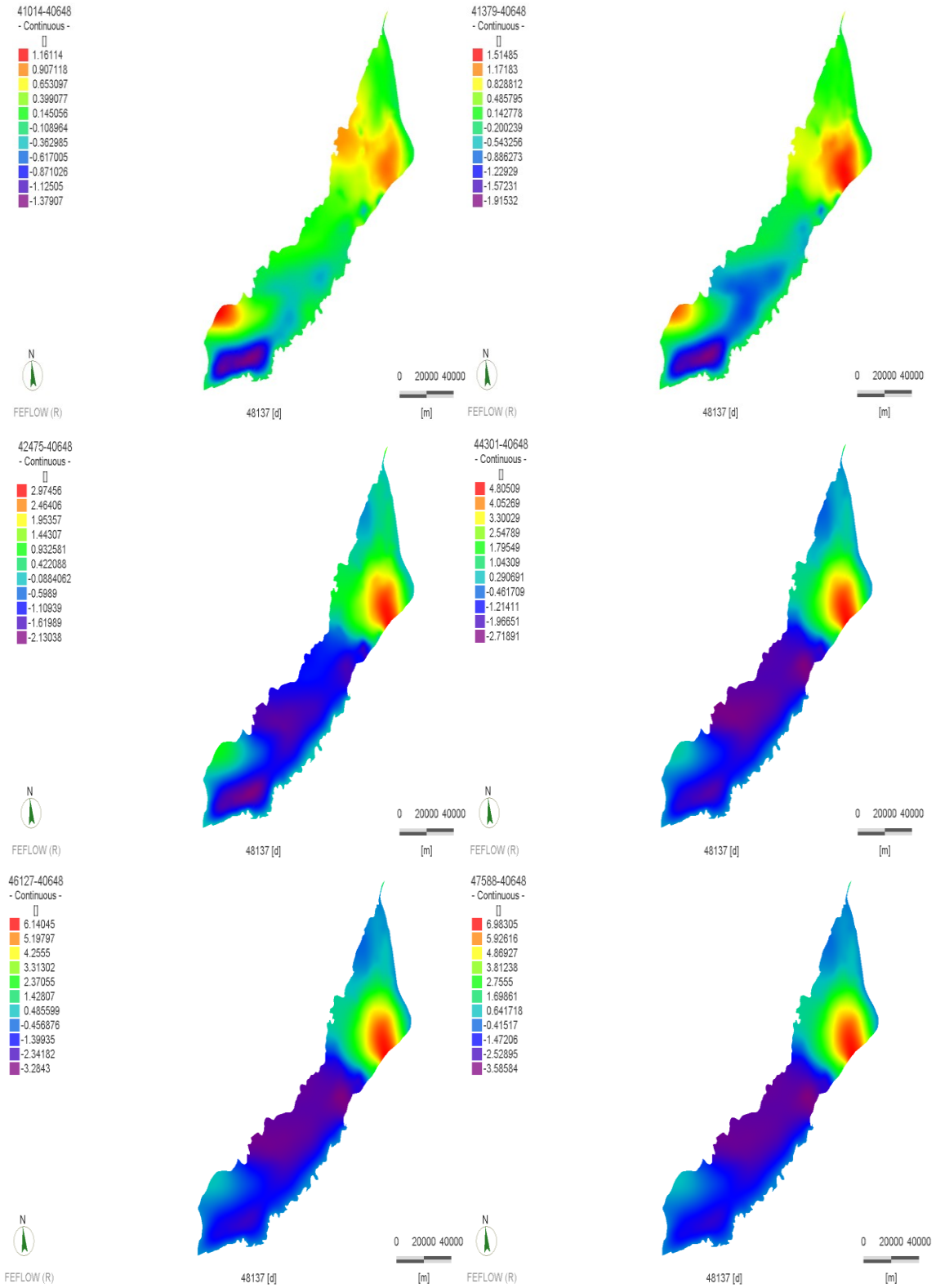
41014-40648
- Continuous -
[]
1.16114
0.907118
0.653097
0.399077
0.145056
-0.108964
-0.362985
-0.617005
-0.871026
-1.12505
-1.37907
N
FEFLOW (R)
48137 [d]
0 20000 40000
[m]
41379-40648
- Continuous -
[]
1.51485
1.17183
0.828812
0.485795
0.142778
-0.200239
-0.543256
-0.886273
-1.22929
-1.57231
-1.91532
N
FEFLOW (R)
48137 [d]
0 20000 40000
[m]
42475-40648
- Continuous -
[]
2.97456
2.46406
1.95357
1.44307
0.932581
0.422088
-0.0884062
-0.5989
-1.10939
-1.61989
-2.13038
N
FEFLOW (R)
48137 [d]
0 20000 40000
[m]
44301-40648
- Continuous -
[]
4.80509
4.05269
3.30029
2.54789
1.79549
1.04309
0.290691
-0.461709
-1.21411
-1.96651
-2.71891
N
FEFLOW (R)
48137 [d]
0 20000 40000
[m]
46127-40648
- Continuous -
[]
6.14045
5.19797
4.2555
3.31302
2.37055
1.42807
0.485599
-0.456876
-1.39935
-2.34182
-3.2843
N
FEFLOW (R)
48137 [d]
0 20000 40000
[m]
47588-40648
- Continuous -
[]
6.98305
5.92616
4.86927
3.81238
2.7555
1.69861
0.641718
-0.41517
-1.47206
-2.52895
-3.58584
N
FEFLOW (R)
48137 [d]
0 20000 40000
[m]

Scenario 3

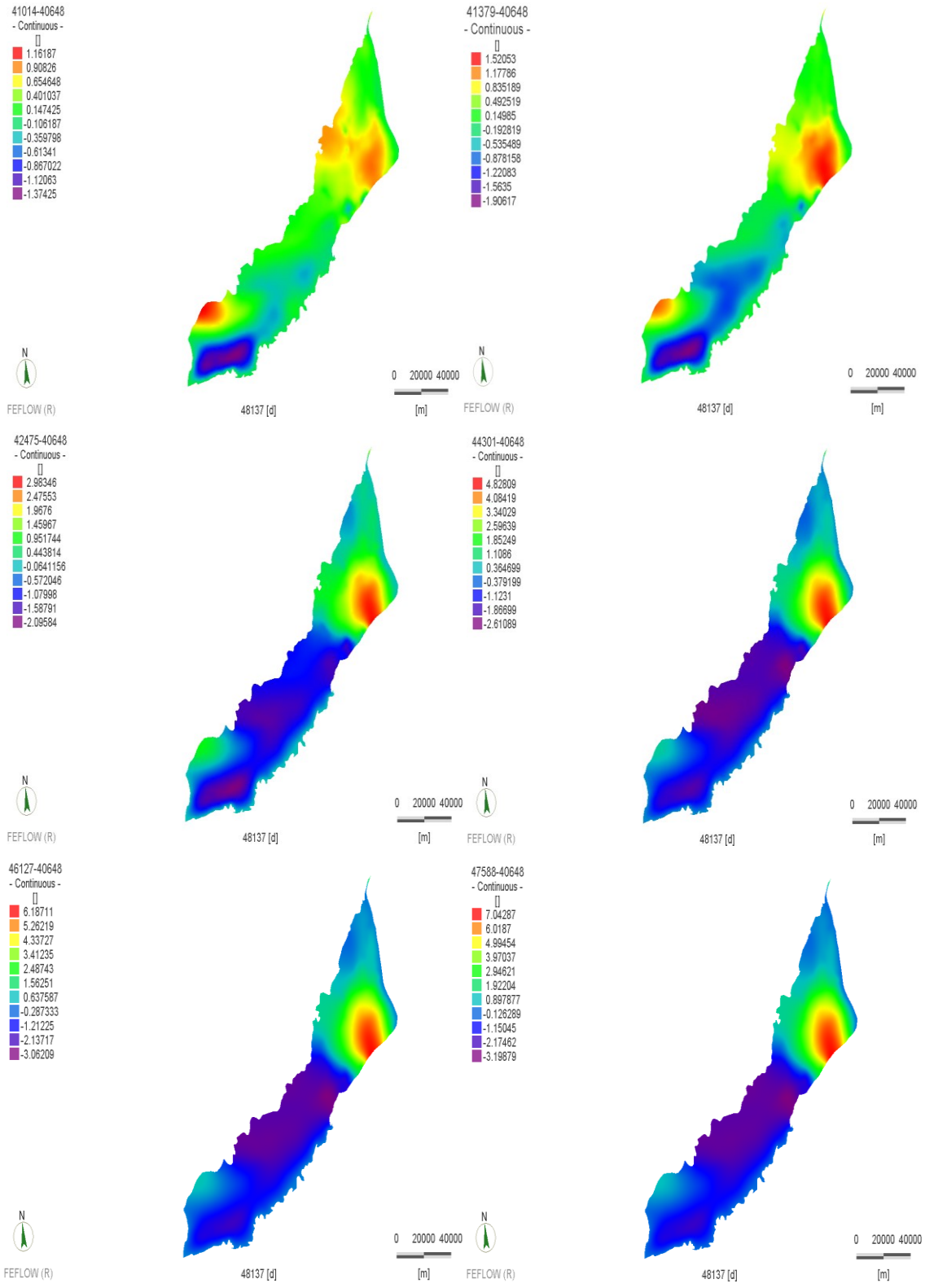
41014-40648
- Continuous -
[]
1.16187
0.90826
0.654648
0.401037
0.147425
-0.106187
-0.359798
-0.61341
-0.867022
-1.12063
-1.37425
N
FEFLOW (R)
48137 [d]
0 20000 40000
[m]
41379-40648
- Continuous -
[]
1.52053
1.17786
0.835189
0.492519
0.14985
-0.192819
-0.535489
-0.878158
-1.22083
-1.5635
-1.90617
N
FEFLOW (R)
48137 [d]
0 20000 40000
[m]
42475-40648
- Continuous -
[]
2.98346
2.47553
1.9676
1.45967
0.951744
0.443814
-0.0641156
-0.572046
-1.07998
-1.58791
-2.09584
N
FEFLOW (R)
48137 [d]
0 20000 40000
[m]
44301-40648
- Continuous -
[]
4.82809
4.08419
3.34029
2.59639
1.85249
1.1086
0.364699
-0.379199
-1.1231
-1.86699
-2.61089
N
FEFLOW (R)
48137 [d]
0 20000 40000
[m]
46127-40648
- Continuous -
[]
6.18711
5.26219
4.33727
3.41235
2.48743
1.56251
0.637587
-0.287333
-1.21225
-2.13717
-3.06209
N
FEFLOW (R)
48137 [d]
0 20000 40000
[m]
47588-40648
- Continuous -
[]
7.04287
6.0187
4.99454
3.97037
2.94621
1.92204
0.897877
-0.126289
-1.15045
-2.17462
-3.19879
N
FEFLOW (R)
48137 [d]
0 20000 40000
[m]

Scenario 4

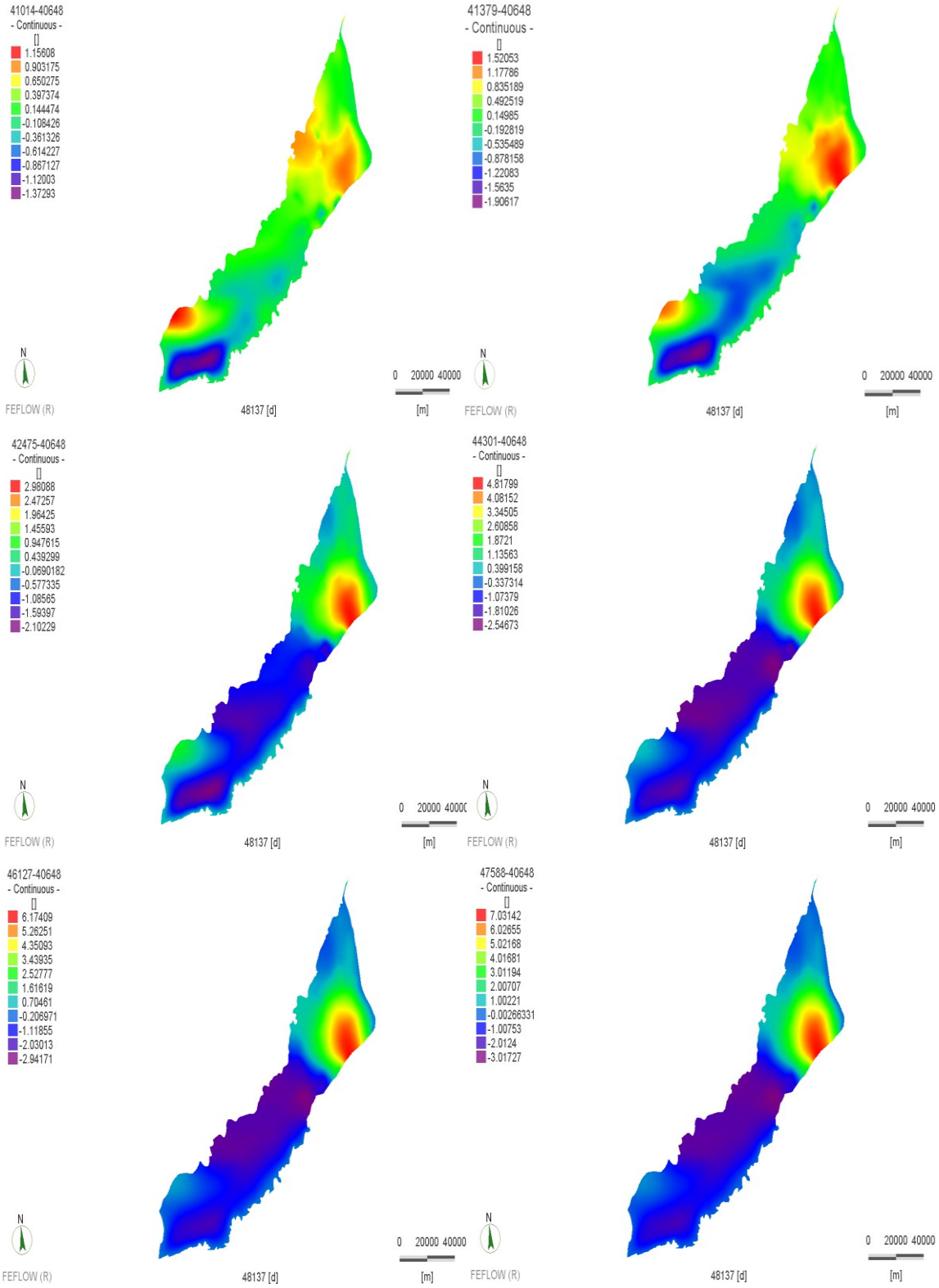
41014-40648
- Continuous -
[]
1.15608
0.903175
0.650275
0.397374
0.144474
-0.108426
-0.361326
-0.614227
-0.867127
-1.12003
-1.37293
N
FEFLOW (R)
48137 [d]
0 20000 40000
[m]
41379-40648
- Continuous -
[]
1.52053
1.17786
0.835189
0.492519
0.14985
-0.192819
-0.535489
-0.878158
-1.22083
-1.5635
-1.90617
N
FEFLOW (R)
48137 [d]
0 20000 40000
[m]
42475-40648
- Continuous -
[]
2.98088
2.47257
1.96425
1.45593
0.947615
0.439299
-0.0690182
-0.577335
-1.08565
-1.59397
-2.10229
N
FEFLOW (R)
48137 [d]
0 20000 40000
[m]
44301-40648
- Continuous -
[]
4.81799
4.08152
3.34505
2.60858
1.8721
1.13563
0.399158
-0.337314
-1.07379
-1.81026
-2.54673
N
FEFLOW (R)
48137 [d]
0 20000 40000
[m]
46127-40648
- Continuous -
[]
6.17409
5.26251
4.35093
3.43935
2.52777
1.61619
0.70461
-0.206971
-1.11855
-2.03013
-2.94171
N
FEFLOW (R)
48137 [d]
0 20000 40000
[m]
47588-40648
- Continuous -
[]
7.03142
6.02655
5.02168
4.01681
3.01194
2.00707
1.00221
-0.00266331
-1.00753
-2.0124
-3.01727
N
FEFLOW (R)
48137 [d]
0 20000 40000
[m]

Scenario 5

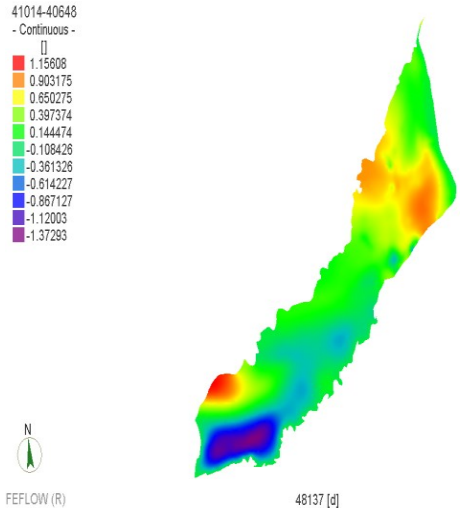
41014-40648
- Continuous -
[]
1.15608
0.903175
0.650275
0.397374
0.144474
-0.108426
-0.361326
-0.614227
-0.867127
-1.12003
-1.37293
N
FEFLOW (R)
48137 [d]
0 20000 40000
[m]

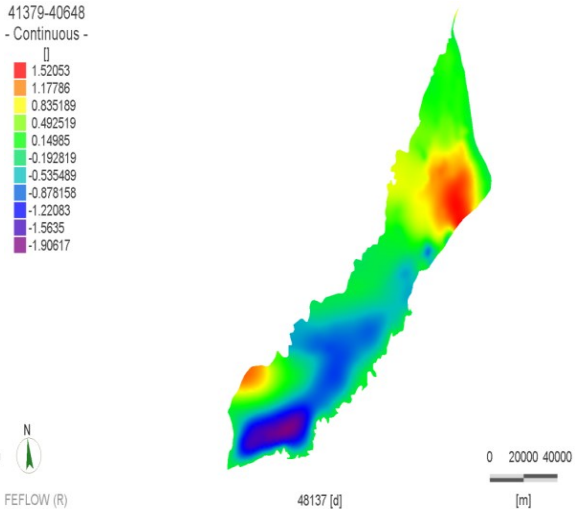
41379-40648
- Continuous -
[]
1.52053
1.17786
0.835189
0.492519
0.14985
-0.192819
-0.535489
-0.878158
-1.22083
-1.5635
-1.90617
N
FEFLOW (R)
48137 [d]
0 20000 40000
[m]

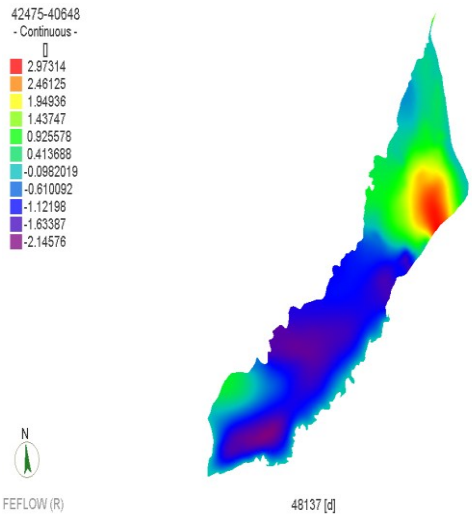
42475-40648
- Continuous -
[]
2.97314
2.46125
1.94936
1.43747
0.925578
0.413688
-0.0982019
-0.610092
-1.12198
-1.63387
-2.14576
N
FEFLOW (R)
48137 [d]
0 20000 40000
[m]

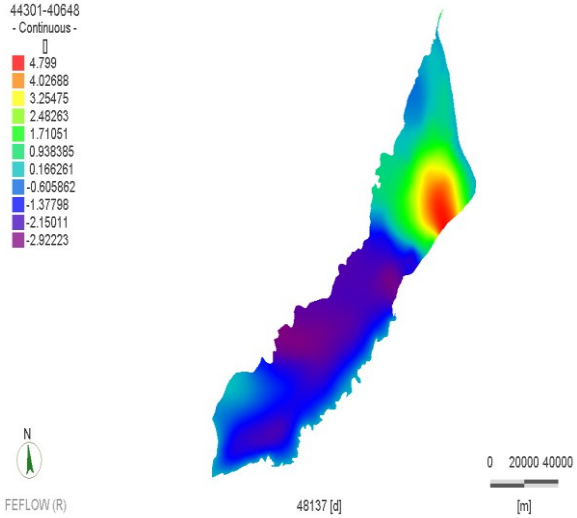
44301-40648
- Continuous -
[]
4.799
4.02688
3.25475
2.48263
1.71051
0.938385
0.166261
-0.605862
-1.37798
-2.15011
-2.92223
N
FEFLOW (R)
48137 [d]
0 20000 40000
[m]

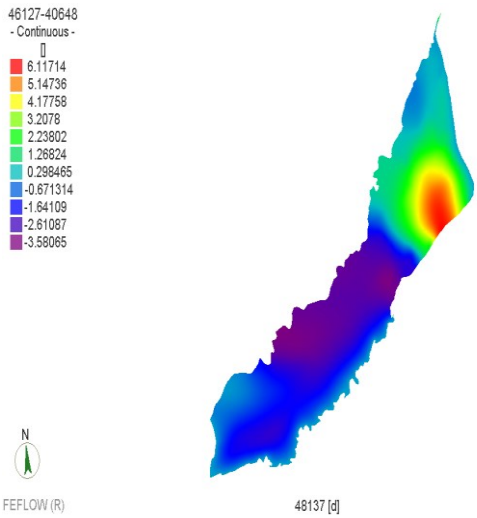
46127-40648
- Continuous -
[]
6.11714
5.14736
4.17758
3.2078
2.23802
1.26824
0.298465
-0.671314
-1.64109
-2.61087
-3.58065
N
FEFLOW (R)
48137 [d]
0 20000 40000
[m]

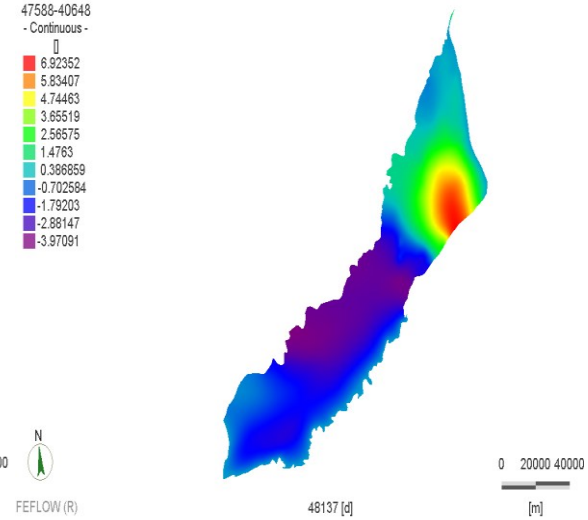
47588-40648
- Continuous -
[]
6.92352
5.83407
4.74463
3.65519
2.56575
1.4763
0.386859
-0.702584
-1.79203
-2.88147
-3.97091
N
FEFLOW (R)
48137 [d]
0 20000 40000
[m]

Scenario 6

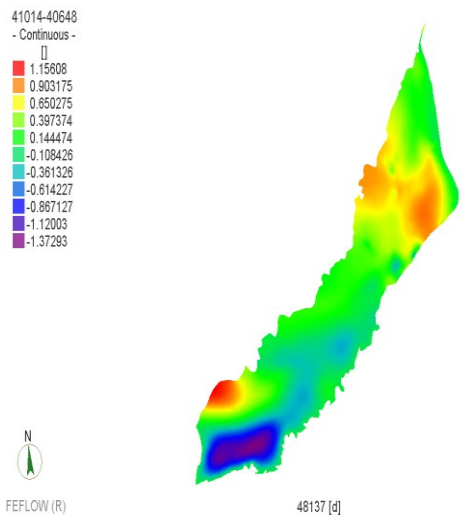
41014-40648
- Continuous -
[]
1.15608
0.903175
0.650275
0.397374
0.144474
-0.108426
-0.361326
-0.614227
-0.867127
-1.12003
-1.37293
N
FEFLOW (R)
48137 [d]
0 20000 40000
[m]

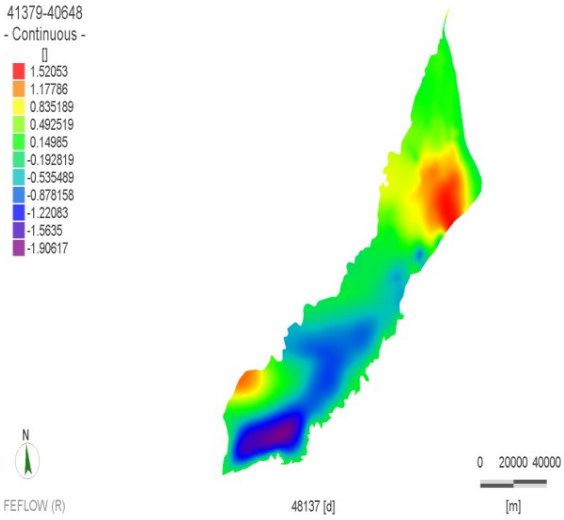
41379-40648
- Continuous -
[]
1.52053
1.17786
0.835189
0.492519
0.14985
-0.192819
-0.535489
-0.878158
-1.22083
-1.5635
-1.90617
N
FEFLOW (R)
48137 [d]
0 20000 40000
[m]

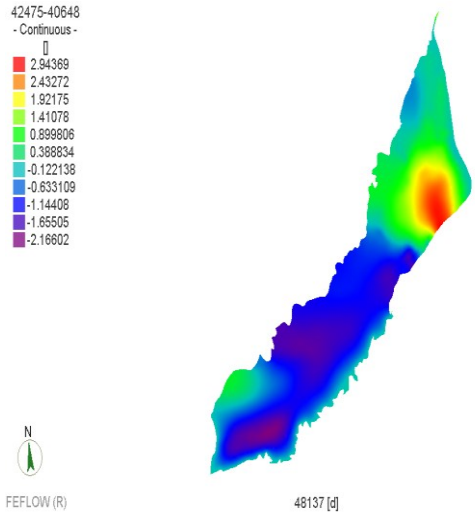
42475-40648
- Continuous -
[]
2.94369
2.43272
1.92175
1.41078
0.899806
0.388834
-0.122138
-0.633109
-1.14408
-1.65505
-2.16602
N
FEFLOW (R)
48137 [d]
0 20000 40000
[m]

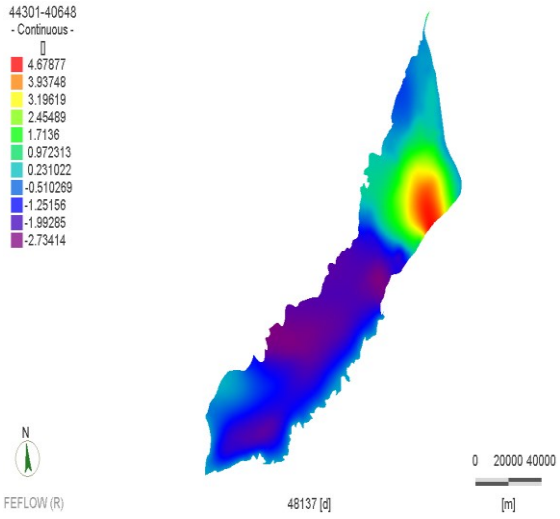
44301-40648
- Continuous -
[]
4.67877
3.93748
3.19619
2.45489
1.7136
0.972313
0.231022
-0.510269
-1.25156
-1.99285
-2.73414
N
FEFLOW (R)
48137 [d]
0 20000 40000
[m]

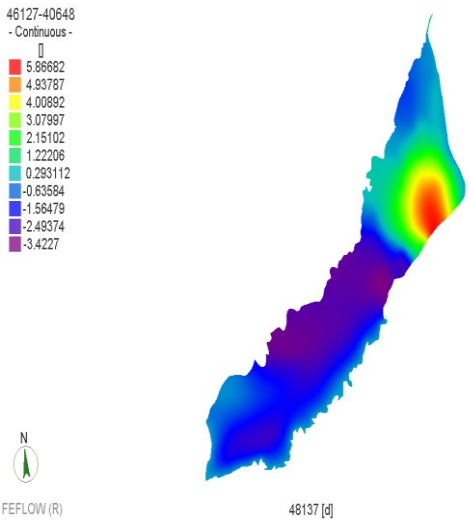
46127-40648
- Continuous -
[]
5.86682
4.93787
4.00892
3.07997
2.15102
1.22206
0.293112
-0.63584
-1.56479
-2.49374
-3.4227
N
FEFLOW (R)
48137 [d]
0 20000 40000
[m]

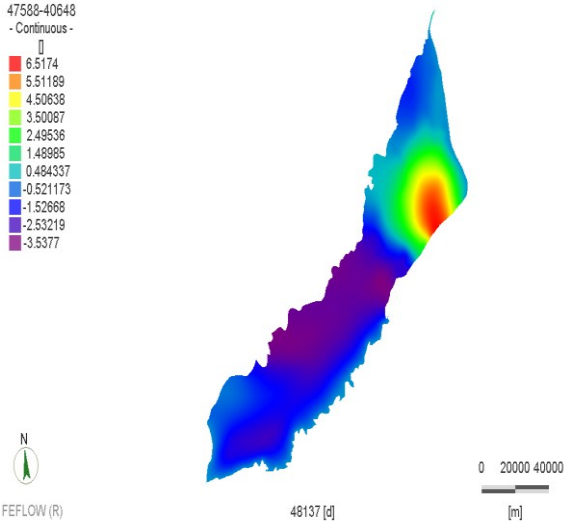
47588-40648
- Continuous -
[]
6.5174
5.51189
4.50638
3.50087
2.49536
1.48985
0.484337
-0.521173
-1.52668
-2.53219
-3.5377
N
FEFLOW (R)
48137 [d]
0 20000 40000
[m]

Scenario 7

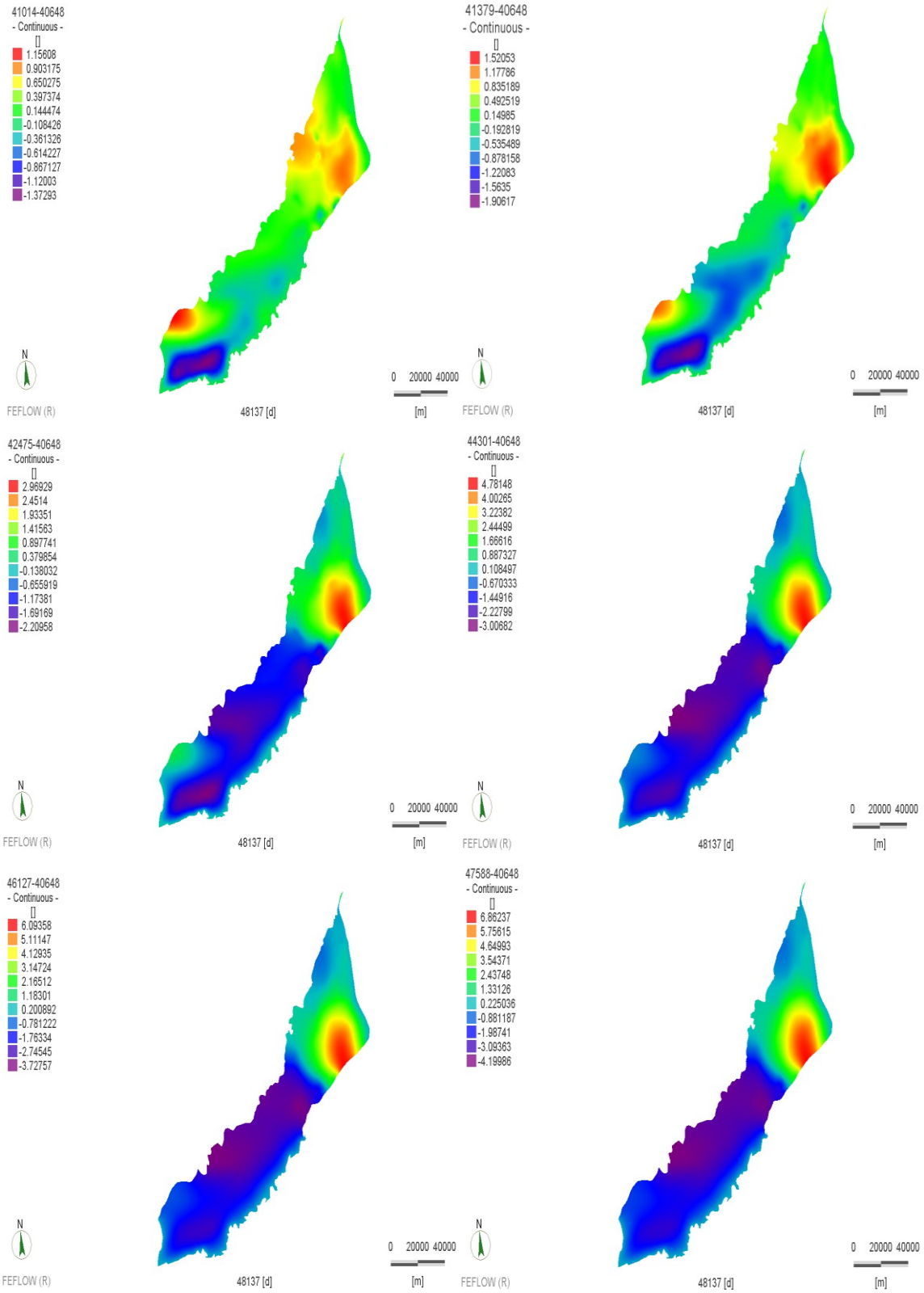
41014-40648
- Continuous -
[]
1.15608
0.903175
0.650275
0.397374
0.144474
-0.108426
-0.361326
-0.614227
-0.867127
-1.12003
-1.37293
N
FEFLOW (R)
48137 [d]
0 20000 40000
[m]
41379-40648
- Continuous -
[]
1.52053
1.17786
0.835189
0.492519
0.14985
-0.192819
-0.535489
-0.878158
-1.22083
-1.5635
-1.90617
N
FEFLOW (R)
48137 [d]
0 20000 40000
[m]
42475-40648
- Continuous -
[]
2.96929
2.4514
1.93351
1.41563
0.897741
0.379854
-0.138032
-0.655919
-1.17381
-1.69169
-2.20958
N
FEFLOW (R)
48137 [d]
0 20000 40000
[m]
44301-40648
- Continuous -
[]
4.78148
4.00265
3.22382
2.44499
1.66616
0.887327
0.108497
-0.670333
-1.44916
-2.22799
-3.00682
N
FEFLOW (R)
48137 [d]
0 20000 40000
[m]
46127-40648
- Continuous -
[]
6.09358
5.11147
4.12935
3.14724
2.16512
1.18301
0.200892
-0.781222
-1.76334
-2.74545
-3.72757
N
FEFLOW (R)
48137 [d]
0 20000 40000
[m]
47588-40648
- Continuous -
[]
6.66237
5.75615
4.64993
3.54371
2.43748
1.33126
0.225036
-0.881187
-1.98741
-3.09363
-4.19986
N
FEFLOW (R)
48137 [d]
0 20000 40000
[m]

Scenario 8

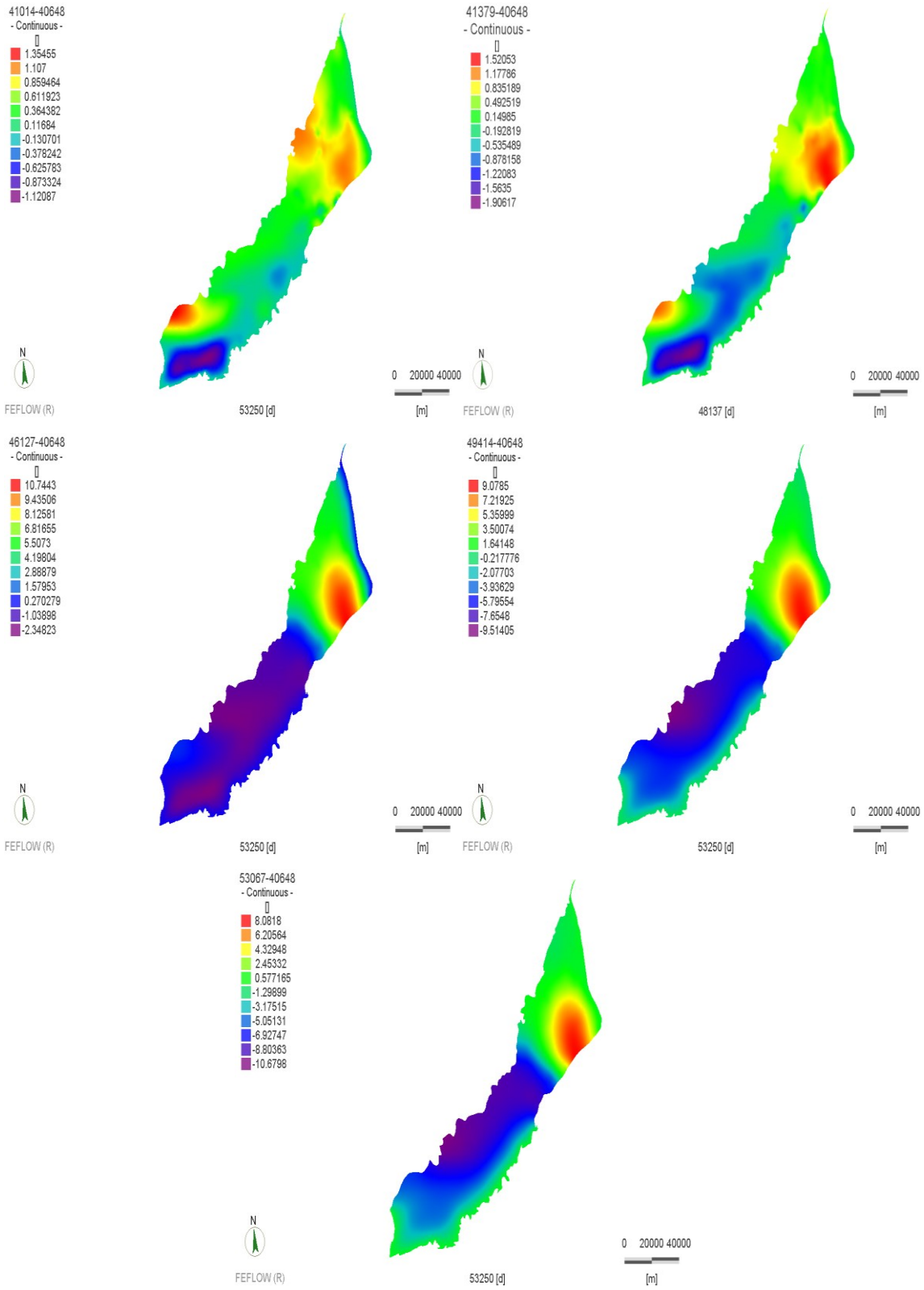
41014-40648
- Continuous -
[]
1.35455
1.107
0.859464
0.611923
0.364382
0.11684
-0.130701
-0.378242
-0.625783
-0.873324
-1.12087
N
FEFLOW (R)
53250 [d]
0 20000 40000
[m]
41379-40648
- Continuous -
[]
1.52053
1.17786
0.835189
0.492519
0.14985
-0.192819
-0.535489
-0.878158
-1.22083
-1.5635
-1.90617
N
FEFLOW (R)
48137 [d]
0 20000 40000
[m]
46127-40648
- Continuous -
[]
10.7443
9.43506
8.12581
6.81655
5.5073
4.19804
2.88879
1.57953
0.270279
-1.03898
-2.34823
N
FEFLOW (R)
53250 [d]
0 20000 40000
[m]
49414-40648
- Continuous -
[]
9.0785
7.21925
5.35999
3.50074
1.64148
-0.217776
-2.07703
-3.93629
-5.79554
-7.6548
-9.51405
N
FEFLOW (R)
53250 [d]
0 20000 40000
[m]
53067-40648
- Continuous -
[]
8.0818
6.20564
4.32948
2.45332
0.577165
-1.29899
-3.17515
-5.05131
-6.92747
-8.80363
-10.6798
N
FEFLOW (R)
53250 [d]
0 20000 40000
[m]

Scenario 9

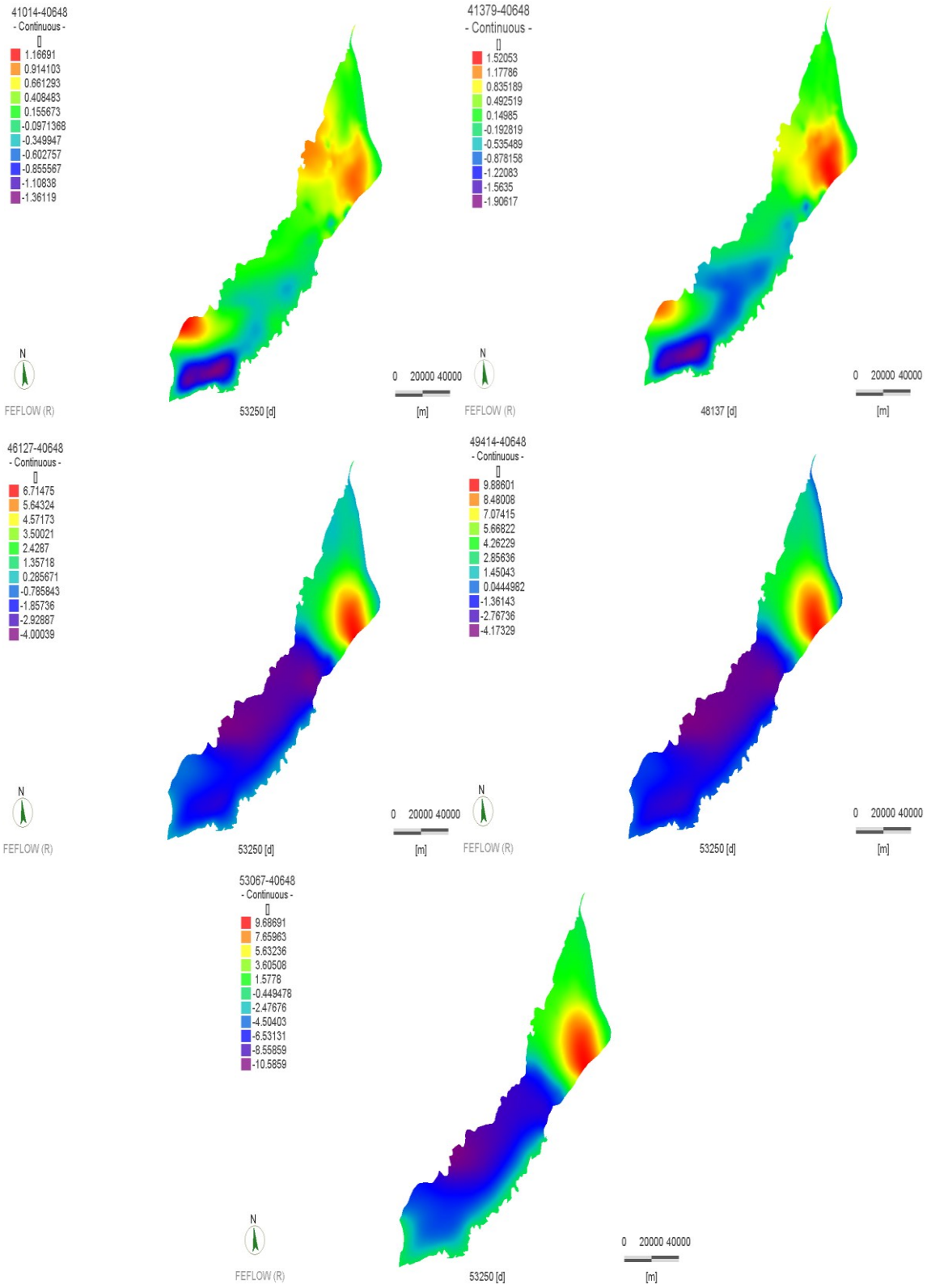
41014-40648
- Continuous -
[]
1.16691
0.914103
0.661293
0.408483
0.155673
-0.0971368
-0.349947
-0.602757
-0.855567
-1.10838
-1.36119
N
FEFLOW (R)
53250 [d]
0 20000 40000
[m]
41379-40648
- Continuous -
[]
1.52053
1.17786
0.835189
0.492519
0.14985
-0.192819
-0.535489
-0.878158
-1.22083
-1.5635
-1.90617
N
FEFLOW (R)
48137 [d]
0 20000 40000
[m]
46127-40648
- Continuous -
[]
6.71475
5.64324
4.57173
3.50021
2.4287
1.35718
0.285671
-0.785843
-1.85736
-2.92887
-4.00039
N
FEFLOW (R)
53250 [d]
0 20000 40000
[m]
49414-40648
- Continuous -
[]
9.88601
8.48008
7.07415
5.66822
4.26229
2.85636
1.45043
0.0444982
-1.36143
-2.76736
-4.17329
N
FEFLOW (R)
53250 [d]
0 20000 40000
[m]
53067-40648
- Continuous -
[]
9.68691
7.65963
5.63236
3.60508
1.5778
-0.449478
-2.47676
-4.50403
-6.53131
-8.55859
-10.5859
N
FEFLOW (R)
53250 [d]
0 20000 40000
[m]

Scenario 10

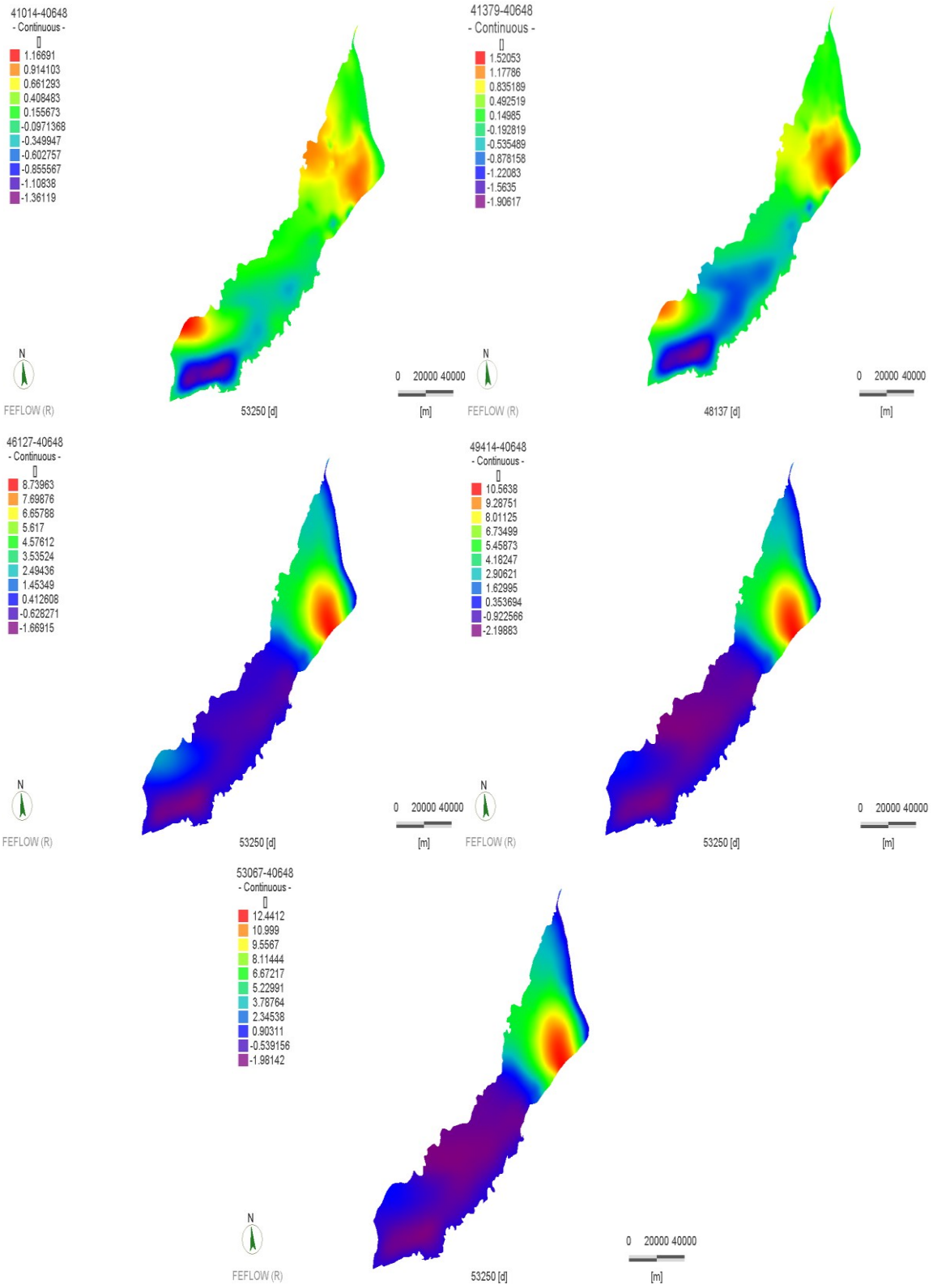
41014-40648
- Continuous -
[]
1.16691
0.914103
0.661293
0.408483
0.155673
-0.0971368
-0.349947
-0.602757
-0.855567
-1.10838
-1.36119
N
FEFLOW (R)
53250 [d]
0 20000 40000
[m]
41379-40648
- Continuous -
[]
1.52053
1.17786
0.835189
0.492519
0.14985
-0.192819
-0.535489
-0.878158
-1.22083
-1.5635
-1.90617
N
FEFLOW (R)
48137 [d]
0 20000 40000
[m]
46127-40648
- Continuous -
[]
8.73963
7.69876
6.65788
5.617
4.57612
3.53524
2.49436
1.45349
0.412608
-0.628271
-1.66915
N
FEFLOW (R)
53250 [d]
0 20000 40000
[m]
49414-40648
- Continuous -
[]
10.5638
9.28751
8.01125
6.73499
5.45873
4.18247
2.90621
1.62995
0.353694
-0.922566
-2.19883
N
FEFLOW (R)
53250 [d]
0 20000 40000
[m]
53067-40648
- Continuous -
[]
12.4412
10.999
9.5567
8.11444
6.67217
5.22991
3.78764
2.34538
0.90311
-0.539156
-1.98142
N
FEFLOW (R)
53250 [d]
0 20000 40000
[m]

Scenario 11

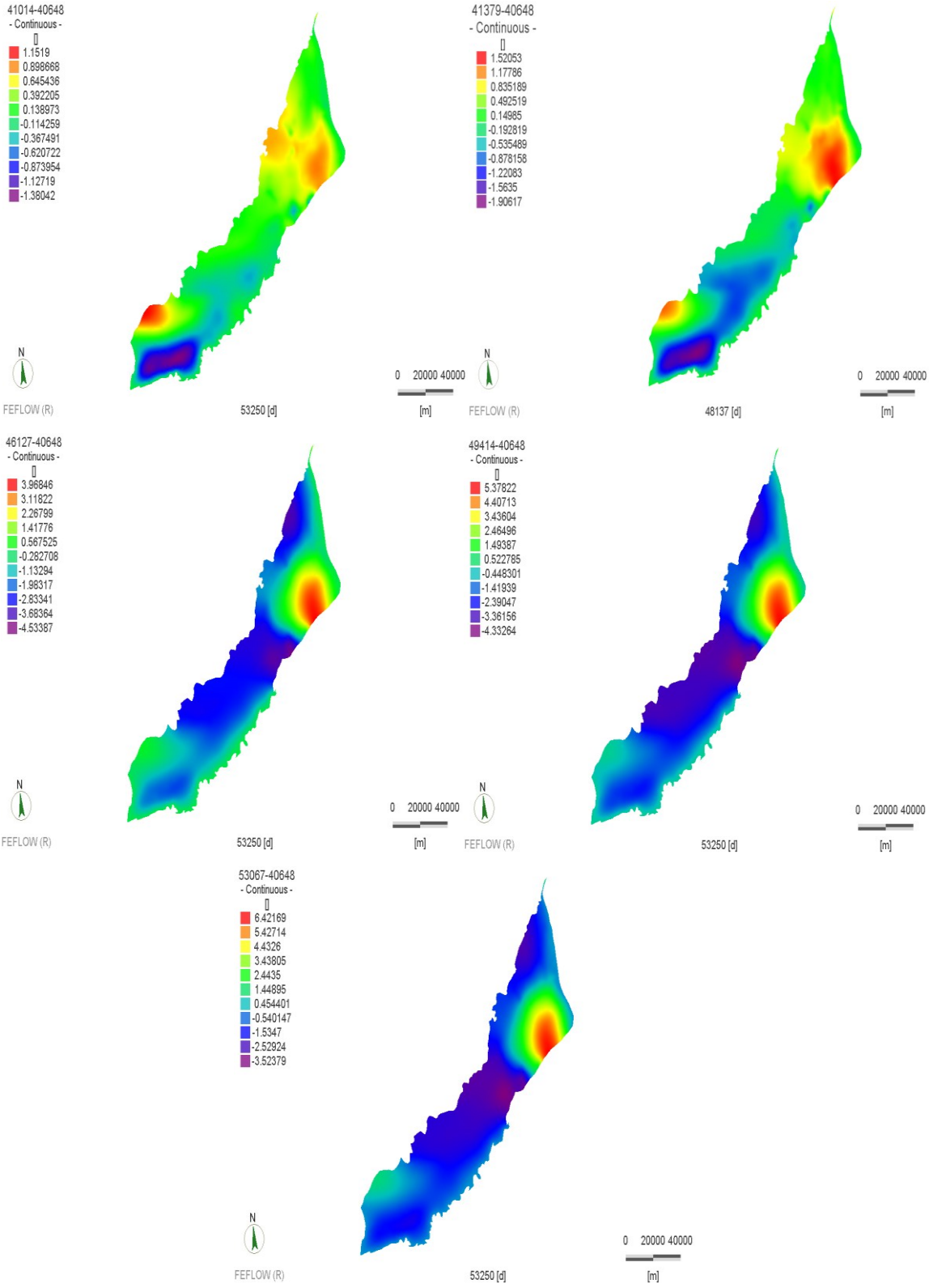
41014-40648
- Continuous -
[]
1.1519
0.898668
0.645436
0.392205
0.138973
-0.114259
-0.367491
-0.620722
-0.873954
-1.12719
-1.38042
N
FEFLOW (R)
53250 [d]
0 20000 40000
[m]
41379-40648
- Continuous -
[]
1.52053
1.17786
0.835189
0.492519
0.14985
-0.192819
-0.535489
-0.878158
-1.22083
-1.5635
-1.90617
N
FEFLOW (R)
48137 [d]
0 20000 40000
[m]
46127-40648
- Continuous -
[]
3.96846
3.11822
2.26799
1.41776
0.567525
-0.282708
-1.13294
-1.98317
-2.83341
-3.68364
-4.53387
N
FEFLOW (R)
53250 [d]
0 20000 40000
[m]
49414-40648
- Continuous -
[]
5.37822
4.40713
3.43604
2.46496
1.49387
0.522785
-0.448301
-1.41939
-2.39047
-3.36156
-4.33264
N
FEFLOW (R)
53250 [d]
0 20000 40000
[m]
53067-40648
- Continuous -
[]
6.42169
5.42714
4.4326
3.43805
2.4435
1.44895
0.454401
-0.540147
-1.5347
-2.52924
-3.52379
N
FEFLOW (R)
53250 [d]
0 20000 40000
[m]

Scenario 12

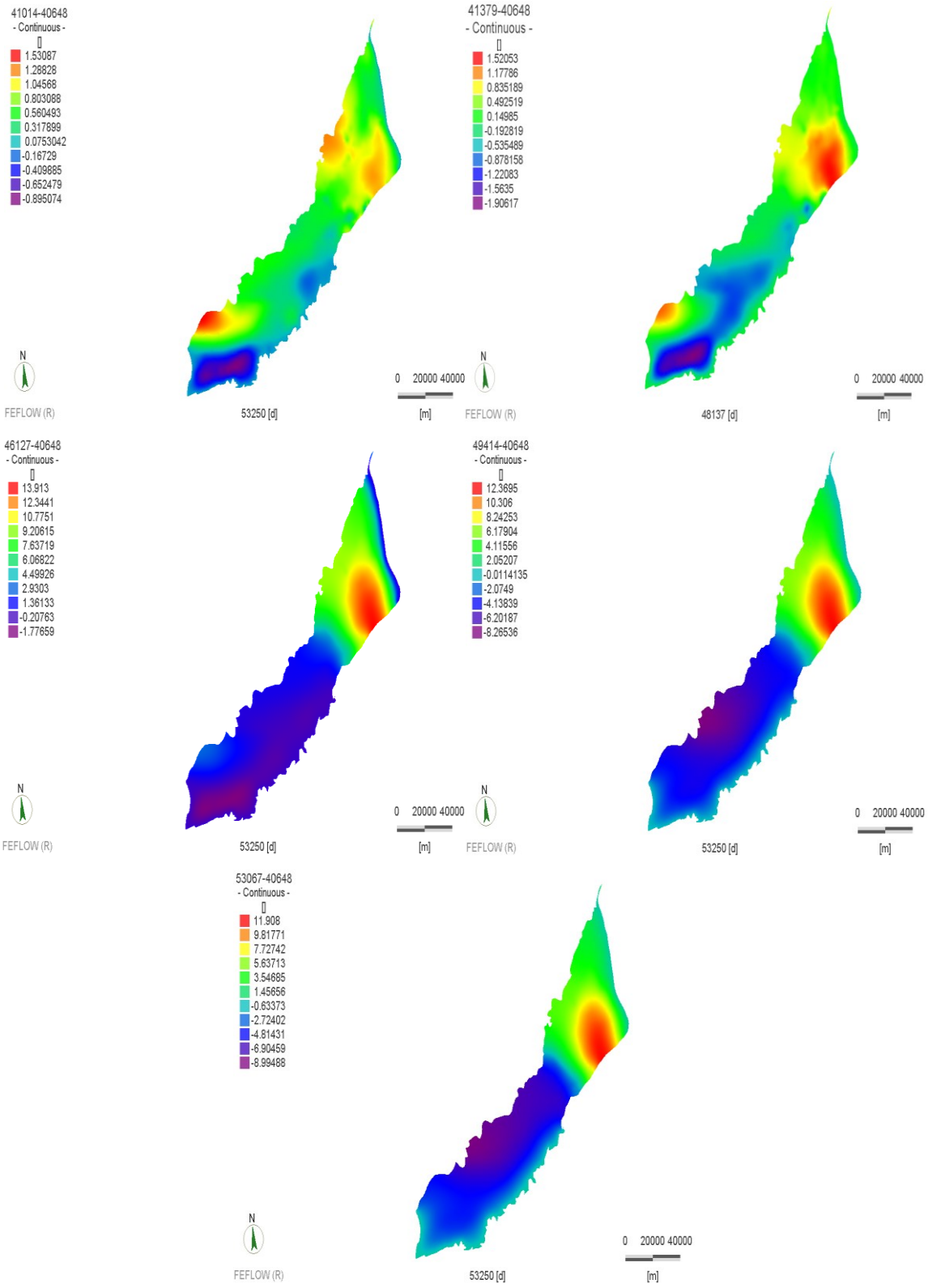
41014-40648
- Continuous -
[]
1.53087
1.28828
1.04568
0.803088
0.560493
0.317899
0.0753042
-0.16729
-0.409885
-0.652479
-0.895074
N
FEFLOW (R)
53250 [d]
0 20000 40000
[m]
41379-40648
- Continuous -
[]
1.52053
1.17786
0.835189
0.492519
0.14985
-0.192819
-0.535489
-0.878158
-1.22083
-1.5635
-1.90617
N
FEFLOW (R)
48137 [d]
0 20000 40000
[m]
46127-40648
- Continuous -
[]
13.913
12.3441
10.7751
9.20615
7.63719
6.06822
4.49926
2.9303
1.36133
-0.20763
-1.77659
N
FEFLOW (R)
53250 [d]
0 20000 40000
[m]
49414-40648
- Continuous -
[]
12.3695
10.306
8.24253
6.17904
4.11556
2.05207
-0.0114135
-2.0749
-4.13839
-6.20187
-8.26536
N
FEFLOW (R)
53250 [d]
0 20000 40000
[m]
53067-40648
- Continuous -
[]
11.908
9.81771
7.72742
5.63713
3.54685
1.45656
-0.63373
-2.72402
-4.81431
-6.90459
-8.99488
N
FEFLOW (R)
53250 [d]
0 20000 40000
[m]

Scenario 13

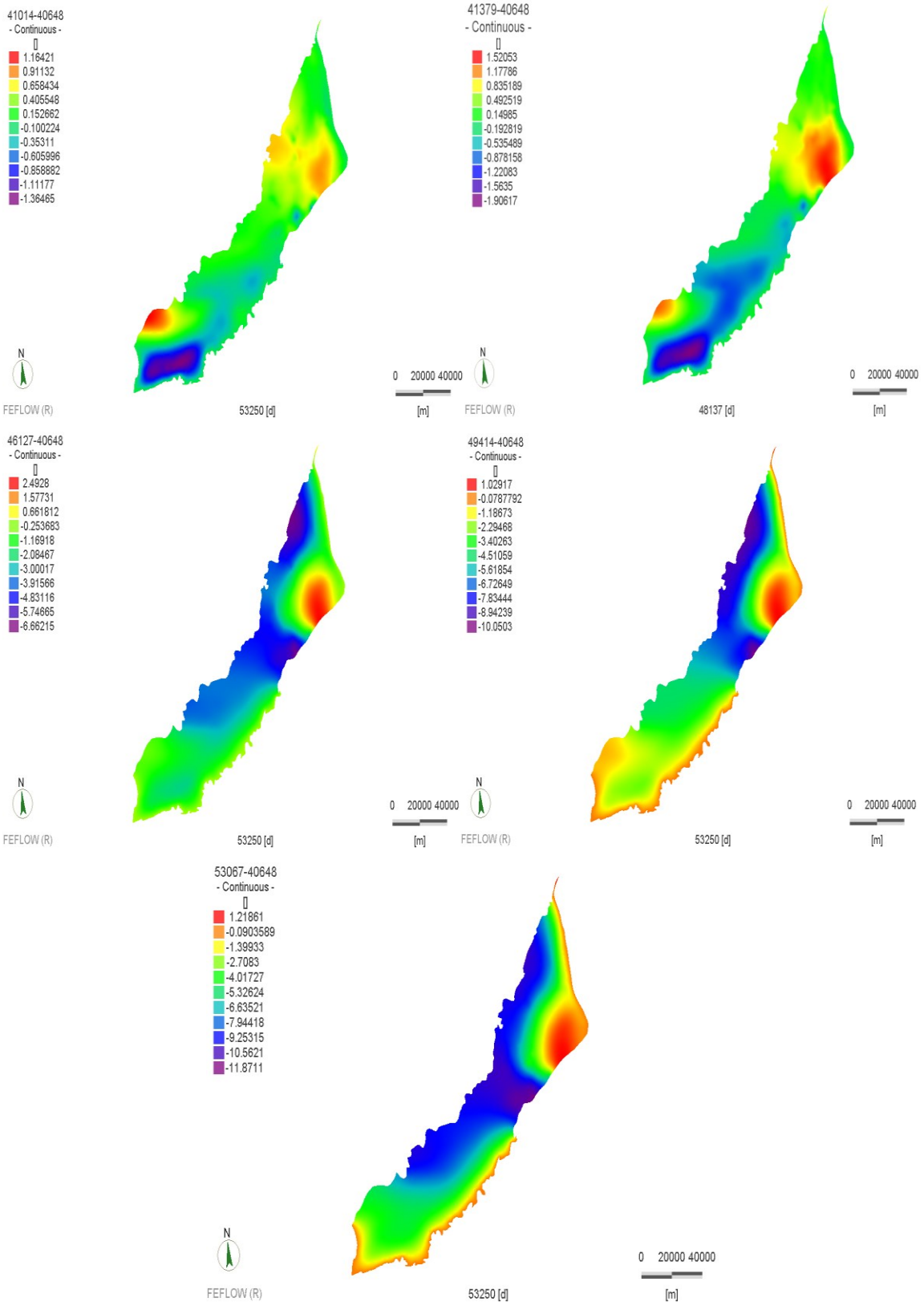
41014-40648
- Continuous -
[]
1.16421
0.91132
0.658434
0.405548
0.152662
-0.100224
-0.35311
-0.605996
-0.858882
-1.11177
-1.36465
N
FEFLOW (R)
53250 [d]
0 20000 40000
[m]
41379-40648
- Continuous -
[]
1.52053
1.17786
0.835189
0.492519
0.14985
-0.192819
-0.535489
-0.878158
-1.22083
-1.5635
-1.90617
N
FEFLOW (R)
48137 [d]
0 20000 40000
[m]
46127-40648
- Continuous -
[]
2.4928
1.57731
0.661812
-0.253683
-1.16918
-2.08467
-3.00017
-3.91566
-4.83116
-5.74665
-6.66215
N
FEFLOW (R)
53250 [d]
0 20000 40000
[m]
49414-40648
- Continuous -
[]
1.02917
-0.0787792
-1.18673
-2.29468
-3.40263
-4.51059
-5.61854
-6.72649
-7.83444
-8.94239
-10.0503
N
FEFLOW (R)
53250 [d]
0 20000 40000
[m]
53067-40648
- Continuous -
[]
1.21861
-0.0903589
-1.39933
-2.7083
-4.01727
-5.32624
-6.63521
-7.94418
-9.25315
-10.5621
-11.8711
N
FEFLOW (R)
53250 [d]
0 20000 40000
[m]

Acknowledgements

While I approach to the completion of my Doctoral degree, I owe a lot to many personalities who continuously showered their favor, support, guidance and prayers. Mere words on a piece of paper cannot recompense their continuous and unconditional care. Nevertheless, I want to extend my deep gratitude to Dr. Gerhard Strauch, Institute of Hydrogeology, Helmholtz Centre for Environmental Research (UFZ), Leipzig, who paved my way to take acceptance from Prof. Dr. Rudolf Liedl, Head, Institute of Groundwater Management (IGW), Technical University Dresden.

Prof. Liedl generously accepted me to supervise my PhD project. He is exceptionally kind, polite and wonderful person whose attitude is always supportive and facilitating. There is not even a single event in my entire stay at IGW, when I felt worry from his side. He always supported me in every step of my research and provided whatever I requested from him and he could have done. Apart from technical supervision of my PhD project, he always vehemently extended his support to facilitate my living. My prayers and well wishes are always for his active and healthy life. It is my deep wish to continue my connection with him in future through further research and, for higher studies.

Many thanks are also due to Dr. Ing. Usman Khalid Awan, Groundwater Hydrologist at ICARDA for his valuable tips and suggestions in fulfilling the requirements of my research project at initial stages. His inspirational personality always proved a motivational force for me due to his critical and innovative ideas.

In addition, I owe many sincere thanks for the Higher Education Commission of Pakistan and Germany Academic Exchange Services (DAAD) for the award of scholarship to pursue my PhD in Germany, while at the same time acknowledging the support received from Graduate Academy, TU Dresden in finalizing my thesis. I also extend my thanks to DHI-WASY for providing me cost free FEFLOW license for my research work. Moreover, special thanks to HIGRADE, UFZ, Leipzig for providing me opportunity to take advance courses which certainly helped me during my research work.

I was blessed to receive every sort of support from IGW team, especially from Ms. Nancy Reimann. She made my stay at IGW so soothing that made my life pleasant. I found her always eager to help me. I am extremely thankful to her for such wonderful hospitality and caring attitude. Guidance received from Dr. Thomas Reimann and Dr. Falk Händel is also highly acknowledged. Lively discussions with Azhar Abbas, ZALF, Müncheberg were cherishing and informative. The company of Saif Al-Amri (late) at IGW proved very helpful in exchanging ideas but after two years he left all of us forever. I pray for his eternal peace in heavens. I would also extend my sincere thanks to Dr. M. Rizwan, Dr. Safdar, Dr. Diana, Thomas Krause, Dr. Marc Walther, Mr. Ronald Oese, Wasim Akram, SA Malik, Aysha Al-Khatri, Afnan Qurban Shaikh in helping to resolve many official and private matters. Special

thanks are also offered to Prof. Dr. Ashfaq Ahmad Chattha, Dr. Adnan Ahmad Shahid, Dr. Muhammad Arshad, Dr. Hamid Hussain Shah, Dr. Jehanzeb Masud Cheema, Abdul Shabbir, Dr. Rashid Mahmood for their continuous encouragement.

Last but not least, my father (late) Ch. Ghulam Ahmad and my mother Riaz Fatima always kept waiting and praying for my successful return. I extend my innermost gratitude to my wife, Sabeeha Akbar, brother, Abdul Jabbar, my sister, Shazia Ambreen, sister in law, Fareeha Jabbar, for their prayers and consoling conversations. I also offer my sincere appreciation for the well-wishes from my father in law (late) Ch. M. Akbar, mother in law, sisters in laws and brothers in laws, nephew and two cute nieces.